uOttawa

L'Université canadienne
Canada's university

FACULTÉ DES ÉTUDES SUPÉRIEURES ET POSTOCTORALES

uOttawa

L'Université canadienne
Canada's university

FACULTY OF GRADUATE AND POSDOCTORAL STUDIES

Jennifer Rosemarie Major
AUTEUR DE LA THÈSE / AUTHOR OF THESIS

M.Sc. (Microbiology and Immunology)
GRADE / DEGREE

Department of Microbiology and Immunology
FACULTÉ, ÉCOLE, DÉPARTEMENT / FACULTY, SCHOOL, DEPARTMENT

Assessing the Oncolytic Potential of Reovirus Reassortants

TITRE DE LA THÈSE / TITLE OF THESIS

Dr. Earl Brown
DIRECTEUR (DIRECTRICE) DE LA THÈSE / THESIS SUPERVISOR

CO-DIRECTEUR (CO-DIRECTRICE) DE LA THÈSE / THESIS CO-SUPERVISOR

EXAMINATEURS (EXAMINATRICES) DE LA THÈSE / THESIS EXAMINERS

Dr. K. Dimock

Dr. I. Lorimer

Gary W. Slater
Le Doyen de la Faculté des études supérieures et postdoctorales / Dean of the Faculty of Graduate and Postdoctoral Studies

Assessing the oncolytic potential of reovirus reassortants

Jennifer Rosmarie Major

Thesis submitted to

The Faculty of Graduate Studies and Research

of

The University of Ottawa

In partial fulfillment of the requirements for the degree

of

Master of Science

Department of Biochemistry, Microbiology and Immunology

Faculty of Medicine

Your file Votre référence
ISBN: 978-0-494-32469-1
Our file Notre référence
ISBN: 978-0-494-32469-1

ABSTRACT

Type 3 Dearing (T3D) reovirus is an oncolytic virus able to lyse a majority of tumor types. The major drawback is that ~20% of tumor types are resistant to lysis by T3D and therefore there is a need to improve the oncolytic ability of reovirus to include resistant tumors. When designing an oncolytic virus, an ideal virus would be sensitive to double stranded protein kinase (PKR) pathway involved in the anti-viral response of normal cells. Previous studies in our lab determined which gene segments were involved in generating high viral yields in the absence of PKR. The M1 gene segment from T3D controls PKR sensitivity and the Type 1 Lange (T1L) L3 gene segment controlled the increased viral yield in the absence of PKR. The hypothesis of this study is that improved oncolysis can be achieved by combining the T1L L3 gene segment with the T3D M1 gene segment through the creation of T1L x T3D reassortants. The reassortant viruses with these gene segments and other unidentified gene segment combinations have the potential to have superior oncolytic ability compared to the parent serotypes.

The Balb/c murine colon carcinoma tumor cell line, CT26, is resistant to lysis by serotype 1 Lang (T1L) and T3D following infection *in vitro* and is thus a demanding model in which to screen T1L x T3D reassortants for improved oncolytic ability. To identify genes involved in viral growth and protein synthesis a panel of T1L x T3D reassortants was monitored for replication and protein synthesis in CT26 cells as well as mouse embryo fibroblasts from wt and the PKR knockout (PKR-/-) Balb-c mice. In epithelial cells the primary gene segment involved in viral yield and protein production in CT26 cells was the T3D S1 gene segment, with secondary contribution from T3D L2, M2 and M3 gene segments for viral yield, and T3D L1 and M2 gene segments for protein

production. However, in fibroblasts the T1L L3 gene segment was important for protein production in the presence of PKR and the T1L L1 and T3D M2 genes segments were involved in protein production in the absence of PKR. Different reovirus genes are involved in the productivity and permissiveness of infection in different cell types.

In contrast to *in vitro* infection, 4 T1L x T3D reassortants, EB88, EB86, EB97, and EB123, possess enhanced ability to prolong survival of Balb/c mice bearing CT26 lung metastases. This finding demonstrated that ability to lyse tumors does not correlate with ability to lyse cells *in vitro* and that specific reovirus reassortants possess enhanced oncolytic properties. Virus infection of CT26 tumors *in vivo* with EB88, EB86, EB97, and EB123 was measured by immunofluorescence with anti-reovirus serum as well as apoptosis over 7 days following infection to show that all reassortants with enhanced oncolytic properties had infections of longer duration and generally more extensive TUNEL positive cells.

I also observed that PKR-/- mice had a unique pattern of infection relative to T1L and T3D; bronchiolar epithelium was infected with T3D but not with T1L, whereas bronchiolar epithelium of wt Balb-c mice was resistant to infection with both viruses. The PKR dependent bronchiolar epithelial tropism mapped to the S1 genome segment. This finding, which contrasts with previous mapping of PKR dependent tropism for fibroblasts to the M1 genome segments, has identified a tissue specific aspect to the PKR dependent control of infection with reoviruses. As >95 % of tumors are epithelial in origin, the difference in PKR dependent infection between fibroblast and epithelium is of relevance to oncolytic viruses which are thought to exploit defects in interferon responsiveness in tumor cells, which are largely epithelial in origin.

On assessing the genotypes of reassortants that possess enhanced oncolytic abilities the T3D-L2 and T3D-M1 genome segments plus T1L-L3 and T1L-M2 genome segments appeared to be functioning to enhance tumor destruction through modulation of cell growth and protein production (L2 and L3-enhanced growth), and interferon /PKR sensitivity (M1-enhanced sensitivity). Although oncolytic properties appear multigenically controlled it is possible to obtain reovirus reassortants with enhanced combinations of proprieties that favor improved abilities to destroy tumors in intact host organisms. This study is thus foundational and has provided important data for further analysis of the mechanisms of reovirus tumor attack and its application to therapy.

DEDICATION

This thesis is dedicated to

My wonderful husband

Gary Haley

ACKNOWLEDGEMENTS

My journey through graduate studies was filled with many wonderful experiences and learning opportunities and would not have been a success without the help of family and friends. I would first like to thank my supervisor Dr. Earl G. Brown for giving me the opportunity to further explore my love for science and research. Thank you for your support, guidance, and encouragement while I developed my skills and conducted this research. My experience working and learning with you will never be forgotten.

To my thesis advisory committee: Dr. John Bell and Dr. Stephanie Bennett, thank you both for all the help, suggestions, and encouragement that you have given along the way.

To all my co-workers (past and present) in Dr. Brown's lab: Jasminka Bozic, Corina Francu, Song Lu, Yishan Li, Liya Kelita, Kathryn Slater, thank you for all the good times and fond memories. Thank you for creating a wonderful environment to work in and thank you for your support on the days when things just don't want to work.

To all the students and staff in Dr. Bell, Dr. Bennett, and Dr. Dimock's labs thank you for fun conversations and all the technical help.

To all the students and staff (past and present) in the BMI department thank you for the technical assistance, good times, and funny experiences and stories that have been shared over the last two years.

To my parents thank you for the love, support, and guidance that you continually give me.

Last but not least special thanks go to my wonderful husband Gary Haley, your constant love and support is second to none. You have allowed me to follow my dreams

and pursue my love of science. Thank you for all your patience and the sacrifices that you have made so that I could continue my studies.

Table of Contents

LIST OF TABLES

LIST OF FIGURES

LIST OF ABBREVIATIONS

BCIP	5-bromo-4-chloro-3-indolyl phosphate
BE	bronchial epithelium
CPE	cytopathic effect
CNS	central nervous system
DMEM	Dulbecco's modified Eagle medium
DR4	death receptor 4
DR5	death receptor 5
dsRNA	double stranded ribonucleic acid
EGFR	epidermal growth factor receptor
eIF2α	eukaryotic initiation factor 2α
FBS	fetal bovin serum
GAP	GTPase activating protein
GDP	guanosine diphosphate
GEF	guanine nucleotide exchange factor
GTP	guanosine triphosphate
h	hour
H & E	Hematoxylin and Eosin
in	intranassal
ISVP	infectious (or intermediate) subvirion particle
iv	intavenous
JAM-A	junctional adhesion molecule A

MB	medulloblastoma
2ME	2-mercaptoethanol
MEF	mouse embryo fibroblast
MEM	minimal essential media
min	minute
MOI	multiplicity of infection
mRNA	messenger ribonucleic acid
NBT	nitro blue tetrazolium
NTR	nontranslated region
ORF	open reading frame
p	probability
PBS	phosphate buffered saline
pfu	plaque forming units
PI3-Kinase	phosphatidylinositol 3-kinase
PKR	double-stranded RNA activated protein kinase
PKR -/-	PKR knockout
PVDF	Polyvinylidene Fluoride
RT	room temperature
SD	standard deviation
SDS-PAGE	sodium dodecyl sulphate-polyacrylamide gel electrophoresis
SOS	son of sevenless
ssRNA	single stranded ribonucleic acid
T1L	type 1 Lang

T2	type 2 Jones
T3D	type 3 Dearing
TNF	tumor necrosis factor
TRAIL	TNF-related apoptosis-inducing ligand
TUNEL	Terminal deoxynucleotidyl Transferase Biotin-dUTP Nick End Labeling
U	units
V	volts

CHAPTER ONE

1. INTRODUCTION

1.1 Reovirus

The mammalian reovirus is a member of the *Orthoreovirus* genus in the family *Reoviridae*. The name reovirus contains the prefix reo which stands for respiratory enteric orphan derived from the fact that reovirus can be isolated from the respiratory and intestinal tracts of humans but has not been associated with specific clinical disease and it is therefore an orphan virus. There are three serotypes of reovirus: type 1 Lang (T1L), type 2 Jones (T2), and type 3 Dearing (T3D). This thesis will deal with the serotypes T1L and T3D and T1L x T3D reassortant viruses and their oncolytic potential.

1.2 Reovirus morphology

Reoviruses are non-enveloped icosahedral viruses, made up of two capsid shells which surround a genome of 10 double-stranded RNA (dsRNA) gene segments (Table 1). There are three forms of the reovirus particle: virion, infectious (or intermediate) subvirion particle (ISVP) and the core (Figure 1). Both the virion and ISVP are infectious particles, able to interact with the cell surface receptors and the virion is the predominant form released from infected cells *in vitro* [66].

Table 1. Characteristics of reovirus structural and nonstructural proteins

Table 1. Characteristics of reovirus structural and nonstructural proteins adapted from [29,66]

Protein	Gene	Protein Mass (kDa)	Copy Number per virion	Location	Functions
λ1	L3	141.9	120	Core capsid Virion, ISVP	RNA bindin; NTPase; helicase; RNA triphosphatase
λ2	L2	144	60	Core spike Virion, ISVP	Guanylyltransferase; methyltransferase
λ3	L1	142.4	12	Core internal Virion, ISVP	RNA-dependent RNA polymerase
μ1	M2	76.2	~ 30	Outer capsid Virion, ISVP	Cell penetration; transcriptase activation
μ1c	M2	72.1	~ 570	Outer capsid Virion, ISVP	
μ2	M1	83.3	~ 20	Core internal Virion, ISVP	Binds RNA; NTPase ?
σ1	S1	49.4	~ 30	Outer capsid Virion, ISVP	Receptor binding protein; hemmaglutinin type-specific antigen
σ2	S2	47.1	150	Core nodule Virion, ISVP	Binds dsRNA
σ3	S4	41.2	600	Outer Capsid Virion	Binds ssRNA; role in assortment and replication
μNS	M3	80	0	Nonstructural	Binds core, role in 2nd transcription probable rolein RNA assortment or replication
μNSC	M3	75	0	Nonstructural	Unknown
σNS	S3	41	0	Nonstructural	Binds ssRNA probable role in RNA assortment or replication
σ1s	S1	14	0	Nonstructural	Dispensable in cell culture

Figure 1: Reovirus Morphology
A. Structure of the reovirus infections virion and viral structural protein arrangement.
www-micro.msb.le.ac.uk/3035/Reoviruses.html
B. Structure of reovirus virion, ISVP and core
http://yin.che.wisc.edu/images.htm

A.

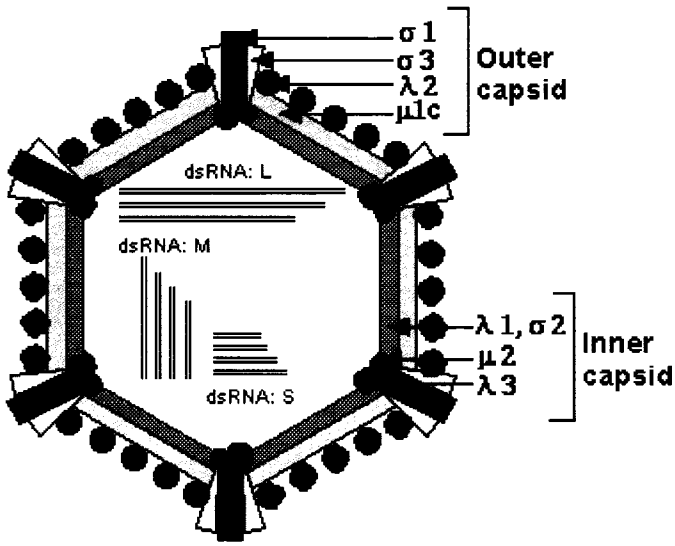

B.

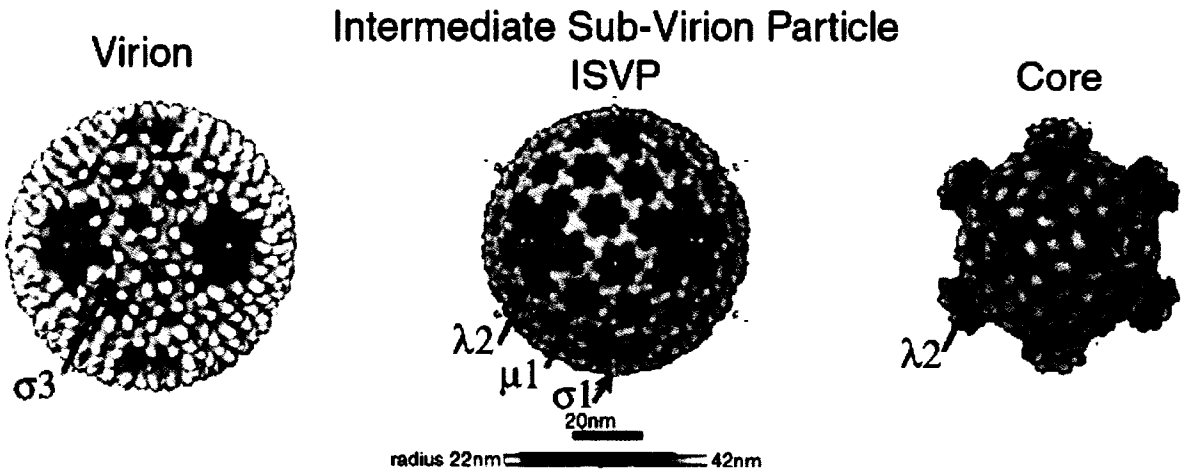

1.2.1 Outer capsid structure

The outer capsid is made up of four proteins: λ2, σ1, σ3 and μ1/μ1c. There are 60 copies of the λ2 protein which is the core spike protein, 600 copies of both σ3 and μ1c structural proteins, and 36 copies of the σ1 protein which is the receptor binding protein [30,78]. Thus, the μ1c (76.2 kDa) and the σ3 (41.2 kDa) proteins are the major components of the outer capsid [29]. The μ1c protein forms a trimer on the surface of the virion and the σ3 protein folds into two lobed structures, the small lobe interacts with μ1c and the large lobe is exposed on the surface of the virion [30,33]. The σ1 (49.4 kDa) [29] receptor binding protein is a fibrous, trimeric protein with a distinct globular head and tail morphology [52,66]. Interactions between σ3 and the μ1 proteins are critical for many different stages in the viral life cycle. The σ3 protein forms a 1:1 complex with μ1c and can interact with as many as three adjacent μ1c molecules [66]. The σ3 protein also interacts with the core spike protein λ2 [66,78]. The μ1 protein is cleaved by carboxyl-terminal endoproteolytic cleavage into μ1N and μ1c and 95% of the μ1 complexed with σ3 is in the μ1c form. The interaction between μ1 and σ3 is also required for the cleavage of μ1 to generate μ1N and μ1c [78]. The three major outer capsid proteins μ1, σ1, and σ3 are modified during the conversion of the virion to an ISVP. ISVPs are generated by proteolytic cleavage during uncoating in cells, or as a result of chymotrypsin treatment *in vitro*, and are characterized by the cleavage of μ1c into δ and φ and the loss of σ3, as well as a conformational change in the σ1 receptor binding protein [39]. It has been suggested that the extensive contact between the μ1/μ1c and σ3 proteins is important for the stability of the outer capsid structure and is therefore important for the survival of the virion during host-to-host transmission [66].

1.2.2 Inner capsid structure

The inner capsid or the core of reovirus is made up of five structural proteins: λ1, λ2, λ3, μ2 and σ2. The λ1 (141.9 kDa) protein is present in 120 copies and is organized as 60 asymmetric dimers to form the inner capsid [29]. The σ2 (47.1 kDa) protein is present in 150 copies and is required for core assembly. It acts as a clamp to hold the capsid shell together [29]. The λ2 (144 kDa) protein is the core spike protein and is present in 60 copies which are organized as pentameric turrets at each of the 12 icosahedral vertices [29]. The λ2 protein interacts with all seven of the other reovirus structural proteins: λ1, λ3, μ2 and σ2 in the inner capsid and μ1/μ1c, σ3, and σ1 in the outer capsid [66]. The λ3 protein (142.4 kDa) is a minor structural protein with only 12 copies present in the inner capsid; structural and functional data suggest that one copy of the λ3 protein is located inside the core shell at each of the icosahedral five-fold axes [29,66]. The μ2 (83.3 kDa) protein is present in 20-24 copies in the inner capsid and currently there is no high resolution structure determination for this protein but, it is believed that the protein is located under each of the core shell icosahedral vertices[29].

1.2.3 Nonstructural proteins

Reovirus has 4 nonstructural proteins, σNS, μNS, μNSC and σ1s. The S3 gene segment codes for the σNS nonstructural protein. The σNS (41kDa) has ssRNA binding ability and is believed to play an important role in the selection, replication and/or packaging or reovirus RNA for the assembly of progeny particles (reviewed in [66]). The M3 gene segment codes for the μNS (80 kDa) and μNSC (75 kDa) nonstructural proteins. The μNSC is formed by alternative translation initiation at the second or third AUG in the M3 mRNA located in the same ORF as μNS [66]. The μNS and μNSC play a role in reovirus replication through their involvement in the formation of inclusion bodies. The S1 gene segment codes

for the σ1s (14 kDa) nonstructural protein, this protein is highly variable between reovirus isolates [66]. The σ1s nonstructural protein is a second translation product and studies suggest that it may be responsible for some of the different biological properties such as, replication, growth, spread and apoptosis, which have been mapped to the S1 gene segment [66].

1.3 Reovirus replication cycle

Reoviruses infect a wide variety of hosts and can be propagated in many different cell lines, with the most common being the mouse L929 fibroblast cell line [96]. The initial step in the replication cycle (Figure 2) is binding of the reovirus to a susceptible host cell, and this process is mediated by the reovirus receptor binding protein σ1. Many functional and biochemical studies have been done to characterize the σ1 protein and its target receptors but not all cellular proteins with which σ1 interacts are known. The presence of sialic acid seems to be an important component of reovirus cellular receptors. Regions in the N-terminal tail of the σ1 protein of T3D have been shown to be responsible for the binding of either α2-3 or α2-6 linked sialic acid [18]. The T1L σ1 protein interacts with glycoconjugates containing α2-3 linked sialic acid on M cell apical surfaces [43]. Sialic acid is not the only cellular receptor targeted by the σ1. The σ1 protein is also able to bind to junctional adhesion molecule A (JAM-A, previously called JAM1) and this interaction is mediated through the C-terminal globular head domain of the σ1 protein [3].

Once reovirus is bound to the host cell viral entry takes place. Reovirus and ISVP can enter the host cell by receptor mediated endocytosis or by directly penetrating the cell membrane, respectively. During receptor mediated endocytosis, the reovirus virion is taken up into an endocytic vesicle that matures into a lysosome. The acidification of the lysosome results in the proteolytic processing of the reovirus virion into an ISVP. Reovirus infection by intact virions can be inhibited

Figure 2: Reovirus replication cycle
http://instruct1.cit.cornell.edu/research/parker_lab/Reovirus.htm

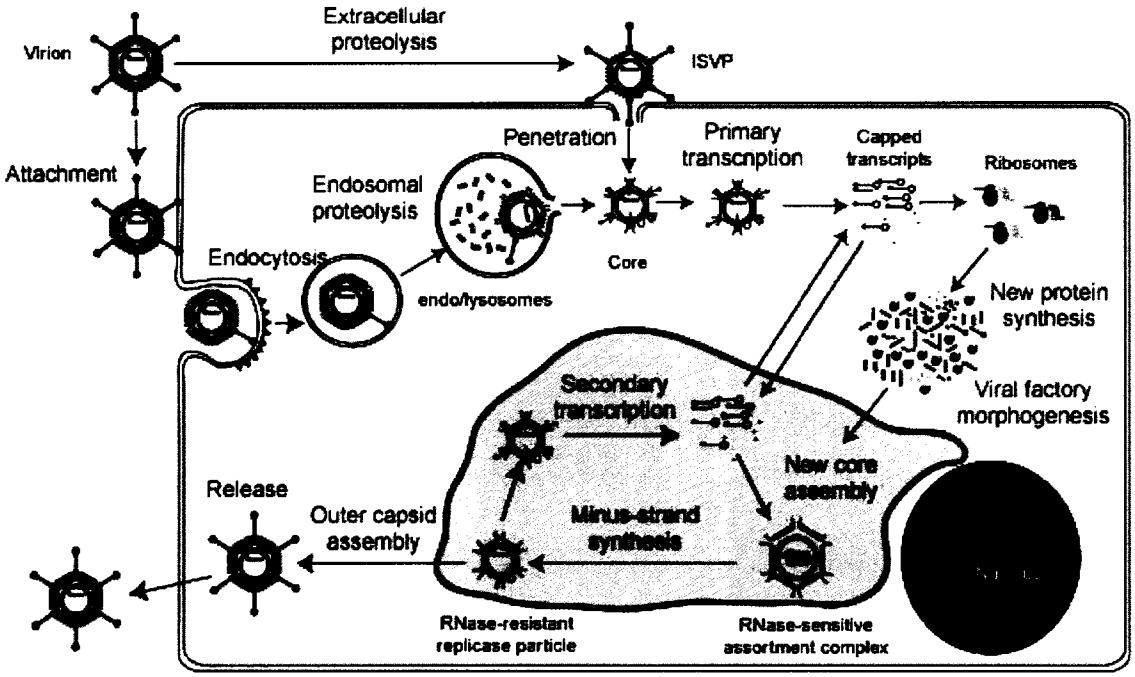

through the use of agents capable of disrupting lysosomal acidification [16]. ISVPs can be generated extracellularly by intestinal proteases *in vivo* [4] and *in vitro* by chymotrypsin. Inhibitors that block infection by intact virions do not block infection by ISVPs [17,65,72]. The ISVP form of the reovirus is able to enter the cell by directly penetrating the cell membrane. ISVPs have been shown to be able to cause membrane perturbations and release ^{51}Cr from preloaded L cells [54] as well as the induction of ion exchange through the formation of multi-sized channels in artificial planar bilayers [95]. These direct interactions between reovirus ISVPs and lipid bilayers suggest direct penetration through the cellular membrane is an alternate route of entry for the virus. The ability of reovirus ISVPs to release ^{51}Cr from L cells was mapped to the M2 gene, which codes for the μ1 protein [54]. The μ1 protein is myristoylated near the N-terminus [67] and contains a cleavage site that is flanked by a pair of amphipathic α helices, which is consistent with membrane insertion motifs found in other proteins [63]. Transmembrane transport was blocked in the temperature sensitive mutant tsA279 and this blockage was mapped to the M2 gene, further supporting a role of the μ1 protein in membrane penetration [42].

Once reovirus has successfully entered the cell the final stage of uncoating occurs and viral replication commences in the cytoplasm. The remaining outer capsid proteins, σ1 and μ1c, are removed from the ISVP to yield the core particle, and the λ2 pentamers undergo a dramatic conformational change that allows the potential diffusion of substrates for transcription, as well as newly synthesized mRNA, out of the core particle and into the cytoplasm of the cell [33]. The reovirus core particle is a multifunctional enzymatic complex and once it is formed in the cytoplasm transcription can take place.

Reovirus replication and assembly takes place in viral inclusion bodies, commonly called viral factories or viroplasms. The morphology of the inclusion bodies is serotype

specific, where T1L forms filamentous inclusion bodies and T3D forms globular inclusion bodies [74]. T1L x T3D reassortant viruses were used to identify that the M1 gene segment, which encodes the μ2 core protein, is the primary genetic determinant for the serotypic difference in morphology [74]. Sequencing of the M1 gene segment from different T1L and T3D isolates revealed that a single amino acid variation at position 208 is responsible for the different inclusion morphologies between serotypes. Initial studies observed that assembly occurred within the structural matrix of the cytoplasm of infected cells, with dsRNA appearing first followed by μNS and σ3, and later on in assembly, by the rest of the viral proteins [80]. It has been shown that all the proteins and the 10 different mRNA molecules are directed to inclusion bodies located in the cytoplasm by the σNS, μNS, and/or μ2 proteins [12-14]. The μNS protein is the most important protein involved in the formation of viral inclusion bodies and the expression of μNS alone is sufficient to form globular inclusion bodies in the absence of other viral proteins [5,12,14]. The μNS protein also associates with the μ2 protein which is a microtubule and RNA-binding protein capable of binding to both single stranded RNA (ssRNA) and dsRNA [10,14]. The μNS protein also interacts with the nonstructural σNS protein which is itself an ssRNA-binding protein [60]. The μNS protein forms the matrix of the inclusion bodies and recruits the core proteins λ1, λ2, and σ2, to the inclusion bodies [13]. When these core proteins were expressed separately in cells they were found to be diffusely distributed throughout the cytoplasm; however, when they were separately co-expressed with the μNS protein, each of the core proteins colocalized with μNS in globular inclusion bodies [13]. Whole core particles released into the cytoplasm during cell entry are also recruited to the viral inclusion bodies by the μNS protein [12]. The ssRNA binding activity of the μNS protein may thus be important for recruiting viral positive-stranded RNA to the inclusion bodies for replication and/or for packaging of viral RNAs [2].

There are two phases of reovirus transcription, a primary and a secondary phase. The mechanism of reovirus transcription is analogous to DNA transcription in that it is conservative with respect to the template and is asymmetric in that only the negative strand of dsRNA serves as the template. Initially only four (L1, M3, S3, and S4) of the ten genome segments are transcribed to produce pre-early mRNA [99]. The four pre-early mRNAs code for the λ3, μNS, σNS, and σ3 proteins, respectively; and once translated by the host ribosomes they act upon the core through an unknown mechanism which results in the transcription of all ten of the genome segments into primary transcripts [29]. The early viral transcripts contain methylated caps which are placed on the 5' end of the nascent transcripts through the action of the guanylytransferase activity of the λ2 protein [57]. This occurs as the mRNAs are exiting the core through the λ2 spike turrets [11,55,56]. Once the mRNA is capped the viral transcripts are then translated by host ribosomes to produce all of the reovirus proteins.

Reovirus assembly occurs in viral inclusion bodies. The assortment process proceeds concomitantly with assembly to ensure that nascent viral particles contain only one of each of the 10 genome segments. The mechanism by which the ten different mRNA molecules are sorted is unknown. However, the σNS and μNS non-structural proteins are likely involved in the assortment process as they are both able to bind to ssRNA and are present in large quantities [36-38,46,86]. Immunoprecipitation studies have indicated that the μNS, σNS, and σ3 proteins form complexes with ssRNA and that the λ2 and λ3 proteins are added to these complexes at the same time that the mRNA is copied into dsRNA [2]. Secondary transcription takes place in "transcriptase particles" and the transcripts produced during this phase of transcription are not capped. It is proposed that the un-capped mRNA are preferentially translated at later times in infection but the switch from cap-dependent to cap-

independent translation is poorly understood [29,66]. Completion of viral inner and outer capsid assembly results in the production of an intracellular infectious virion and shuts down transcriptase activity. Mature virions are released from the infected cell when the cell lyses.

1.4 Reovirus genome and reassortment

Reovirus was the first dsRNA virus discovered in nature. Reovirus has a segmented dsRNA genome made up of 10 genome segments. These genome segments are classified according to size, there are: 3 large gene segments (L1-L3) ranging in size from 3,854 to 3,916 base pairs (bp); 3 medium gene segments (M1-M3) ranging in size from 2,203 to 2,304 bp; and 4 small small gene segments (S1-S4) ranging in size from 1,196 to 1,463 bp [29,66]. The 10 genome segments code for 11 proteins: 8 structural proteins and 3 non-structural proteins. Sequencing of the 60-90 residues at the 5' and 3' termini revealed that each of the 10 gene segments contains a completely conserved consensus sequences. On each positive-strand of the 10 genome segments there is a conserved GCUA tetranucleotide at the 5' end and a conserved UCAUC pentanucleotide at the 3' end [29]. Each genome segment contains an open reading frame (ORF) and short nontranslated regions (NTR) at the 5' and 3' end of the gene segment. The NTRs vary in length between each of the gene segments ranging from 12 bp in the S1 gene to 32 bp in the S4 gene at the 5' end and from 35 bp in the L1 gene to 83 bp in the M1 gene at the 3' end [29,66,102] The function of the NTR is not fully understood but it is believed that the NTR sequences, as well as some parts of the ORF, may act as signals that direct genomic assembly or assortment. Using a reovirus reverse genetic system, Roner *et al.* discovered a 96 nucleotide region in the 5' end of the S2 gene that is essential for the incorporation of the *in vitro* generated dsRNA into new progeny viral particles [77]. Through the use of high passage T1L x T3D reassortant mutants containing

deletions in the M1 gene segment, Zou and Brown discovered the minimum essential sequence in the ORF of the M1 gene that is essential for M1 replication and assembly [105].

The reovirus segmented genome provides reovirus with the unique ability to generate reassortant viruses through the process of genome segment reassortment that occurs when a cell is co-infected with two parental viruses. In a co-infected cell, gene segments are chosen from a mixed pool of gene segments for encapsidation and this results in progeny viruses that contain mixed genetic information provided from both parental viruses.

Sequence analysis done on the genome segments of reassortant viruses identified repetitive mutations that occur each time reassortant viruses are formed. These mutations vary slightly depending on the acceptor virus. When T3D is accepting gene segments from either T1L or T2J, the T3D s4 genome segment will contain the mutation $G^{624} \rightarrow A$ and $G^{74} \rightarrow A$ [50]. However, each segment accepted by T1L from one of the other serotypes must contain mutations that render the gene segment more similar to the T1L genome segment that is being replaced [50].

Analysis of T1L x T3D reassortants demonstrated that T3D is able to readily generate deletion mutants whereas T1L does not. This could indicate that each serotype has a different mechanism of reassortment. The use of T1L x T3D reassortants at high passages demonstrated the ability to generate deletion mutants lacking either the L1, L2, L3 or M1 genome segments [15,68,69,105]. The ability of the T1L x T3D reassortants to generate the deletion of gene segments was mapped to the M3 and L2 genes when these genes were of heterologous origin [15].

The T1L and T3D serotypes have been used to generate a large panel of reovirus reassortants for use in genetic studies. In theory, if the 10 genome segments of both T1L and T3D were subject to random segregation, the resulting progeny reassortant viruses could

contain 1024 potential gene combinations [64]. However, when reassortant progeny arise from co-infected cells the reassortment frequency of the genes has rarely ever been observed above 25% [64]. When statistical analysis was performed on a panel of 83 reassortants derived from the T1L and T3D serotypes it revealed the statistically significant ($p < 0.005$) nonrandom associations of parental alleles in the L1-L2, L1-M1, L1-S1, and L3-S1 segment pairs [64]. It is believed that the nonrandom segregation of certain segment pairs may be influenced both by the evolution of reoviruses in nature and in the laboratory, and these associations may also represent necessary interactions between different viral components [64]. Nonrandom segregation was also demonstrated in mice where T1L x T3D reassortant viruses were isolated from suckling mice that had been infected perorally with both T1L and T3D serotypes. The two most prevalent reassortant viruses contained mainly T1L genes with only a few genes derived from T3D [101].

1.5 Reovirus pathogenesis

Reoviruses are ubiquitous in the environment and can be isolated from a wide variety of mammals including humans. Serological data indicate that throughout their lives humans are repeatedly infected with reovirus [79]; but, reovirus infection is not associated with any serious disease in humans. However, reovirus infection in rodents spreads systemically and is a good model system to study reovirus pathogenesis.

Reovirus T1L and T3D differ in their tropism for different organs. In the central nervous system (CNS), the S1 gene segment, which codes for the receptor binding protein σ1 and the non-structural protein σ1s, determines the pathology following reovirus infection. Newborn mice infected with T3D develop fatal encephalitis with neuronal destruction; however, when infected with T1L they develop a nonfatal ependymal infection without neuronal damage [100]. The S1 gene segment is also responsible for the pathogenesis of viral

pneumonia in reovirus infected rat lungs. More neutrophils were recruited to the site of infection in lungs infected with reovirus T3D than lungs infected with T1L and this difference was mapped to the S1 gene segment [62]. Examination of reovirus induced acute myocarditis in mice revealed that the S1 gene segment determines the efficiency with which reovirus infects cardiac myocytes but, that RNA synthesis, and not the generation of infectious virus, was the determinant of the severity of myocarditis [81]. Another study of reovirus induced myocarditis revealed that gene segments coding for viral core proteins λ2, λ3, and μ2, affected the outcome of reovirus induced myocarditis [82]. IFN-β induction in reovirus infected cardiac myocyte cultures correlated with viral myocarditic potential and was associated with the M1, S2, and L2 gene segments [83]. In addition, severe combined immunodeficient (SCID) mice infected with T1L x T3D reassortants were used to identify organ-specific virulence gene segments [40]. The S1, L2, M1 and L1 gene segments accounted for more than 90% of the increased virulence seen with T1L infection [40]. The L1 and L2 gene segments were involved in the severity of viral hepatitis and the viral titers in the brain, intestines and liver. The M1 gene segment was found to be independently important for high liver titers and the severity of hepatitis, whereas the S1 gene segment and not the M1 gene segment was the critical determinant of viral titers in both the intestines and the brain [40]. The M1 gene segment is also a factor in the ability of T1L to grow in cultured bovine aortic endothelial cells [58] and in cultured mouse cardiac cells [59]. The mechanisms of serotype-dependent replication and tropism are reliant on the gene segments involved in controlling the infection in different cell types (Table 2).

Table 2: The roles of reovirus gene segments in pathogenesis

Gene	Protein	Role in Pathogenesis
L1	λ3 -RNA dependent RNA polymerase	involved in severity of hepatitis and viral titers in brain, intestines, and liver
L2	λ2 - core spike protein	involved in severity of hepatitis and viral titers in brain, intestines, and liver
M1	μ2 - core protein	key determinant of growth in normal tissues, hepatitis in adult SCID mice, and myocarditis in suckling mice and plays a role in IFN induction and sensitivity
M2	μ1 - major outer capsid protein	Critical determinant for apoptosis
S1*	σ1 - receptor binding protein	involved in the serotype specific productivity of infection
	σ1s - nonstructural protein	plays a role in apoptosis critical determinant for tissue tropism severity of myocarditis viral pneumonia in infected Rat lungs
S2	σ2 - core protein binds dsRNA	IFN-β induction in infected cardiac myocyte and viral myocarditis

* In most cases these studies did not differentiate between the receptor binding protein σ1 or the nonstructural protein σ1s.

1.6 Reovirus induced apoptosis

The study of reovirus has provided insight into many general mechanisms of viral infections including apoptosis. Reovirus has been shown to induce apoptosis in a wide variety of cultured cells *in vitro* and in tissue *in vivo* [25]. Reovirus-induced apoptosis is a key element in infection and pathogenesis *in vivo* and is the mechanism of virus induced injury in specific organs such as the heart and the CNS [32,45,75]. Inhibition of apoptosis through the use of caspase inhibitors reduces the amount of tissue injury following infection [32]. Reovirus-induced apoptosis has been well studied and requires both death receptor and mitochondrial-mediated cell death pathways [19-24,28,51]. Apoptosis following reovirus infection involves members of the tumor necrosis factor (TNF) receptor superfamily, more specifically the cellular receptors DR4 and DR5 [21]. Reovirus infection induces both the release of the TNF-related apoptosis-inducing ligand (TRAIL) and an increase in expression of DR4 and DR5 in infected cells *in vitro* [21]. The binding of TRAIL to its cellular receptors DR4 and DR5 mediates apoptosis following reovirus infection [21]. Apoptosis can be blocked in reovirus infected cells by using anti-TRAIL antibodies and soluble TRAIL receptors supporting reovirus' use of TRAIL-mediated apoptosis in infected cells [21]. Reovirus has also been shown to induce TRAIL-mediated apoptosis in human cancer cell lines *in vitro* [22]. In addition, the combination of a soluble TRAIL treatment and reovirus infection synergistically augmented TRAIL-mediated apoptosis in infected human cancer cells *in vitro* [22].

1.7 Reovirus as an oncolytic virus

Oncolytic viruses have either been naturally selected or genetically engineered to selectively replicate and kill tumor cells. Conventional chemotherapeutics are currently the best treatments available to treat cancers; however, they are limited due to drug resistant

mechanisms that develop over time in tumor cells. Unlike conventional theraputics, oncolytic viruses have the potential to be multi-modal therapies. Oncolytic viruses can be rapidly engineered so that they are tumor specific, genes can be added that code for toxic payloads that are delivered directly to the tumor, and viruses have an innate capacity to stimulate the immune system resulting the production of cytokines and tumor-specific inflammation (reviewed in [6,7,73]).

The oncolytic ability of reovirus is not a new concept, since early studies demonstrated that reovirus was preferentially cytotoxic in certain transformed cell lines [41], and that T3D preferentially infected and lysed SV40-transformed human embryonic lung cells (WI38) relative to normal WI38 cells [34]. These early studies demonstrated that certain features of reovirus replication resulted in different effects in normal and transformed human cells, and that the lytic response of reovirus seemed to be selective for transformed cells. In more recent studies done by Lee and colleagues, it was demonstrated that normal mouse cell lines, NR6 and B82, could be made susceptible to reovirus T3D infection through the activation of the epidermal growth factor receptor (EGFR) signaling pathway [90]. T3D is able to bind the EGFR [92]. It is believed that T3D benefits from the activation of downstream cellular machinery as a result of the functional signaling transduction pathway mediated through the EGFR in transformed cells and not as a result of T3D's ability to recognize EGFR. Therefore, to further examine the hypothesis that reovirus T3D is dependent on activation of the signaling pathway, Lee *et al.* conducted experiments to determine whether or not transformation of resistant NIH 3T3 cells with the oncogenic v-erbB could make the NIH 3T3 cells susceptible to reovirus infection. The oncogenic v-erbB is a truncated EGFR that lacks the extracellular binding domain but possesses constitutive, ligand-independent tyrosine kinase activity. Indeed transformation of NIH 3T3 cells with v-erbB did render

these cells susceptible to reovirus infection [89]. When the transformed cells were treated with the tyrosine kinase inhibitor Genistein, the enhanced viral protein synthesis conferred by v-erbB was abolished [89]. This finding supports the theory that the mechanism of enhancement of infection in transformed cells is through the opportunistic utilization of an already activated signal transduction pathway. It is now clear that T3D exploits an activated Ras pathway for its own replication in transformed cells. Activated intermediates in the Ras signaling pathway such as Son of Sevenless (SOS, a Ras GDP exchange factor) have been shown to confer reovirus susceptibility to otherwise resistant NIH 3T3 cells [88].

1.7.1 Reovirus and the Ras pathway

Ras proteins form a subfamily of small GTP-binding proteins that are involved in the regulation of a wide variety of cellular functions such as cell proliferation, differentiation, morphology and apoptosis [91]. Ras protein activity is regulated by guanine nucleotide exchange factor (GEF) and GTPase activating proteins (GAP) and activation is induced by a large variety of extracellular signals, most notably those associated with tyrosine kinase activity such as EGFR [91]. Activation of the EGFR signaling cascade occurs as a result of ligand binding, followed by receptor oligomerization and the subsequent activation of tyrosine kinase activity and autophosphorylation of specific tyrosine receptors. Ras proteins are located in the cytoplasm at the inner surface of the plasma membrane and cycle between the inactive GDP-bound state and the active GTP-bound state. Ras activation is promoted by the GEF SOS which is recruited to the plasma membrane by adaptor molecules that have been activated by the autophosphorylation of the tyrosine receptors. Once at the plasma membrane SOS stimulates a Ras protein and converts the GDP bound form to the GTP bound form and Ras becomes active [91]. The activated Ras-GTP stimulates over 18 different downstream effectors. The best characterized of these effector molecules are the Raf

kinases, the phosphatidylinositol 3-kinase (PI3-Kinase) and the GEFs for the small G protein Ral pathway [85]. Experiments by Norman *et al.* demonstrated that the Ras/RalGEF/p38 pathway is involved in the selective replication of reovirus in transformed cells [71]. An active mutant form of RalGEF permitted reovirus replication in the absence of activated Ras, and the use of a dominant negative form of Ral, which is the target protein for RalGEF-mediated GDP/GTP exchange, abolished reovirus infection in permissive Ras transformed cells [71]. Inhibitors of p38, a downstream effector of RalGEF, also suppress reovirus replication in cells transfected with active mutants of Ras and RalGEF, suggesting that more than one downstream effector of the Ras pathway is involved in reovirus selectivity for transformed cells [71].

When Ras is constitutively active it promotes metastasis, angiogenesis, and the loss of growth control. Mutations which result in active forms of Ras have been discovered in more than 30% of all human cancers [88,94]; however, this does not account for the mutations or oncogenic changes that occur either up or downstream of Ras that are proposed to occur in 80% of tumor cell types. The ability of reoviruses to replicate and lyse cells with aberrant Ras signal pathways, and the fact that these pathways are involved in many tumor types, demonstrates the promising potential of reovirus as a cancer therapeutic.

1.7.2 Reovirus and PKR

The proposed mechanism that allows reovirus to be selective for cells with an active Ras pathway involves the release of a block in protein synthesis. When protein synthesis was monitored using ^{35}S-methionine labeling and immunofluoresecent microscopy, it was observed that reovirus protein expression was significantly reduced in untransformed cells [71,88]. When the cell lysates of infected NIH 3T3 cells were analyzed, a 65 kDa phosphorylated protein was discovered. This protein was not present in the cell lysates

collected from uninfected cells or in either infected or uninfected transformed NIH 3T3 cells [88]. The 65 kDa protein was determined to be the double-stranded RNA activated protein kinase (PKR) [88]. PKR expression is upregulated in response to IFN stimulation from virally infected cells. The binding of dsRNA to PKR results in PKR dimerization, autophosphorylation and activation. The mechanism by which PKR blocks protein production is through the phosphorylation of the eukaryotic initiation factor 2α (eIF2α). When eIF2α is phosphorylated it prevents the loading of Met-tRNA and the formation of the 43S initiation complex and, this blocks translation at the ribosome (reviewed in [85]). Therefore, the activation of PKR in infected cells is responsible for the block in protein synthesis observed in normal cells. Both the deletion of the PKR gene and the chemical inhibition of PKR phosphorylation restores reovirus translation and protein production in untransformed cells [88] and therefore this observation provides evidence that PKR plays a direct role in determining resistance to reovirus replication in untransformed cells.

The role of PKR goes beyond inducing an antiviral state in infected cells. There is accumulating evidence that implicates PKR in signal transduction, cell growth, differentiation and apoptosis and, under normal conditions, PKR may have tumor suppressor functions [49]. In fact, the PKR gene is absent or inactive in many different tumor types [6,84,93]. The actions of PKR block protein production and this is an undesired trait for malignant transformed cells. The link between oncogenic Ras activation and the inactivation of PKR is not yet fully understood; however, it is hypothesized that PKR is blocked in Ras transformed cells. This block may be mediated by either the presence of an inhibitor that blocks the phosphorylation and therefore activation of PKR or by a phosphatase that removes the phosphate from activated PKR to return it to its inactive form (Figure 3) [85].

Figure 3: The possible link between Ras activation and the inactivation of PKR in transformed cells (from reference 85)

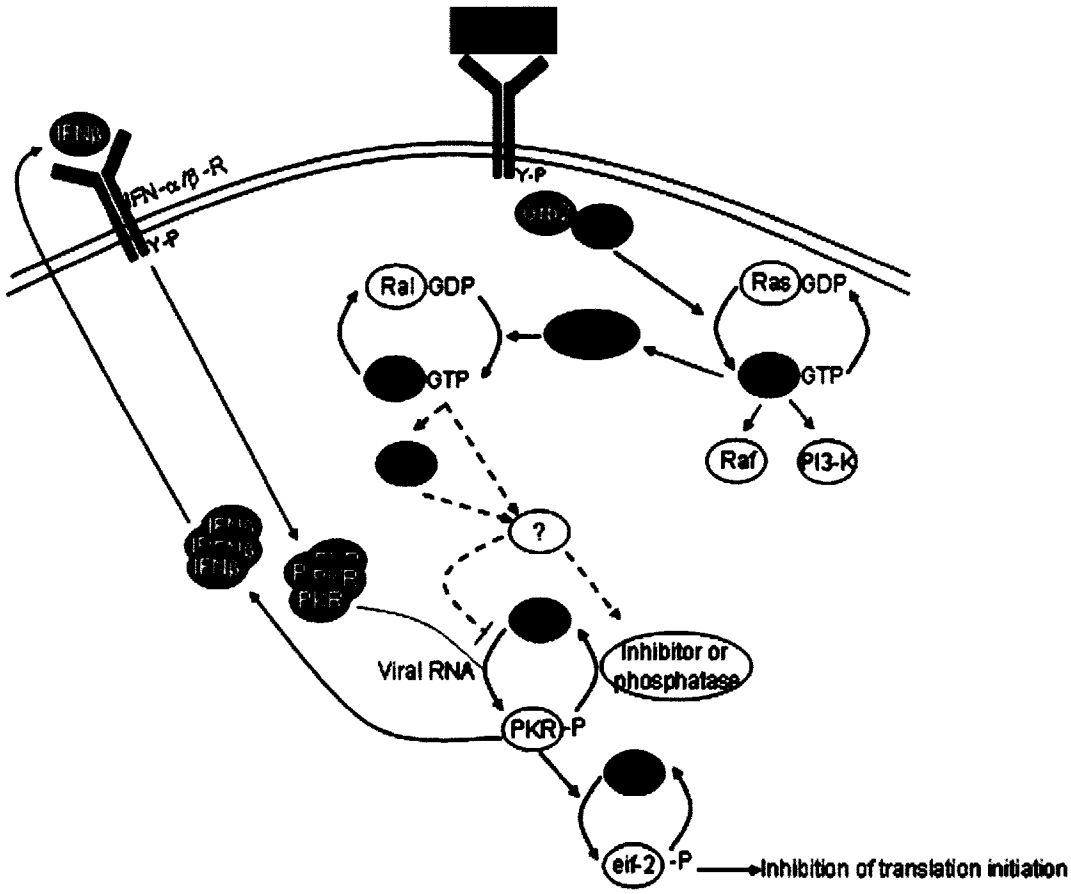

1.7.3 Reovirus in *in vitro* and *in vivo* cancer models

Reovirus T3D has been a very successful oncolytic virus in many different experimental cancer models. In human medulloblastoma (MB) cells derived from surgical specimens, reovirus T3D was able to kill >90% of the cells 48 h after infection *in vitro* [104]. When these MB cells were put into nude mice, a single reovirus treatment was able to produce long-term survival in the nude mice bearing MB tumors [104]. In animal models, reovirus treatment also resulted in the regression of established human colon and ovarian tumors and histological studies revealed that reovirus infection was restricted to the tumor cells [44]. Studies using reovirus in a bilateral *in vivo* breast cancer model demonstrated that reovirus could not only cause treatment regression in breast cancer tumors at the site of injection, but it could also cause regression of tumors that are remote from the site of injection [70]. This demonstrates the ability of reovirus to act as a systemic cancer therapeutic. In addition, reovirus was shown to be an effective oncolytic against human head and neck squamous carcinoma cells both *in vitro* and *in vivo* [48]. The ability of T3D reovirus to lyse a majority of tumor types including breast, colon, ovarian, glioblastoma and lymphatic tumors [1,44,70,103], in these experimental settings, makes it an attractive candidate for a novel cancer therapeutic. Further studies are needed to better understand the mechanisms of reovirus oncolysis and to address the problem of resistant tumor types.

CHAPTER TWO

2. RATIONALE AND OBJECTIVES

The study of oncolytic viruses as potential cancer therapeutics is an exciting and promising field of study. T3D reovirus, as an oncolytic virus, is able to lyse a majority of tumor types such as breast, colon, ovarian, glioblastoma and lymphatic tumors [1,44,70,103]. The major drawback is that ~20% of tumor types are resistant to lysis by T3D [1,26,103] and therefore there is a need to improve the oncolytic ability of reovirus to include resistant tumor types.

The segmented nature of the reovirus genome allows for the exchange of genome segments, and therefore biological properties, among different reovirus strains. Cells that are co-infected with 2 parental strains, T1L and T3D in the case of this study, will yield progeny viruses called reassortants that contain different combinations of the 10 genome segments. These new reovirus reassortants have novel biological properties due to the unique combinations of genome segments that they carry. Thus, reovirus reassortants provide a powerful tool to study reovirus biology as well as a new tool to uncover the genetic modifications that may give rise to superior oncolytic reoviruses.

The genetic basis for reovirus PKR sensitivity, with respect to viral growth, was previously established by our lab (Brown unpublished data). The replication of the T1L and T3D strains was compared in mouse embryo fibroblasts (MEF) and PKR knockout MEF (PKR -/-) cells. It was observed that both T1L and T3D grew to higher titers in the PKR -/- cells, but that TIL grew better than T3D in both PKR-/- and MEF cells. A panel of T1L x T3D reassortants was then used to determine which gene segments were involved in generating high viral yields in the absence of PKR. As a result of this study it was

demonstrated that the M1 gene segment from T3D controls PKR sensitivity and the T1L L3 gene segment controlled the increased viral yield in the absence of PKR. When designing an oncolytic virus, an ideal virus would be sensitive to PKR, so that it will not replicate efficiently in normal cells, and be able to produce high viral yields in the absence of PKR, which is a common phenotype in many tumors.

Improving viral oncolysis is an exercise in applied pathogenesis where aspects of viral infection are optimized for tumor destruction and not disease. This can be achieved by optimizing the basic infection process through the creation of reovirus reassortants with the desirable gene segment combinations that will increase not only the yield of virus in resistant tumor cells but also increase their oncolytic ability. First, it is critical to determine all gene segments involved in viral oncolysis. The novel approach taken in this study involves screening the ability of reovirus reassortants to find second generation oncolytic reoviruses that have superior oncolytic potential over the parental strains. This study also furthers our understanding of reovirus genetics and biology in resistant tumor cells.

Hypothesis: The oncolytic ability of reovirus can be improved through the modulation of viral replication and pathogenesis to include resistant tumor types through the generation of reovirus reassortants. The improved oncolysis can be achieved by combining the T1L L3 gene segment with the T3D M1 gene segment through the creation of T1L x T3D reassortants. The reassortant viruses with these gene segments and other unidentified gene segment combinations have the potential to have superior oncolytic ability over the parent serotypes.

Objectives:

A. Use reovirus reassortants to better understand the genetic basis for the difference observed in oncolysis in the resistant CT26 murine colon tumor cell line, by assessing both viral yield and protein production following infection.

B. Use reovirus reassortants to assess the role of PKR in viral protein production *in vitro* using mouse embryo fibroblasts, and in viral lung tropism *in vivo* using TIK (murine PKR) knockout mice. Studies of reovirus tropism in the lung will assess the role of PKR in the lung epithelium.

C. Assess reovirus reassortants *in vivo* in a lung tumor model through analysis of viral growth, antigen expression, and expression of apoptotic markers in tumor bearing lungs, as well as through survival studies of CT26 tumor-bearing mice.

CHAPTER THREE

3. MATERIALS AND METHODS

3.1 Cells and viruses

Mouse connective tissue L929 tumor cells, wild type mouse embryo fibroblast (MEF) and MEF PKR knockout (PKR -/-)cells, as well as murine colon carcinoma CT26 cells were propagated in adherent culture in minimum essential medium (MEM) (Gibco BRL Life Technologies, Burlington, ON) supplemented to contain 5% fetal bovine serum (FBS), 2mM L-glutamine, 100 U/ml penicillin /100 μg/ml streptomycin sulfate and 0.22% $NaHCO_3$ and kept at 37°C and 3.5% CO_2. Reovirus strains used in this research, type 1 Lang (T1L) and type 3 Dearing (T3D), were laboratory stocks initially obtained from B. N. Fields. The T1L X T3D reassortant viruses were produced previously by Dr. Earl G. Brown (Brown *et al.*, 1983). A list of all viruses used in this study and their gene segments can be found in Table 3.

Table 3. Reovirus: Parental strains and T1L x T3D reassortants and gene segment map

Virus	L1	L2	L3	M1	M2	M3	S1	S2	S3	S4
T1L	L	L	L	L	L	L	L	L	L	L
T3D	D	D	D	D	D	D	D	D	D	D
G2	L	D	L	L	L	L	D	L	L	L
G16	L	L	L	D	L	L	L	D	L	L
H15	L	D	D	L	D	D	D	D	D	L
H17	D	D	L	L	D	D	L	D	D	L
H60	D	D	L	L	D	D	D	D	D	L
EB1	L	D	L	L	D	L	L	L	D	L
EB18	D	D	L	D	D	D	L	L	D	L
EB28	D	D	L	D	D	D	D	L	D	D
EB31	L	L	L	D	L	L	L	D	D	L
EB39	L	D	D	L	D	D	D	D	D	D
EB68	L	D	L	L	D	L	L	L	D	D
EB73.1	L	D	L	L	D	D	D	D	D	D
EB86	L	D	D	D	D	L	D	D	D	L
EB87	L	D	L	L	D	L	L	D	L	L
EB88	D	D	D	D	L	D	D	D	D	D
EB96	L	D	L	D	L	L	L	L	D	L
EB97	D	D	L	D	D	D	D	D	D	L
EB108	L	D	L	D	L	L	L	L	D	D
EB118	D	D	L	L	D	D	D	D	L	L
EB123	D	D	L	D	D	D	D	D	L	D
EB128	D	D	L	D	D	D	L	D	D	L
EB129	D	D	D	D	D	L	D	L	L	D
EB145.1	D	D	D	D	D	D	D	D	D	L
EB146.1	L	D	L	L	D	D	D	D	D	D

3.2 Growth and plaque assay of reovirus and reovirus reassortants

For the preparation of virus stocks L929 cell monolayers were grown in T-75 flasks and were infected with reovirus derived from a single isolated plaque. Subsequent stocks were prepared by absorbing 0.5 ml volumes of virus stocks. The progression of cytopathic effect (CPE) was observed daily and the virus was harvested when CPE had reached 90% or greater. The virus was harvested from infected cells by three freeze-thaw cycles. Cell debris was removed from samples by centrifugation and the virus stock, supernatant, was then aliquoted and stored at -80°C.

To determine viral growth and protein production in CT26 cells, 6 well dishes were seeded with CT26 cells and grown to confluency. Supernatant was removed and the CT26 monolayers were infected with 0.1 - 0.25 ml of T1L, T3D or reovirus reassortants at a

multiplicity of infection (MOI) equal to 10. Infected monolayers were incubated for 30 – 45 min at 37°C and the dishes were rocked every 15 min to ensure an even distribution of the virus. Following incubation 3 ml of supplemented MEM was added to each well and the infected dishes were placed at 37°C. Three days post-infection virus samples were harvested to titer and protein samples were harvested for western blot analysis.

To determine protein production in MEF and PKR -/- cells, 6 well dishes were seeded with MEF or PKR -/-cells and grown to confluency. Supernatant was removed and the monolayers were infected with T1L, T3D or reovirus reassortants at an MOI =10. Infected monolayers were incubated for 30 – 45 min at 37°C and the dishes were rocked every 15 min to ensure an even distribution of the virus. Following incubation 3 ml of supplemented MEM was added to each well and the infected dishes were placed at 37°C. Two days post-infection protein samples were harvested for western blot analysis.

To determine the titer of the harvested virus, preparations were serially diluted in PBS (145 mM NaCL, 2.2 mM NaH_2PO_4, and 7.6 mM. $NaHPO_4$). The diluted virus (100 μl) was applied onto L929 monolayers in 6 well dishes. The 6 well dishes with infected monolayers were incubated for 30 -45 min at 37°C and the dishes were rocked every 15 min to ensure an even distribution of the virus. Following incubation 3 ml of overlaying medium (1% agar, 1 x 199 medium, 5% FBS, 100 U/ml penicillin, 100 μg/ml streptomycin, and 0.225% $NaHCO_3$) at 37°C was added to each infected well. Overlay medium was added to the wells every three days and on the 6^{th} or 9^{th} day 3 ml of overlay containing 0.15% neutral red was added to each well. The plaques were counted the following day to determine viral titer.

3.3 Antibodies

Table 4. Antibodies

Antibody	Primary or Secondary	Source	Working Dilution
Rabbit anti-T1L	Primary	E.G. Brown	1:500 (IB); 1:200 (IF)
Rabbit anti-T3D	Primary	E.G. Brown	1:500 (IB); 1:200 (IF)
Rabbit anti-active caspase 3	Primary	BD Bioscience	1:500 (IF)
Anti-Rabbit FITC	Secondary	Jackson ImmunoResearch	1:200 (IF)
Anti-Rabbit CY3	Secondary	Jackson ImmunoResearch	1:800 (IF)
Anti-Rabbit IgG	secondary	Sigma	1:10 000 (IB)

IB = immunoblot
IF = immunofluorescence

3.4 Immunoblotting

Infected cell monolayers were lysed in SDS sample buffer (62.5 mM Tris-HCL pH 6.8, 10% glycerol, 2% SDS, 0.05% bromophenol blue, and 5% 2-mercaptoethanol (2-ME) freshly added). Cellular DNA was then sheared by passage through a 26 gauge need of a tuberculin syringe 5 times. The proteins were separated by sodium dodecyl sulphate-polyacrylamide gel electrophoresis (SDS-PAGE) and then transferred to PVDF membrane (Immobilon-P, Millipore Corp., Mississauga, ON) by semi-dry transfer at 15V for 45 min. The dried membrane was blocked with 5% skim milk in PBS for 1 h at RT. This was followed by the addition of primary antibody in fresh 5% skim milk in PBS and incubation for 2 h at 4°C. The membrane was then washed three times for 10 min in PBS and once for 10 min in TBS (150 mM NaCl, 50 mM Tris-HCl pH 7.5) to remove phosphate and incubated with secondary antibody in 5% milk in TBS for 1 h at room temperature. Finally the

membrane was washed four times for 10 min in TBS before reaction with the chromogenic substrate, nitro blue tetrazolium (NBT) (33μg/ml) plus 5-bromo-4-chloro-3-indolyl phosphate (BCIP) (3.3 μg/ml), in alkaline phosphatase buffer (100 mM NaCl, 5 mM $MgCl_2$ and 100 mM Tris-HCl pH 9.5).

3.5 Densitometry

Densitometry was done on the M protein bands (labeled as μ's in figures) using Scion Image Beta 4.0.3 computer software.

3.6 Immunocytochemisty to detect viral antigens

Cover slips were placed in the wells of a 6 well plate and 1 ml of 0.1% gelatin solution (0.1% gelatin (SIGMA, Oakville, ON) in sterile ddH_2O) was added to the well to cover the entire cover slip. The cover slips were left in a sterile fume hood over night to allow the gelatin time to adhere to the glass. Any excess gelatin solution was removed the next day.CT26 cells were seeded on 22x22 mm glass cover slips coated with gelatin (0.1% in sterile ddH_2O) in 6 well plates. Cells were then either mock infected or infected with reovirus or reovirus reassortants at an MOI = 10. Viruses used were T1L, T3D, EB88, EB96, EB97, or EB123. Infection was allowed to progress for either 1, 2 or 3 days. The cover slips were washed once in PBS. Cells were fixed by incubating the cover slips in 3.7% formaldehyde in PBS for 20 min at room temperature. The cover slips were washed 3 times in PBS, 5 min per wash, and incubated in primary antibody diluted in Ab buffer (PBS, 3% BSA, 0.3% Triton-x) in a humidified chamber over night at 4°C. The cover slips were then washed 3 times in PBS, 5 min per wash, and incubated with secondary antibody diluted in Ab buffer for 1 hr at room temperature. The cover slips were washed 3 times in PBS, 5 min per wash, and incubated in Hoechst dye (0.2 μg/ml) for 5 min at room temperature. The

cover slips were washed 3 times in PBS, 5 min per wash, and mounted on slides using Vectashield mounting medium (Vector Labs, Peterborough, UK).

3.7 Infection of Balb/c mice bearing CT26 lung tumors

All protocols for this study were approved by the University of Ottawa Animal Care Committee and conformed to the Canadian Council on Animal Care Guidelines. To establish the *in vivo* tumor model adult female Balb/c mice 4-6 weeks old (Charles River, St. Hyacinthe, PQ) were administered 3.0×10^5 CT26 cells intravenously (*iv*). Seven days after receiving the CT26 cells the mice were anaesthetized with halothane (3% in oxygen), 2-4 min, and given their first treatment of virus (1.0×10^7 plaque forming units (pfu)) for inspiration intra-nasally (*in*). Virus suspended in 0.05 ml PBS was placed onto the nosepad and inhaled; this method introduces virus into the lungs. Depending on the study the mice either received 1 or 3 treatments. Those mice that received multiple treatments received the first treatment 7 days after receiving CT26 cells and then an additional treatment every 2 days until a total of 3 treatments had been given. The mice were placed into different treatment groups and given one of the following viruses; T1L, T3D, EB88, EB96, EB97, EB123, or the PBS mock treatment. The mice were monitored to assess post-treatment survival. Other sets of CT26 tumor bearing Balb/c mice were given one dose of the above mentioned viruses and then collected at 1, 2, 3, or 7 days post-treatment. The mice were given a lethal intra-peritoneal injection of 0.1 ml of sodium pentobarbital (Euthansol) (65mg/ml) and were deeply anesthetized, transcardially perfused and the lungs were collected, stained and visualized for the presence of viral antigen and apoptotic markers.

3.8 Infection of TIK knockout mice

The mouse homologue of PKR is termed TIK. TIK knockout mice with a Balb/c background were generously provided by Dr. John Bell. These mice were intranasally infected with virus, either T1L, T3D, or one of the 24 reassortants used in this study. The mice received a viral dose of 1.0×10^7 pfu, and the infection was allowed to progress for 3 days. At 3 days post-infection the mice were transcardially perfused and the lungs were collected, stained and visualized for the presence of viral antigen.

3.9 Transcardial perfusion and tissue preparation

Mice were given a lethal intra-peritoneal injection of 0.1 ml of sodium pentobarbital (Euthansol) (65mg/ml) and were deeply anesthetized. The mice were transcardially perfused with 20 ml PBS to removed red blood cells from the tissues, followed by 20 ml of 3.7% formaldehyde fixative in PBS, both at room temperature. The lungs were removed and placed in 3.7% formaldehyde in PBS over night at 4°C. The 3.7% formaldehyde fixative was removed and the tissue was cryoprotected by overnight incubation in 20% sucrose in PBS with 0.001% sodium azide at 4°C. The sucrose solution was changed daily for 3 days. Lungs were then flash frozen using compressed CO_2 gas in OCT compound (Fisher Scientific, Ottawa) and were then cut on a CM190 Leica cryostat into 10 μm sections and placed on slides. Tissue sections mounted on slides were kept at -20°C.

3.10 Immunohistochemistry for frozen tissue sections.

Tissue mounted on slides was equilibrated in PBS for 5 min. Tissue was incubated with primary antibody diluted in Ab buffer in a humidified chamber over night at 4°C. Slides were washed 3 times in PBS, 5 min per wash, and incubated with secondary antibody diluted in Ab buffer for 1 hr at room temperature. Slides were washed 3 times in PBS, 5 min per wash, and incubated in Hoechst dye (0.2 μg/ml) for 5 min at room temperature. Slides

were washed 3 times in PBS, 5 min per wash, and mounted with cover slips using anti-fade mounting medium (pH 8.0; 1mg p-phenylendiamine, PBS, 90% glycerol).

3.11 TUNEL

Tissue mounted on slides was equilibrated in PBS for 5 min. Tissue was fixed in 3.7% formaldehyde in PBS for 20 min at room temperature. Slides were washed 3 times in PBS, 5 min per wash, and tissue was permeabilized in 0.1% Na Citrate and 0.1% Triton-x for 5 min on ice. Tissue was incubated in cold (-20 ^{o}C) 2:1 (Ethanol: Acetic Acid) solution for 2 min on ice. Slides were washed 3 times in PBS, 5 min per wash, and incubated in the TUNEL (Roche) reaction mixture (1:10 mix enzyme: labeling) for 1 hr at 37^{o}C in a humidified chamber. Slides were washed 3 times in PBS, 5 min per wash, and incubated in Hoechst dye (0.2 μg/ml) for 5 min at room temperature. Slides were washed 3 times in 10 mM PBS, 5 min per wash, and cover slipped using anti-fade mounting medium.

3.12 Histopathology

Lungs sections were given to the Department of Pathology and Laboratory Medicine, University of Ottawa, and were stained with Hematoxylin and Eosin (H&E).

3.13 Microscopy and Imaging

Fluorescently stained cells and tissue were observed using an inverted fluorescent microscope (BMAX Series Microscopes, Olympus America Inc.) using the 20x and 40x objective lenses. The H & E stained tissue were observed in a BH2 Research Microscope (Olympus America Inc.) using the 10x objective lens. All final image compositions were done using Adobe Photoshop 7.0 (Adobe Systems, San Jose, CA).

3.14 Statistics

Values are presented as means ± SD. Graphs were generated in Graphpad Prism (San Diego, CA, v. 3.02 © 2000). Wilcoxon Rank-sum analysis was done using software from http://home.clara.net/sisa/ordinal.htm. Values that were $p<0.05$ were considered significant.

CHAPTER FOUR

4. RESULTS

4.1 Reovirus protein expression in CT26 cells *in vitro*

Previous preliminary *in vivo* studies done by our lab have shown that reovirus reassortants had different abilities in promoting survival in Balb/c mice bearing CT26 lung tumors. When a large panel of T1L x T3D reovirus reassortants was screened in the in vivo lung tumor model 4 reovirus reassortants were able to promote long term survival > 45 days following a single dose of virus (1 x10^7 pfu) *in* (Figure 4). The average time of death for the PBS control animals was 18 days post-treatment. The 4 reassortants able to yield long term survival were EB88, EB96, EB97, and EB123. Observing the genotype of these reassortants shows that they all possess the T3D M1 gene segment and the T1L L3 gene segment was present in 3 of the 4 (Table 5). These 4 reassortants differ in the combinations of their other gene segments. The diversity of the genotypes suggests that there may be multiple factors for improving oncolysis. In order to gain a better understanding of why these reassortant viruses were able to achieve better survival in the lung tumor model then both parental serotypes further experiments were done to understand the genetic characteristics for improved oncolysis. *In vitro* studies were done using the 4 reovirus reassortant to examine protein expression following infection in permissive (L929) and non-permissive (CT26) cell lines. L929 and CT26 cells were seeded on cover slips and then infected with reovirus reassortants at an MOI = 10. L929 cells were infected with either T1L or T3D and at 24hr post-infection the cells were fixed and stained for the presence of viral antigen using anti-reovirus antibodies (Figure 5).

Figure 4: Survival graph of Balb/c mice bearing CT26 lung tumors following a single intranasal dose of virus ($1.0x10^7$ pfu)
A large panel of T1L x T3D reassortants were used to treat Balb/c mice bearing CT26 lung tumors in order to assess survival post-treatment. Reassortants EB88, EB96, EB97, and EB123 were able to prolong survival for more then 45 days post treatment.

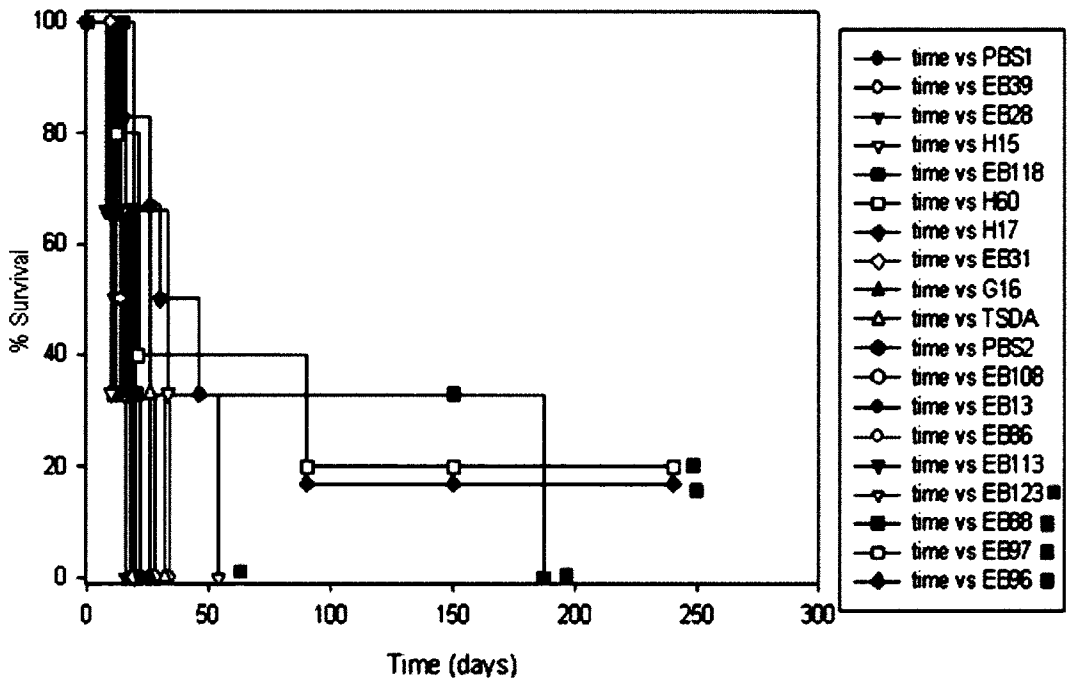

Table 5: Gene map for the 4 key reovirus reassortants that prolonged the survival of mice bearing CT26 tumors

Virus	L1	L2	L3	M1	M2	M3	S1	S2	S3	S4
T1L	L	L	L	L	L	L	L	L	L	L
T3D	D	D	D	D	D	D	D	D	D	D
EB88	D	D	D	D	L	D	D	D	D	D
EB96	L	D	L	D	L	L	L	L	D	L
EB97	D	D	L	D	D	D	D	D	D	L
EB123	D	D	L	D	D	D	D	D	L	D

Figure 5: Fluorescent antibody staining for reovirus antigen in infected L929 cells and CT26 cells 24 h post-infection (20X magnification)
L929 cells were infected with either T1L or T3D using an MOI = 10 and then 24 h post-infection were stained for the presence of reovirus antigen. CT26 cells were mock infected or infected T1L, T3D, EB88, EB96, EB97, or EB123 using an MOI = 10. This composite is made up of photographs of Cy3 conjugated antibodies labeling reovirus antigens and Hoechst dye labeling the cell nucleus. 24 h post-infection cells were stained for the presence of reovirus antigen. Scale bars are 10 microns.

L929 + T1L

L929 + T3D

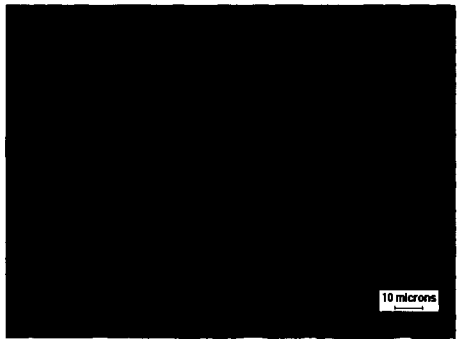

CT26 + Mock

CT26 + T1L

CT26 + T3D

CT26 + EB88

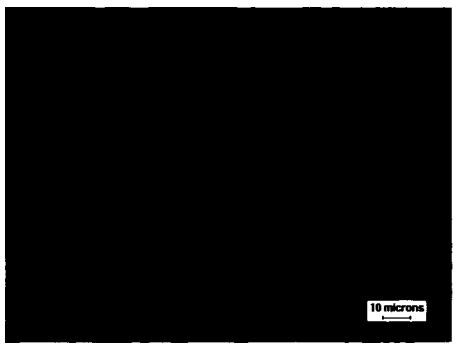

CT26 + EB96

CT26 + EB97

CT26 + EB123

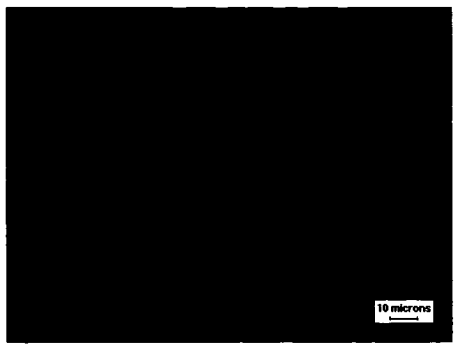

The CT26 cells were either mock infected or infected with T1L, T3D, EB88, EB96, EB97, and EB123. At 24 and 72 hr post-infection the CT26 cells were fixed and stained for the presence of detectable viral protein expression using ant-reovirus antibodies (Figure 5 & 6). In the permissive L929 cells, high levels of viral antigen were detected in all cells infected with either T1L or T3D 24 hr post-infection. In the resistant CT26 cell line lower levels of T1L and T3D viral antigen were detected at both 24 and 72 hr post-infection than observed in the permissive cell line where a minority of cells are showing detectable protein expression. Also the T3D protein expression levels appeared to be higher than the T1L antigen levels after infection of the CT26 cells, where as the protein expression levels for both were similar in the permissive L929 cells. The levels of viral protein expression detected among the different reovirus reassortants differed from one to another; some reassortants produced more protein expressing cells in the infected monolayers. The different viral responses as seen in the levels of viral antigen observed in the CT26 cells suggest a different pattern of infection for each of the parental serotypes and the reassortant viruses. It appears that although all cells are infected only a minority of cells are producing high levels of protein at any given time. These cells are not killed by infection but are persistently infected with virus. To gain a better understanding of the genetic basis for the difference in oncolysis in the resistant CT26 cell line I then examined the infectious yield and protein expression levels using western blot analysis of an expanded panel of 24 reassortants

Figure 6: Fluorescent antibody staining for reovirus antigen in infected CT26 cells 72 h post-infection (20X magnification)
CT26 cells were either mock infected or infected T1L, T3D, EB88, EB96, EB97, or EB123 using an MOI = 10. 72 h post-infection cells were stained for the presence of reovirus antigen. This composite is made up of photographs of Cy3 conjugated antibodies labeling reovirus antigens and Hoechst dye labeling the cell nucleus. Scale bar are 10 microns.

CT26 + Mock

CT26 + T1L

CT26 + T3D

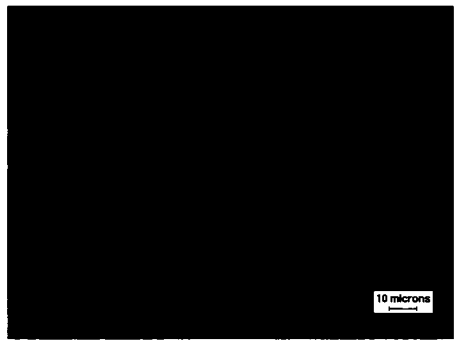

CT26 + EB88

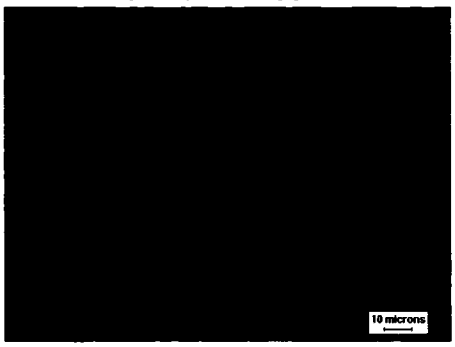

CT26 + EB96

CT26 + EB97

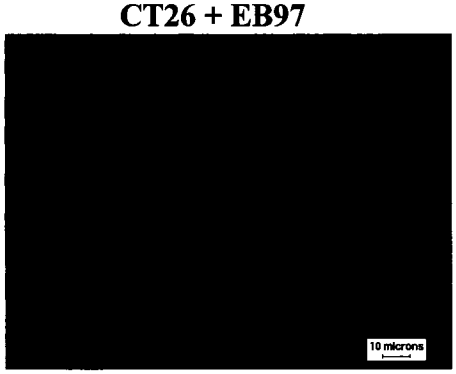

CT26 + EB123

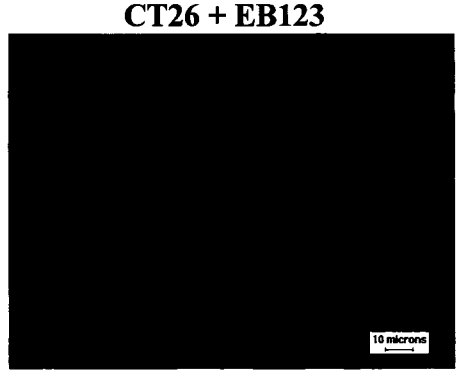

4.2 Viral growth in CT26 cells

To examine viral growth in the resistant CT26 cells, 6 well dishes were seeded with CT26 cells and were either mock infected or infected in triplicate with one of the parental serotypes, T1L or T3D, or one of the 24 reovirus reassortants. Three days post-infection virus was collected from the infected cells and a plaque assay was performed to determine viral titer. The plaque assay results indicate different levels of viral yield among the parental serotypes and the 24 reovirus reassortants (Figure 7). The parental serotypes and reovirus reassortants were then ranked from highest to lowest yield based on the average viral titers taken from three separate experiments. Using Wilcoxon Rank-sum analysis the gene segments important for high viral yield in CT26 cells were determined. The results of the analysis showed that the gene segments important for viral yield in CT26 cells were the L2 ($p = 0.0028$), M2 ($p = 0.0043$), M3 ($p = 0.0137$), and S1 ($p = 0.000036$) gene segments from the parental serotype T3D (Figure 7c). Mapping to the S1 gene segment of T3D was the most significant. The S1 gene segment encodes the σ1 receptor binding protein and the σ1s non-structural protein. The L2 gene segment encodes the λ2 outercapsid protein which is the core spike protein. The M2 gene segment encodes the μ1 outer capsid protein which is cleaved to μ1c. The M3 gene segment encodes the non-structural protein μNS which is a coordinating protein in assembly.

Interestingly the 4 reassortants that produced greater survival *in vivo* gave very different results *in vitro*. Two gave high viral yield and two gave low viral yield in the CT26 cells. This indicates that the ability to replicate in CT26 cells does not correlate with tumor destruction.

Figure 7: Growth of T1L x T3D reassortants in CT26 cells
CT26 cells were infected with T1L, T3D or one of the 24 reovirus reassortants MOI = 10. 3 days post-infection the viral titer was determined by plaque assay. **A**. Graph of viral titers 3 days post-infection in CT26 cells. Values are represented as average values ± SD (n = 3). **B**. Ranking of reovirus reassortants from highest to lowest based on viral titer. Gene map for each reassortant virus is also included. Reovirus reassortants with improved oncolysis *in vivo* are in bold **C**. Many reovirus reassortants grow better than either parent and this is primarily due to the S1 gene segment and secondarily L2, M2, and M3 gene segments from T3D (using Wilcoxin Rank-sum analysis)

A. CT26

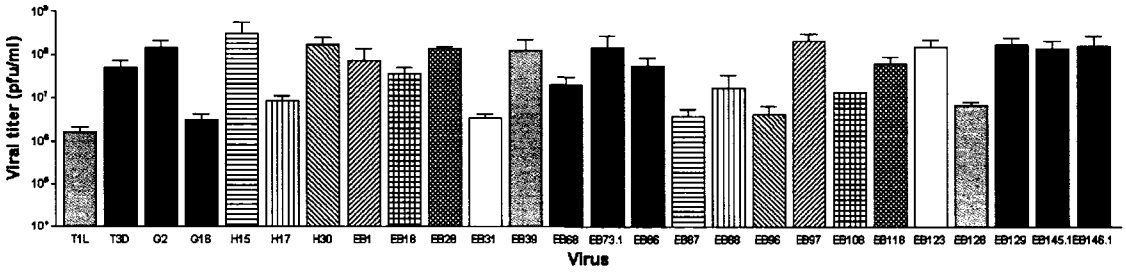

B.

Rank	Virus	Viral Titer	L1	L2	L3	M1	M2	M3	S1	S2	S3	S4
1	H15	3.03E+08	L	D	D	L	D	D	D	D	D	L
2	**EB97**	**2.15E+08**	**D**	**D**	**L**	**D**	**D**	**D**	**D**	**D**	**D**	**L**
3	EB129	1.68E+08	D	D	D	D	D	L	D	L	L	D
4	EB146.1	1.67E+08	L	D	L	L	D	D	D	D	D	D
5	**EB123**	**1.56E+08**	**D**	**D**	**L**	**D**	**D**	**D**	**D**	**D**	**L**	**D**
6	G2	1.44E+08	L	D	L	L	L	L	D	L	L	L
7	EB73.1	1.44E+08	L	D	L	L	D	D	D	D	D	D
8	EB28	1.37E+08	D	D	L	D	D	D	D	L	D	D
9	EB145.1	1.35E+08	D	D	D	D	D	D	D	D	D	L
10	EB39	1.23E+08	L	D	D	L	D	D	D	D	D	D
11	H60	1.05E+08	D	D	L	L	D	D	D	D	D	L
12	EB1	7.23E+07	L	D	L	L	D	L	L	L	D	L
13	EB118	6.10E+07	D	D	L	L	D	D	D	D	L	L
14	EB86	5.62E+07	L	D	D	D	D	L	D	D	D	L
15	T3D	5.03E+07	D	D	D	D	D	D	D	D	D	D
16	EB18	3.53E+07	D	D	L	D	D	D	L	L	D	L
17	EB68	2.00E+07	L	D	L	L	D	L	L	L	D	D
18	**EB88**	**1.71E+07**	**D**	**D**	**D**	**D**	**L**	**D**	**D**	**D**	**D**	**D**
19	EB108	1.32E+07	L	D	L	D	L	L	L	L	D	D
20	H17	8.33E+06	D	D	L	L	D	D	L	D	D	L
21	EB128	6.67E+06	D	D	L	D	D	D	L	D	D	L
22	**EB96**	**4.09E+06**	**L**	**D**	**L**	**D**	**L**	**L**	**L**	**L**	**D**	**L**
23	EB87	3.80E+06	L	D	L	L	D	L	L	D	L	L
24	EB31	3.33E+06	L	L	L	D	L	L	L	D	D	L
25	G16	3.00E+06	L	L	L	D	L	L	L	D	L	L
26	T1L	1.55E+06	L	L	L	L	L	L	L	L	L	L

C.

Gene Segmen	L1	L2	L3	M1	M2	M3	S1	S2	S3	S4
p value	0.1400	**0.0028**	0.0783	0.7315	**0.0043**	**0.0137**	**0.000036**	0.3430	0.3536	0.0632

4.3 Protein production in CT26 cells

In order to more accurately measure the protein production levels of reovirus infected CT26 cells 6 well dishes were seeded with CT26 cells and then either mock infected or infected with one of the parental serotypes or one of the reovirus reassortants using an MOI = 10. Three days post-infection the proteins were collected and fractionated by SDS-PAGE, transferred to an immobilon p membrane and the protein bands were visualized by immunoblot using anti-reovirus antibodies and BCIP/NBT colourimetric reaction. Densitometry was used to quantify the protein band intensity of the μ proteins (Figure 8). In order to rank the different reoviruses based on protein band density, T3D, which had the highest protein band density among the two parental serotypes, was considered as yielding 100% protein production and all the other protein band intensities were compared to T3D and quantified as a percent protein band density relative to this "standard" level (Figure 9). The average percent protein density was determined for each of the parental serotypes and the 24 reassortants from the results of three separate experiments. The average percent relative protein density was used to rank the different reoviruses from highest to lowest percent protein density and then Wilcoxin Rank-sum analysis was performed to determine which gene segments are important for protein production in CT26 cells. The results of the analysis showed that the L1 ($p = 0.015$), M3 ($p = 0.0059$), and S1 ($p = 0.0000093$) gene segments from the T3D parental serotype are most important for controlling high protein production levels in the resistant CT26 cell line relative to the corresponding gene segments from T1L (Table 6). Mapping to the S1 gene segment of T3D is most significant for high levels of protein production in CT26 cells. The S1 gene segment from T3D was also the most significant for high viral yield in the resistant CT26 cells line. The L1 gene segment which was not important for viral yield but seems to play a role in protein production,

encodes the λ3 inner capsid protein which is the viral RNA dependent RNA polymerase. This gene segment may control gene expression via control of RNA synthesis.

Figure 8. Western blot of proteins produced in CT26 cells
The μ proteins were used for densitometry measurements. The three gels represent protein bands for the parental strains and the entire panel of reovirus reassortants.

Protein production in CT26 cells

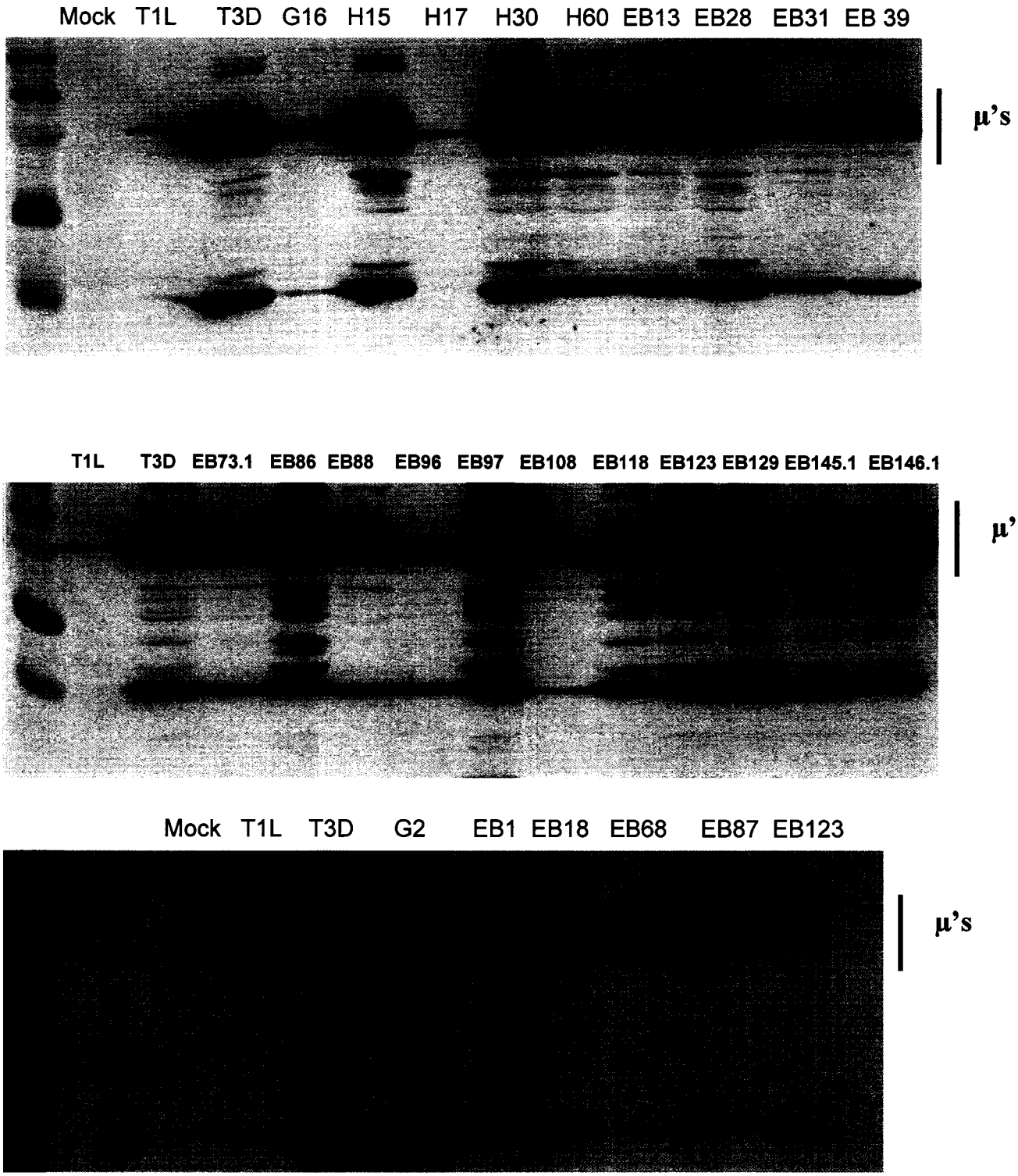

Figure 9: Protein production of T1L x T3D reassortants in CT26 cells
CT26 cells were infected with T1L, T3D or one of a large paned or reovirus reassortants MOI = 10. 3 days post-infection the proteins were collected and separated by SDS-PAGE and the protein band density was determined for each virus. **A.** Graph of percent protein density 3 days post-infection in CT26 cells. Values are represented as average values ± SD (n = 3). **B.** Ranking of reovirus reassortants from highest to lowest based on protein band density. Gene map for each reassortant virus. Reovirus reassortants with improved oncolysis *in vivo* are in bold.

A. CT26

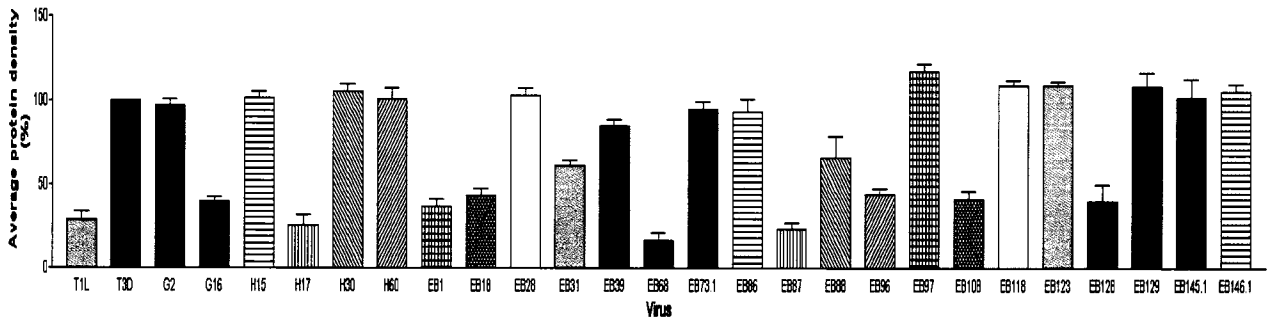

B.

Rank	Virus	Ave. Density (%)	SD	L1	L2	L3	M1	M2	M3	S1	S2	S3	S4
1	**EB97**	**117.19**	**7.47**	**D**	**D**	**L**	**D**	**D**	**D**	**D**	**D**	**D**	**L**
2	EB118	108.88	4.34	D	D	L	L	D	D	D	D	L	L
3	**EB123**	**108.6**	**4.59**	**D**	**D**	**L**	**D**	**D**	**D**	**D**	**D**	**L**	**D**
4	EB129	108.23	13.75	D	D	D	D	D	L	D	L	L	D
5	EB146.1	104.73	8.14	L	D	L	L	D	D	D	D	D	D
6	EB28	102.44	8.45	D	D	L	D	D	D	D	L	D	D
7	H15	101.59	6.06	L	D	D	L	D	D	D	D	D	L
8	EB145.1	101.2	20.15	D	D	D	D	D	D	D	D	D	L
9	H60	100.43	11.21	D	D	L	L	D	D	D	D	D	L
10	T3D	100	0	D	D	D	D	D	D	D	D	D	D
11	G2	96.67	6.04	L	D	L	L	L	L	D	L	L	L
12	EB73.1	94.68	7.83	L	D	L	L	D	D	D	D	D	D
13	EB86	92.88	13.63	L	D	D	D	D	L	D	D	D	L
14	EB39	84.54	7.41	L	D	D	L	D	D	D	D	D	D
15	**EB88**	**65.89**	**22.54**	**D**	**D**	**D**	**D**	**L**	**D**	**D**	**D**	**D**	**D**
16	EB31	61.2	5.22	L	L	L	D	L	L	L	D	D	L
17	**EB96**	**43.88**	**7.42**	**L**	**D**	**L**	**D**	**L**	**L**	**L**	**L**	**D**	**L**
18	EB18	43.82	6.94	D	D	L	D	D	D	L	L	D	L
19	EB108	41.5	9.28	L	D	L	D	L	L	L	L	D	D
20	EB126	40.08	17.83	D	D	L	D	D	D	L	D	D	L
21	G16	39.41	5.59	L	L	L	D	L	L	L	D	L	L
22	EB1	36.47	7.64	L	D	L	L	D	L	L	L	D	L
23	T1L	28.7	9.04	L	L	L	L	L	L	L	L	L	L
24	H17	25.8	9.36	D	D	L	L	D	D	L	D	D	L
25	EB87	23.09	7.14	L	D	L	L	D	L	L	D	L	L
26	EB68	16.37	8.1	L	D	L	L	D	L	L	L	D	D

Table 6: Probability of roles for individual gene segments involved in protein production following infection of CT26, MEF, and PKR -/- cells

Probability values where determined by Wilcoxin Rank-sum analysis that compared the average ranks of each allele (T1L vs T3D) for each gene segment. 3 days post-infection in CT26 cells many reovirus reassortants produce more proteins than both parents and this is primarily due to the S1 gene segment and secondarily to the L1 and M3 gene segments from T3D. 2 days post-infection in MEF cells many reassortant viruses produce more proteins than both parents and this is due to the L3 gene segment from T1L. 2 days post-infection in PKR -/- cells many reovirus reassortants produce more proteins that both parents and this is due primarily to the L1 gene segment from T1L, and secondarily to the M2 gene segment from T3D.

p values						
Gene Segment	**CT26** Parental origin		**MEF** Parental origin		**MEF PKR-/-** Parental origin	
	D	**L**	**D**	**L**	**D**	**L**
L1	**0.015**	0.985	0.286	0.714	0.999	**0.00041**
L2	0.059	0.941	0.752	0.248	0.093	0.907
L3	0.087	0.913	0.970	**0.030**	0.815	0.185
M1	0.177	0.823	0.479	0.521	0.561	0.439
M2	0.056	0.944	0.580	0.420	**0.020**	0.980
M3	**0.0059**	0.994	0.758	0.242	0.077	0.923
S1	**0.0000093**	1.000	0.572	0.428	0.057	0.943
S2	0.093	0.907	0.617	0.383	0.657	0.343
S3	0.625	0.375	0.668	0.332	0.535	0.465
S4	0.134	0.866	0.437	0.563	0.134	0.866

4.4 Protein production in the presence or absence of PKR

Reovirus T3D is sensitive to the PKR antiviral response in normal MEF cells due to the nature of its M2 gene segment. The PKR status of CT26 tumor cells is not known. It is known that T3D reovirus has a natural preference to replicate in many transformed cells with mutations in the Ras pathway that is known to down regulate the PKR response. Interestingly the genetic basis for T3D replication in CT26 cells is primarily due to the S1 gene segment and secondarily due to the L2, M2 and M3 gene segments but without a role for the M1 gene segment. To be able to gain a better understanding for the reasons why certain reovirus reassortants have an improved oncolytic ability over their parental serotypes we need to gain an understanding of how these reovirus reassortants respond both in the presence and absence of PKR. Through the use of a large panel of reovirus reassortants it has been previously determined in our laboratory that the T3D M1 gene segment controls PKR sensitivity *in vitro*, and the T1L L3 gene segment is involved in increased viral yield in the absence of PKR (unpublished). In order to get a better understanding of the role of PKR during infection the panel of 24 reovirus reassortants was used to characterize the genetic basis for the difference in protein production both in the presence and absence of PKR in MEF cells. MEF and PKR -/- were used to examine protein production levels 48 hr post-infection. Six-well dishes were seeded with either MEF or PKR-/- cells and were then either mock infected or infected with one of the parental serotypes or one of the 24 reovirus reassortants using an MOI = 10. At 48 hr post-infection the proteins were collected and separated by SDS-PAGE, transferred to immobilon p membrane and the protein bands were visualized by immunoblot using anti-reovirus antibodies and BCIP/NBT colorimetric reaction. Densitometry was then used to quantify the protein band intensity of the μ proteins (Figure 10 & 12). In order to rank the different reoviruses bases on protein band density for

the MEF cells line T1L had the highest protein band density among the two parental serotypes and was therefore considered as 100% protein production and all the other protein band intensities were compared to T1L and quantified as a percent relative protein density (Figure 11). However, for the PKR -/- cells T3D had the highest protein band density and therefore it was considered as the protein production reference standard (i.e 100% value) and all the other protein band intensities were compared to it and quantified as a percent relative protein density (Figure 13). The average relative percent protein density was determined for each of the parental serotypes and the 24 reassortants from the results of three separate experiments. The relative protein densities were used to rank the different reoviruses from highest to lowest percent protein density and then Wilcoxon Rank-sum analysis was performed to determine which gene segments are important for protein production in the MEF and PKR -/- cells.

In the MEF cells the gene segment associated with high protein production in the presence of PKR mapped to the L3 ($p = 0.030$) gene segment from the parental serotype T1L (Table 6). The L3 gene segment encodes the λ1 inner capsid protein which has RNA binding activity for both ssRNA and dsRNA, it also has NTPase activity. It has previously been observed in our lab that the L3 gene segment from T1L is involved in the increased viral yield in the absence of PKR in the PKR -/- cells.

In the PKR -/- cells the gene segments associated with high protein production in the absence of PKR were the L1 ($p = 0.00041$) genome segment from T1L and the M2 ($p = 0.020$) gene segment from T3D (Table 6). The data identify a lack of correlation between viral yield and protein synthesis in PKR -/- cells indicating that a difference in some aspect of viral replication independent of amount of protein is controlling the amount of infectious virus produced in the absence of PRK.

Figure 10: Western blot of proteins produced in MEF cells
The μ proteins were used for densitometry measurements. The three gels represent protein bands for the parental strains and the entire panel of reovirus reassortants.

Protein production in MEF cells

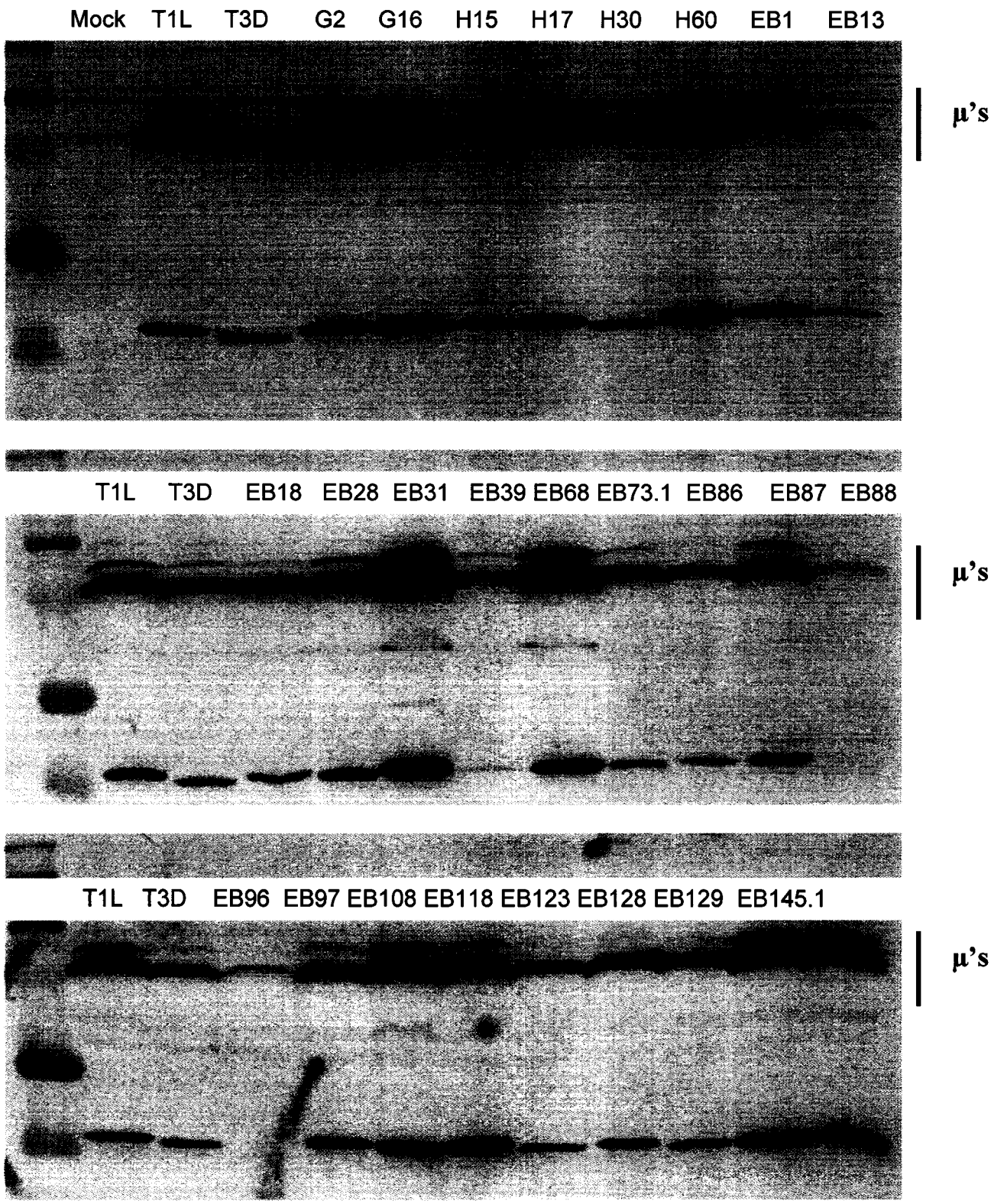

Figure 11: Protein production of T1L x T3D reassortants in MEF cells
MEF cells were infected with T1L, T3D or one of a large paned or reovirus reassortants MOI = 10. 2 days post-infection the proteins were collected and separated by SDS-PAGE and the protein band density was determined for each virus. **A.** Graph of percent protein density 2 days post-infection in MEF cells. Values are represented as average values ± SD (n = 3). **B.** Ranking of reovirus reassortants from highest to lowest based on protein band density. Gene map for each reassortant virus. Reovirus reassortants with improved oncolysis *in vivo* are in bold.

A. MEF

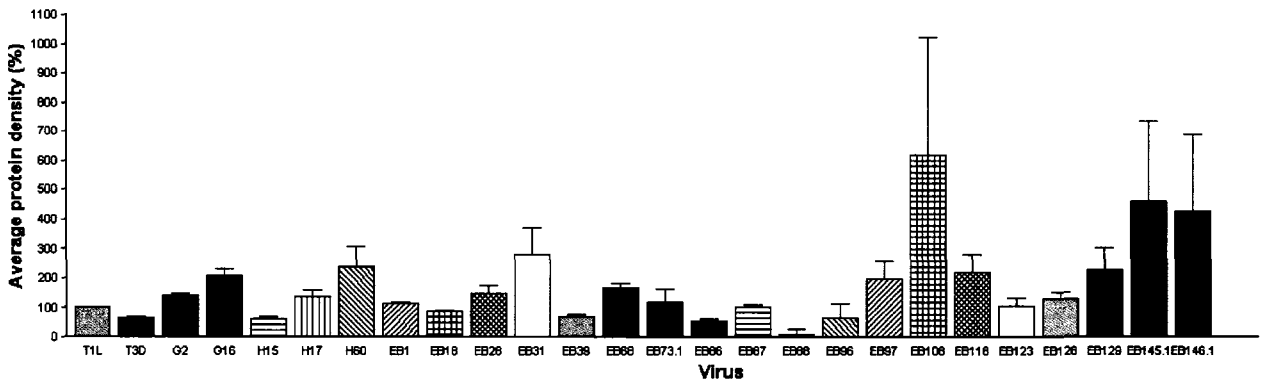

B.

Rank	Virus	Ave	SD	L1	L2	L3	M1	M2	M3	S1	S2	S3	S4
1	EB108	619.13	694.46	L	D	L	D	L	L	L	L	D	D
2	EB145.1	460.72	473.62	D	D	D	D	D	D	D	D	D	D
3	EB146.1	427.32	450.41	L	D	L	L	D	D	D	D	D	L
4	EB31	277.74	90.34	L	L	L	D	L	L	L	D	D	L
5	H60	236.24	119.77	D	D	L	L	D	D	D	D	D	L
6	EB129	226.13	131.63	D	D	D	D	D	L	D	L	L	D
7	EB118	217.82	107.44	D	D	L	L	D	D	D	D	L	L
8	G16	205.62	43.11	L	L	L	D	L	L	L	D	L	L
9	**EB97**	**196.96**	**103.76**	**D**	**D**	**L**	**D**	**D**	**D**	**D**	**D**	**D**	**L**
10	EB68	166.24	27.35	L	D	L	L	D	L	L	L	D	D
11	EB28	148.19	43.19	D	D	L	D	D	D	D	L	D	D
12	G2	139.19	11.16	L	D	L	L	L	L	D	L	L	L
13	H17	136.65	35.47	D	D	L	L	D	D	L	D	D	L
14	EB126	126.96	43.29	D	D	L	D	D	D	L	D	D	L
15	EB73.1	115.02	80.3	L	D	L	L	D	D	D	D	D	D
16	EB1	112	11.45	L	D	L	L	D	L	L	L	D	L
17	**EB123**	**106.57**	**43.59**	**D**	**D**	**L**	**D**	**D**	**D**	**D**	**D**	**L**	**D**
18	T1L	100	0	L	L	L	L	L	L	L	L	L	L
19	EB87	99.85	13.02	L	D	L	L	D	L	L	D	L	L
20	EB18	87.75	2.83	D	D	L	D	D	D	L	L	D	L
21	EB39	66.85	11.59	L	D	D	L	D	D	D	D	D	D
22	**EB96**	**63.75**	**84.63**	**L**	**D**	**L**	**D**	**L**	**L**	**L**	**L**	**D**	**L**
23	T3D	63.13	6.84	D	D	D	D	D	D	D	D	D	D
24	H15	61.01	12.27	L	D	D	L	D	D	D	D	D	L
25	EB86	52.74	11.69	L	D	D	D	D	L	D	D	D	L
26	**EB88**	**6.78**	**32.78**	**D**	**D**	**D**	**D**	**L**	**D**	**D**	**D**	**D**	**D**

Figure 12: Western blot of proteins produced in PKR -/- cells
The μ proteins were used for densitometry measurements. The three gels represent protein bands for the parental strains and the entire panel of reovirus reassortants.

Protein production in PKR -/- cells

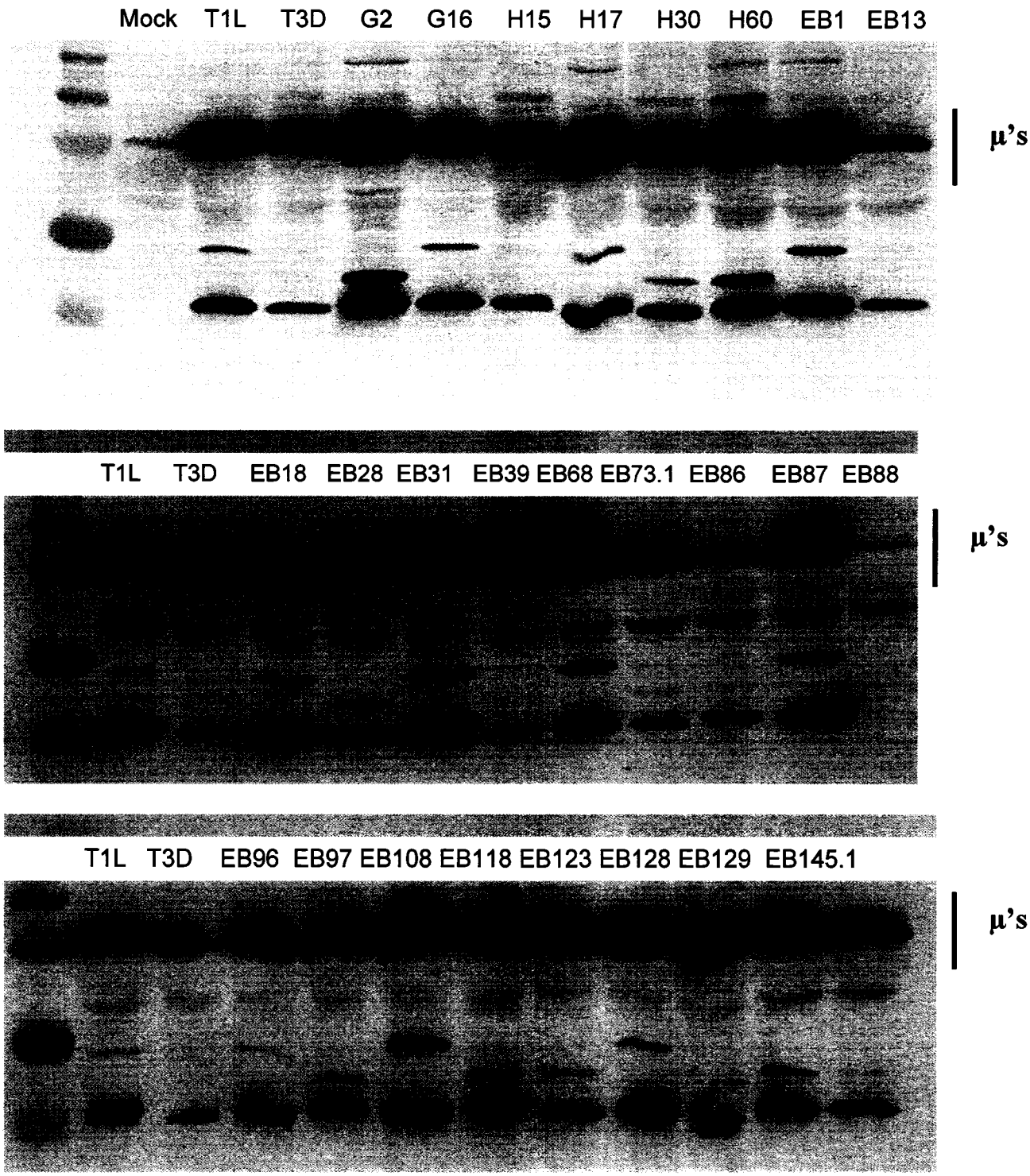

Figure 13: Protein production of T1L x T3D reassortants in PKR -/- cells
PKR -/- cells were infected with T1L, T3D or one of a large paned or reovirus reassortants MOI = 10. 2 days post-infection the proteins were collected and separated by SDS-PAGE and the protein band density was determined for each virus. A. Graph of percent protein density 2 days post-infection in PKR -/- cells. Values are represented as average values ± SD (n = 3). B. Ranking of reovirus reassortants from highest to lowest based on protein band density. Gene map for each reassortant virus. Reovirus reassortants with improved oncolysis *in vivo* are in bold.

A. PKR -/-

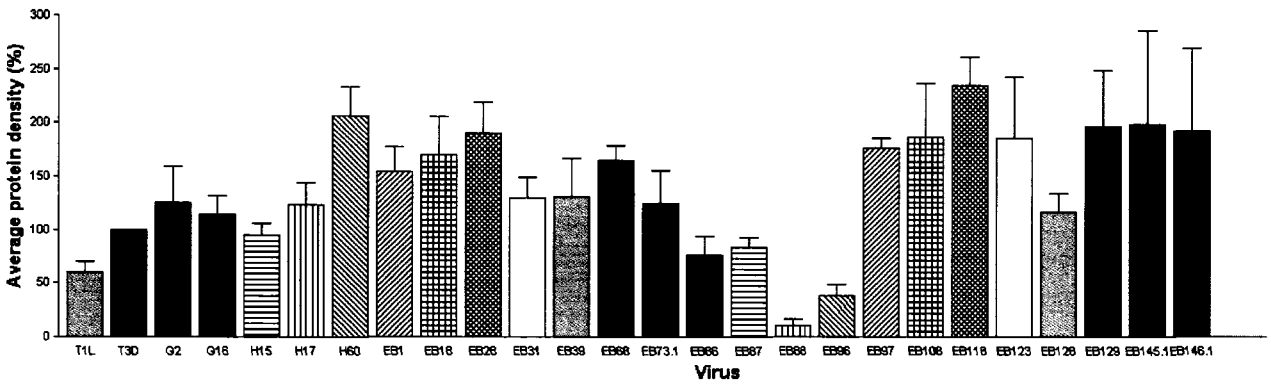

B.

Rank	Virus	Ave	SD	L1	L2	L3	M1	M2	M3	S1	S2	S3	S4
1	EB118	234.68	45.41	D	D	L	L	D	D	D	D	L	L
2	H60	206.88	45.43	D	D	L	L	D	D	D	D	D	L
3	EB145.1	198.77	149.76	D	D	D	D	D	D	D	D	D	D
4	EB129	196.64	89.72	D	D	D	D	D	L	D	L	L	D
5	EB146.1	192.48	132.29	L	D	L	L	D	D	D	D	D	L
6	EB26	190.46	49.04	D	D	L	D	D	D	D	L	D	D
7	EB108	185.5	88.79	L	D	L	D	L	L	L	L	D	D
8	**EB123**	**185.06**	**99.89**	**D**	**D**	**L**	**D**	**D**	**D**	**D**	**D**	**L**	**D**
9	**EB97**	**176.05**	**14.92**	**D**	**D**	**L**	**D**	**D**	**D**	**D**	**D**	**D**	**L**
10	EB18	169.27	62.6	D	D	L	D	D	D	L	L	D	L
11	EB68	164.16	23.35	L	D	L	L	D	L	L	L	D	D
12	EB1	154.13	39.73	L	D	L	L	D	L	L	L	D	L
13	EB39	130.3	62.92	L	D	D	L	D	D	D	D	D	D
14	EB31	129.7	33.82	L	L	L	D	L	L	L	D	D	L
15	G2	125.33	58.18	L	D	L	L	L	L	D	L	L	L
16	EB73.1	124.06	53.96	L	D	L	L	D	D	D	D	D	D
17	H17	123.03	36.15	D	D	L	L	D	D	L	D	D	L
18	EB126	115.67	30.78	D	D	L	D	D	D	L	D	D	L
19	G16	114.26	30.21	L	L	L	D	L	L	L	D	L	L
20	T3D	100	0	D	D	D	D	D	D	D	D	D	D
21	H15	94.24	19.79	L	D	D	L	D	D	D	D	D	L
22	EB87	83.31	16.38	L	D	L	L	D	L	L	D	L	L
23	EB86	76.35	29.9	L	D	D	D	D	L	D	D	D	L
24	T1L	59.8	17.61	L	L	L	L	L	L	L	L	L	L
25	**EB96**	**37.58**	**18.58**	**L**	**D**	**L**	**D**	**L**	**L**	**L**	**L**	**D**	**L**
26	**EB88**	**10.3**	**10.34**	**D**	**D**	**D**	**D**	**L**	**D**	**D**	**D**	**D**	**D**

4.5 The role of PKR in viral tropism in the lung

Since we observed different genetic patterns of protein expression and viral yield in MEF, PKR-/- and epithelial tumor (CT26) cells we examined the tropism of reovirus T1L and T3D in PKR +/+ and PRK-/- mouse lungs. This was done to separate the role of tumor cell transformation from that of normal cells since the fibroblasts are normal and CT26 cells are transformed cells. In wild-type Balb/c mice lungs only the alveolar regions of the lungs were infected by T1L and T3D. However, when TIK knockout mice (TIK -/-) were infected with T1L and T3D a different pattern of infection was observed (Figure 14). In the absence of PKR T3D was able to infect the bronchial epithelial cells of the lung which are restricted sites in wild-type Balb/c mice. To characterize the role PKR plays in viral tropism seen in the lung and to gain a better understanding of the reovirus gene segments involved TIK -/- mice were infected with either one of the parental serotypes or one of the 24 reovirus reassortants. Mice were anesthetized and given 1.0×10^7 pfu of virus *in.* The lungs were collected 3 days post-infection and stained for the presence of reovirus antigen using anti-reovirus antibodies to determine the pattern of infection in the TIK -/- mice lungs. The reovirus reassortants were separated based on whether or not they had the ability to infect the bronchial epithelial cells in the absence of PKR. Gene segment mapping was then done to determine which gene segments were involved in the different infection patterns (Table 7). All of the reovirus reassortants that were able to infect the bronchial epithelial cells in the TIK -/- mice had the S1 gene segment from the parental T3D strain. The reovirus reassortants that were only able to infect the alveolar cells in the lung all had the S1 gene segment from the parental serotype T1L. In the absence of PKR the parental serotype T3D and reovirus reassortants with the S1 gene segment from T3D were able to infect bronchial

Figure 14: Infection patterns of T1L and T3D in Balb/c and TIK -/- mice (40X magnification)

Balb/c and TIK -/- mice were given $1.0x10^7$ pfu of either T1L or T3D intranasally and lungs were collected 3 days post-infection. Panels a, c, e, g, and i are phase contrast images. The arrows are pointing to the bronchial epithelium. Panels a, b, c, and d are images from infected Balb/c lung tissue. In panels b and d both T1L and T3D antigen is only present in alveolar region of the lungs. Panels e and f are uninfected TIK -/- lungs. Panels g, h, i and j are images from infected TIK -/- lung tissue. In panel h T1L antigen is only present in alveolar region of the lung. In panel j T3D antigen is present in both the alveolar region and bronchial epithelial cells of the lung. This composite is made up of photographs of FITC conjugated antibodies labeling reovirus antigens in frozen sections of mouse lung showing the location of viral infection. The photographs were taken in the most brightly fluorescing areas, and may not be representative of the entire lung section. Scale bars are 10 microns.

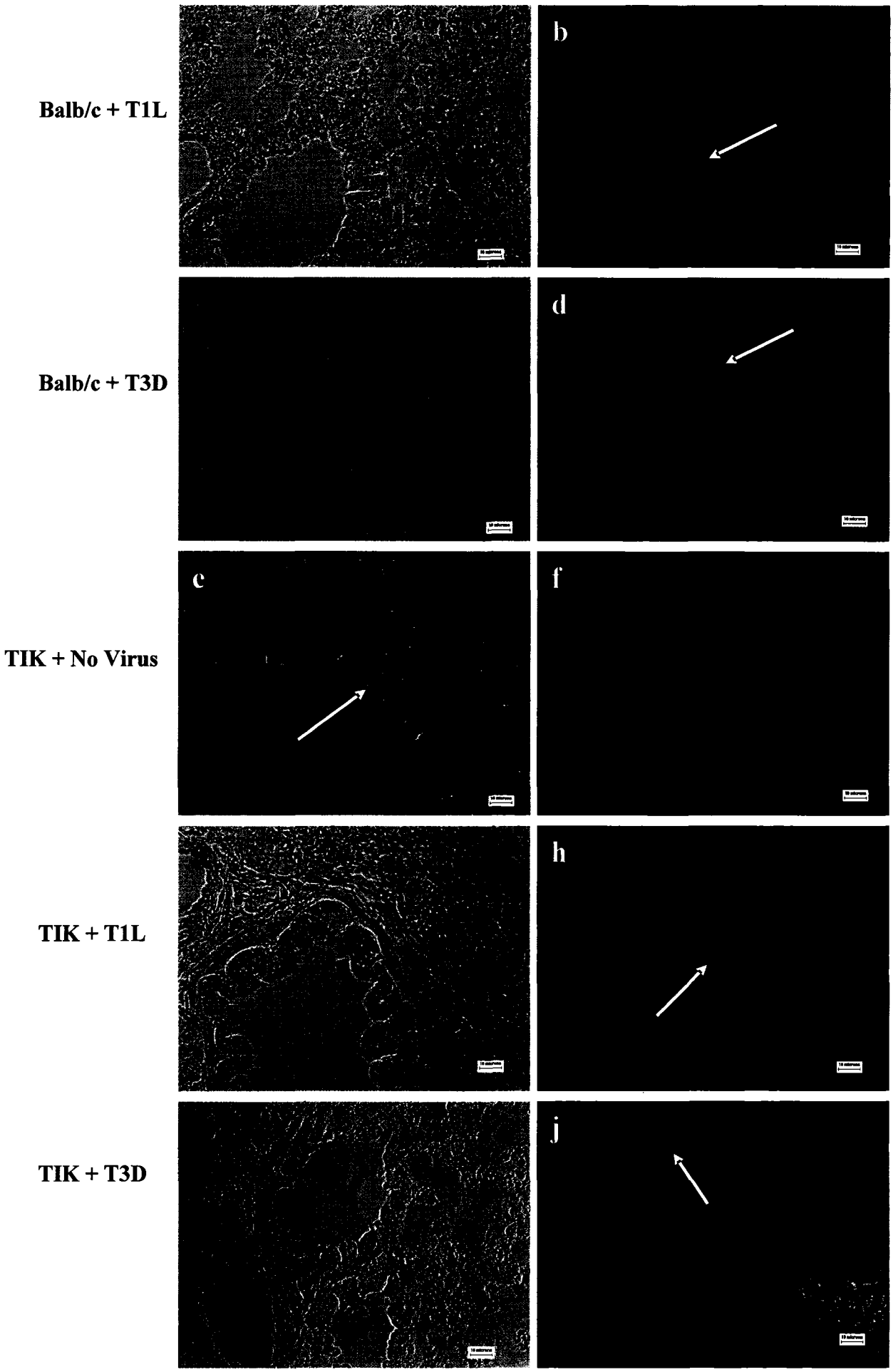

Table 7: Gene mapping of the infection patterns of a large panel of T1L x T3D reassortants 3 days post-infection in the TIK -/- mouse lung.
Reovirus reassortants are separated into two groups base on whether or not the reassortant has the ability to infect the bronchial epithelial cells in the TIK -/- mouse lungs. The ability to infect bronchial epithelial cells is due to the S1 gene segment of T3D.

Virus	L1	L2	L3	M1	M2	M3	S1	S2	S3	S4	Infection in BEC
T3D	D	D	D	D	D	D	**D**	D	D	D	Yes
H15	L	D	D	L	D	D	**D**	D	D	L	Yes
H60	D	D	L	L	D	D	**D**	D	D	L	Yes
EB28	D	D	L	D	D	D	**D**	L	D	D	Yes
EB39	L	D	D	L	D	D	**D**	D	D	D	Yes
EB73.1	L	D	L	L	D	D	**D**	D	D	D	Yes
EB86	L	D	D	D	D	L	**D**	D	D	L	Yes
EB88	D	D	D	D	L	D	**D**	D	D	D	Yes
EB97	D	D	L	D	D	D	**D**	D	D	L	Yes
EB118	D	D	L	L	D	D	**D**	D	L	L	Yes
EB123	D	D	L	D	D	D	**D**	D	L	D	Yes
EB129	D	D	D	D	D	L	**D**	L	L	D	Yes
EB145.1	D	D	D	D	D	D	**D**	D	D	L	Yes
EB146.1	L	D	L	L	D	D	**D**	D	D	D	Yes
T1L	L	L	L	L	L	L	L	L	L	L	No
G16	L	L	L	D	L	L	L	D	L	L	No
H17	D	D	L	L	D	D	L	D	D	L	No
EB31	L	L	L	D	L	L	L	D	D	L	No
EB96	L	D	L	D	L	L	L	L	D	L	No
EB108	L	D	L	D	L	L	L	L	D	D	No

epithelial cells which are protected when PKR is present in wild-type mice. This suggests that PKR plays a role in protecting epithelial cells from reovirus infection. In order to determine if the different infection patterns seen in the TIK -/- mice are due to the S1 gene segment alone, TIK -/- mice were infected with single segment reassortant reoviruses. The 1HA3 virus contains all T1L gene segments with the exception of the S1 gene segment that is from T3D. The 3HA1 virus contains all T3D gene segments with the exception of the S1 gene segment that is from T1L. At 3 days post-infection the lungs were collected and stained using anti-reovirus antibodies for the presence of viral antigen to determine the pattern of infection (Figure 15). The 1HA3 virus was able to infect the bronchial epithelial cells; however, the 3HA1 virus was only able to infect the alveolar regions in the lung. Therefore, only the S1 gene segment from T3D is necessary for reovirus to infect the bronchial epithelial cells in the absence of PKR. Thus, the S1 gene segment is a good candidate that may increase oncolytic ability in types of cancer that affect epithelial cells. Other studies in our laboratory have shown that T1L grew to high titers in Balb/c lungs indicating that the T1L virus may employ PKR to achieve optimal replication. T3D grew to higher titers in PKR -/- lung consistent with the infection of bronchial epithelial cells in the absence of PKR.

Figure 15: Infection patterns of 1HA3 and 3HA1 in TIK -/- mouse lungs 3 days post-infection (40X magnification)
TIK -/- were infected with either 1HA3 or 3HA1, $1.0x10^7$ pfu intranasally. 1HA3 is able to infect the bronchial epithelial cells while viral antigen cannot be detected for 3HA1.

TIK + 1HA3

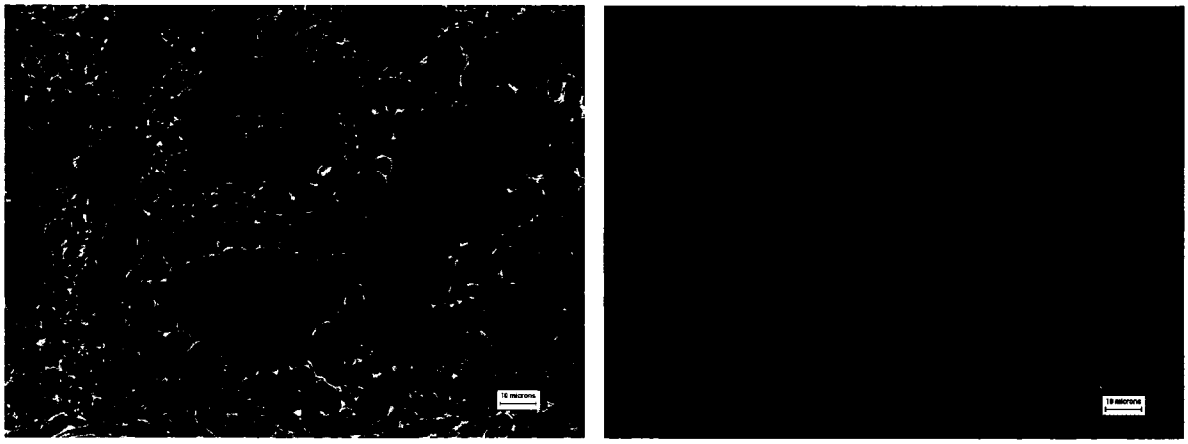

TIK + 3HA1

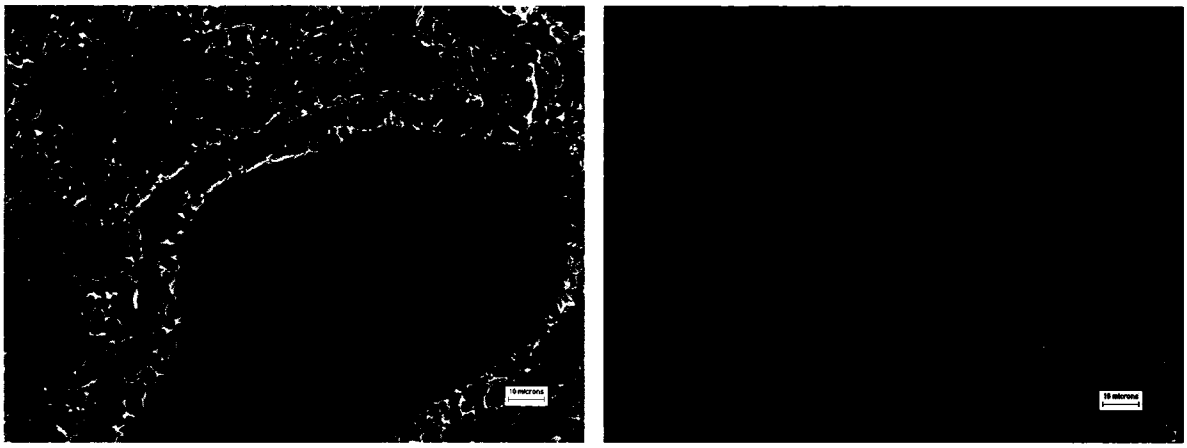

4.6 Assessing reovirus reassortants *in vivo* in a lung tumor model

For the purpose of this study, to assess virus growth in tumors, tumors were allowed more time to grow to facilitate visualization of the tumors and whether or not viral antigen could be detected in the tumors. The mice were monitored for signs of respiratory distress which indicates that they are suffering due to increased tumor burden. Therefore, once the mice showed signs of respiratory distress as determined by animal care staff they were given the viral treatment. Balb/c mice were given a single treatment of virus (1.0×10^7 pfu *in*) at day 8 days following the delivery of CT26 tumors. The lungs were collected at the appropriate times post-treatment and stained for the presence of reovirus proteins.

4.6.1 Reassortant gene mapping

The infection of CT26 tumors *in vivo* by the 4 reovirus reassortants that have been previously shown to increase survival in Balb/c mice bearing lung tumors, EB88, EB96, EB97, and EB123, was monitored. The gene segment maps of all four reassortants were compared to determine which gene segments from each of the parental serotypes, T1L and T3D that they have in common (Table 5). Three of the four reassortants have the S1 gene segment from T3D which was shown to be important in viral growth *in vitro* in the CT26 cell line. Interestingly EB96 does not have the S1 gene segment from T3D, which was shown to be the most significant gene segment involved in both viral growth and protein production *in vitro*. EB96 only has one gene segment that was shown to be important for viral yield in CT26 cells, the L2 gene segment from T3D, but was able to increase survival in Babl/c mice bearing CT26 lung tumors.

4.6.2 Viral growth in CT26 tumor bearing lungs

To get a better understanding of the productivity of infection in tumor bearing lungs, Balb/c mice were given a single viral treatment (1.0×10^7 pfu *in*) and 2 days post-treatment the mice were euthanized, the lungs were collected and the viral titer in the lungs was determined by plaque assay (Figure 16). In the CT26 cells *in vitro* T3D had a higher viral yield than T1L. However in the tumor bearing lungs T1L gave the highest viral yield over T3D and all 4 of the reassortant viruses. Among the reassortant viruses EB123 and EB97 produced the most virus in tumor bearing lungs. These two reassortants also gave high viral titers in the CT26 cells *in vitro*.

Figure 16: Viral titer in CT26 tumor bearing lungs 2 days post-treatment
Balb/c mice bearing CT26 lung tumors were given a single dose of 1.0×10^7 pfu of virus intransally and viral titer was determined 2 days post-treatment. Each bar represents the average titer obtained from two different mice infected with one of the 6 viruses, with error bars showing the standard deviation.

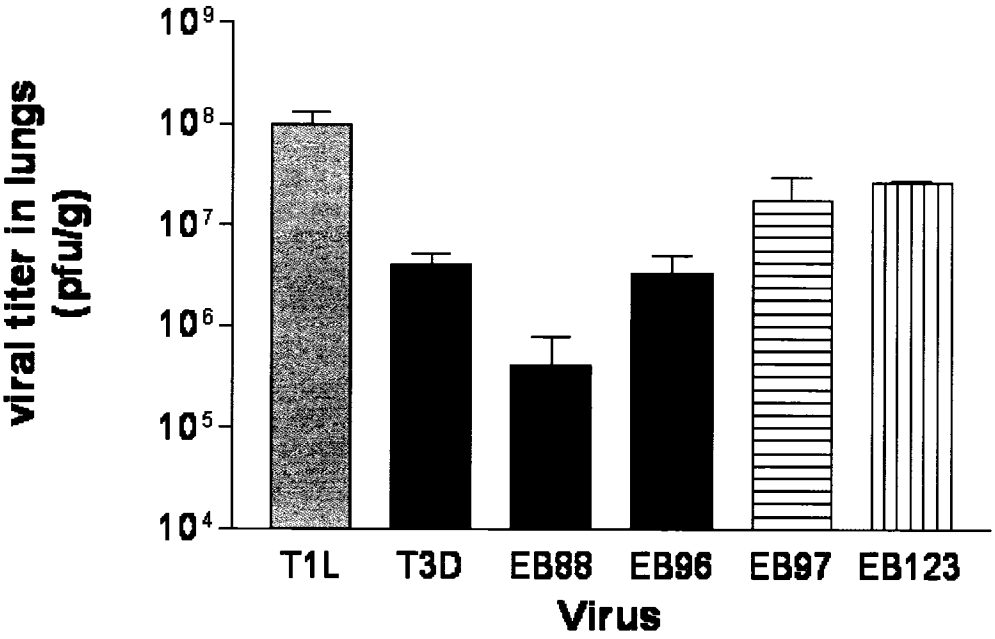

4.6.3 H & E in tumor bearing lungs

Balb/c mice bearing CT26 lung tumors were given a single treatment of virus 1.0×10^7 pfu *in* and lungs were collected at 1, 2, 3, and 7 days post-treatment. The lungs were stained for the presence of H & E. The H & E staining allows for the histological examination of the lung tissue and the tumors present in the lungs (Figure 17). Tumor break down was observed as early as 1 day post-treatment and became more prominent by 3 days post-treatment in tumors from lungs treated with the reassortant viruses. It important to note that tumor break down was observed in PBS treated lungs and suggests that there is an immune component involved in this breakdown. However, by 7 days post-treatment there was a dramatic difference in tumor size in lungs treated with EB88 and EB96 compared to lungs treated with EB97. At 7 days post-treatment lungs from mice treated with EB88 and EB96 had tumors were significantly reduced in size compared to EB97 treated mice. Seven days post-treatment there are no longer any animals that had survived in the PBS, T1L, T3D or EB123 treated groups.

Figure 17: Lung pathology of Balb/c mice bearing CT26 tumors following a single intranasal viral treatment (10X magnification)
Balb/c mice bearing CT26 lung tumors were given a single dose of virus $1.0x10^7$ pfu intranasally and lungs were collected 1, 2, 3, and 7 days post-treatment. This composite is made up of photographs of H & E stained mouse lung sections showing tumor burden in each of the different treatment groups at several post-treatment time points

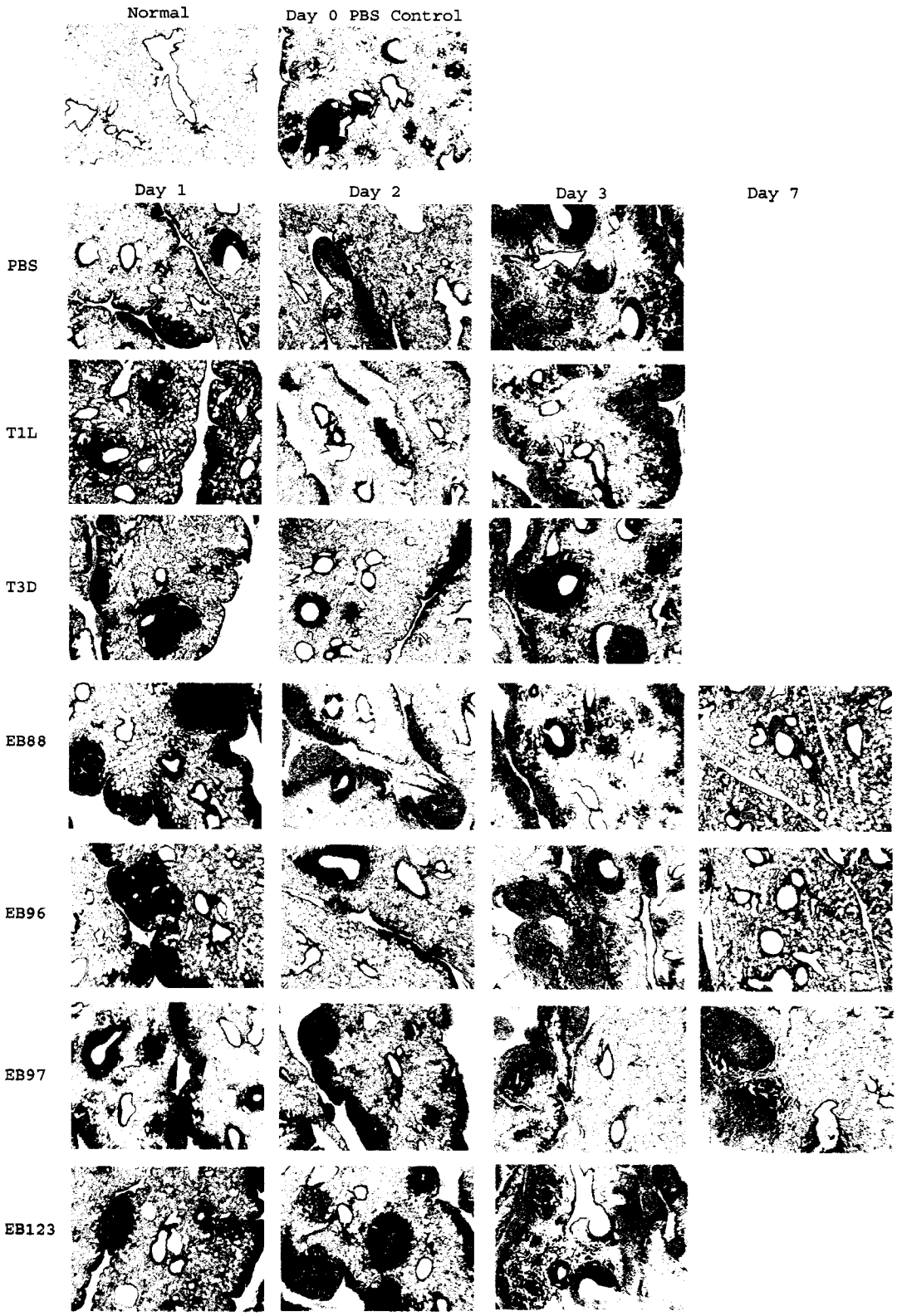

4.6.4 Reovirus protein expression in CT26 tumor bearing lungs

The amount of viral antigen in CT26 tumor bearing lungs was assessed at 1, 2, 3 and 7 days post-treatment (Figures 18, 19, 20 and 21). At 1, 2, and 3 days post-treatment the lungs treated with EB123 had the highest amount of viral antigen detected by immunohistochemistry (qualitative analysis). EB123 had the highest viral yield in the lungs compared to the other three reassortants and it also produced high amounts of viral protein in the CT26 cells *in vitro*. At 7 days post-treatment there were no longer any PBS or EB123 treated animals as they had all died due to tumor burden; however viral antigen could still be detected in the lungs treated with reovirus reassortants EB88 and EB96. Interestingly EB88, but not EB96, produced high levels of protein in CT26 cells *in vitro*, yet both EB88 and EB96 persisted to infect cells and produce detectable protein *in vivo* 7 days post-treatment.

Figure 18: Fluorescent antibody staining for reovirus antigens in CT26 tumor bearing lungs 1 day post-treatment (20X and 40X magnification)
Balb/c mice bearing CT26 lung tumors were given a single dose of virus $1.0x10^7$ pfu intranasally and lungs were collected 1 day post-treatment. This composite is made up of photographs of Cy3 conjugated antibodies labeling reovirus antigens on frozen sections of mouse lung showing the location of viral infection. The 20X images contain both labeled viral antigen and Hoechst dye labeling the cell nucleus. The square in the 20X image represents the area magnified by the 40X image. The 40X images contain only Cy3 labeled viral antigen. The photographs were taken in areas containing CT26 tumors showing the most brightly fluorescing areas and may not be representative of the entire lung section. Scale bars are 10 microns.

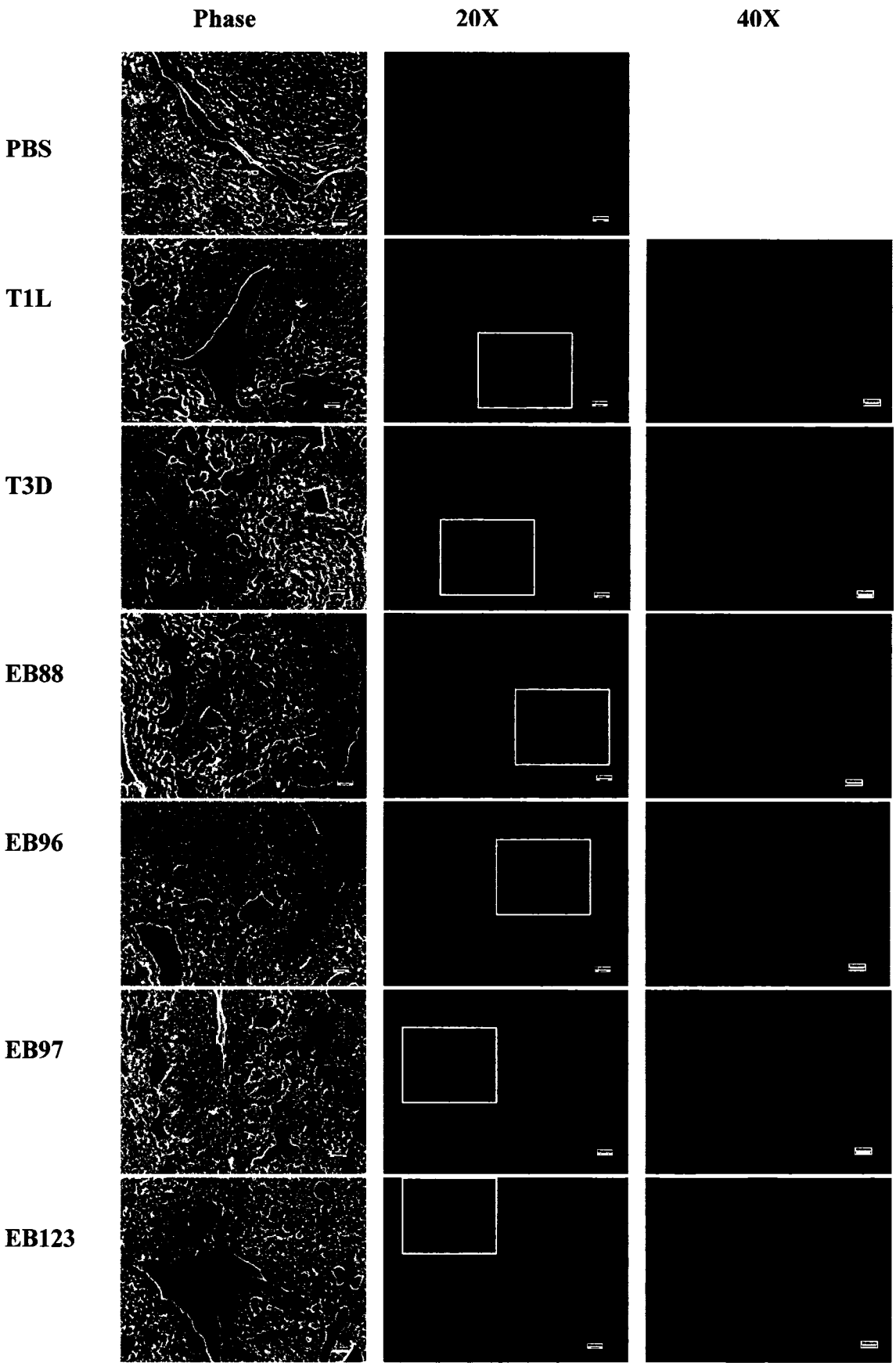

Figure 19: Fluorescent antibody staining for reovirus antigens in CT26 tumor bearing lungs 2 days post-treatment (20X and 40X magnification)
Balb/c mice bearing CT26 lung tumors were given a single dose of virus $1.0x10^7$ pfu intranasally and lungs were collected 2 days post-treatment. This composite is made up of photographs of Cy3 conjugated antibodies labeling reovirus antigens on frozen sections of mouse lung showing the location of viral infection. The 20X images contain both labeled viral antigen and Hoechst dye labeling the cell nucleus. The square in the 20X image represents the area magnified by the 40X image. The 40X images contain only Cy3 labeled viral antigen. The photographs were taken in areas containing CT26 tumors showing the most brightly fluorescing areas and may not be representative of the entire lung section. Scale bars are 10 microns.

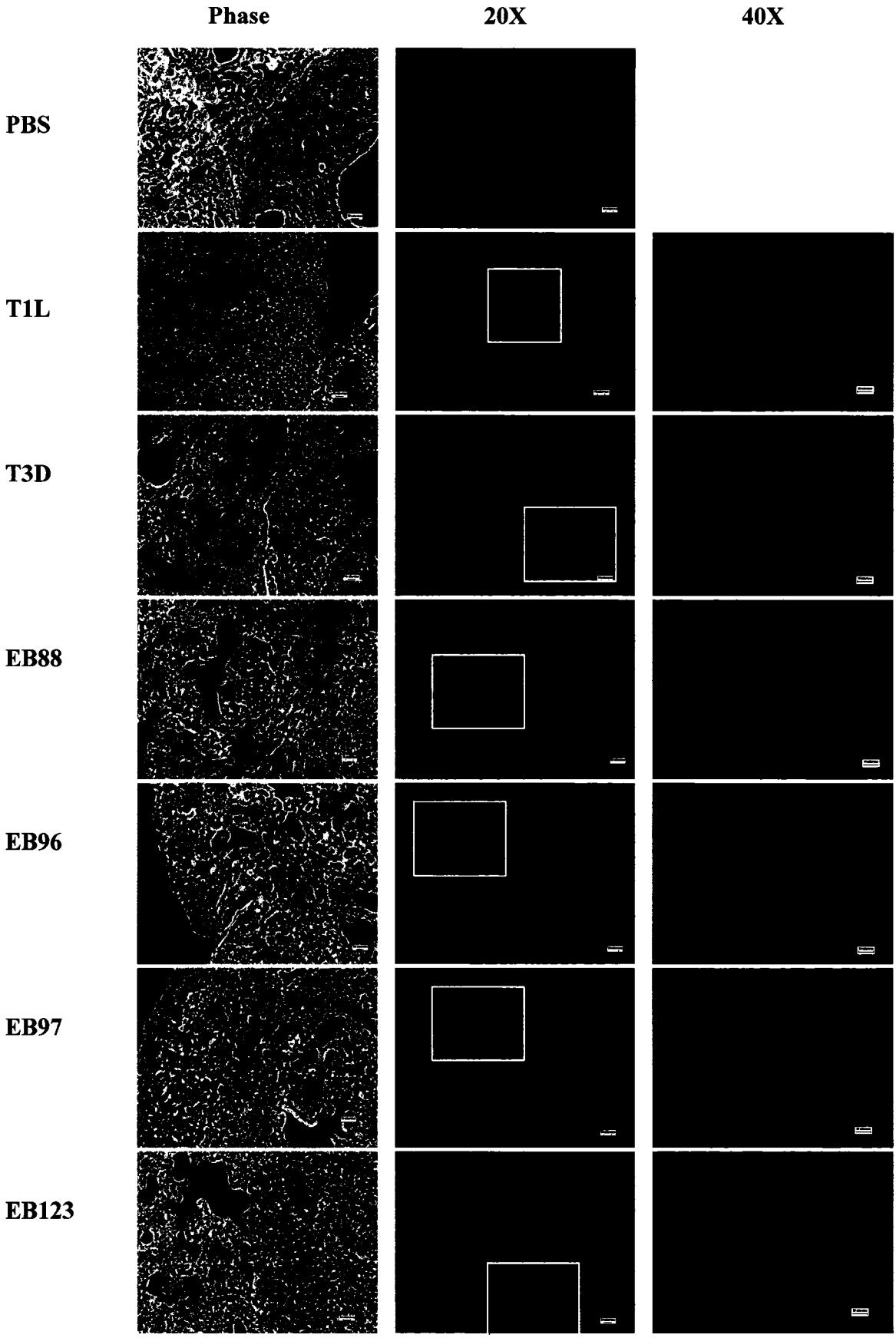

Figure 20: Fluorescent antibody staining for reovirus antigens in CT26 tumor bearing lungs 3 days post-treatment (20X and 40X magnification)
Balb/c mice bearing CT26 lung tumors were given a single dose of virus $1.0x10^7$ pfu intranasally and lungs were collected 3 days post-treatment. This composite is made up of photographs of Cy3 conjugated antibodies labeling reovirus antigens on frozen sections of mouse lung showing the location of viral infection. The 20X images contain both labeled viral antigen and Hoechst dye labeling the cell nucleus. The square in the 20X image represents the area magnified by the 40X image. The 40X images contain only Cy3 labeled viral antigen. The photographs were taken in areas containing CT26 tumors showing the most brightly fluorescing areas and may not be representative of the entire lung section. Scale bars are 10 microns

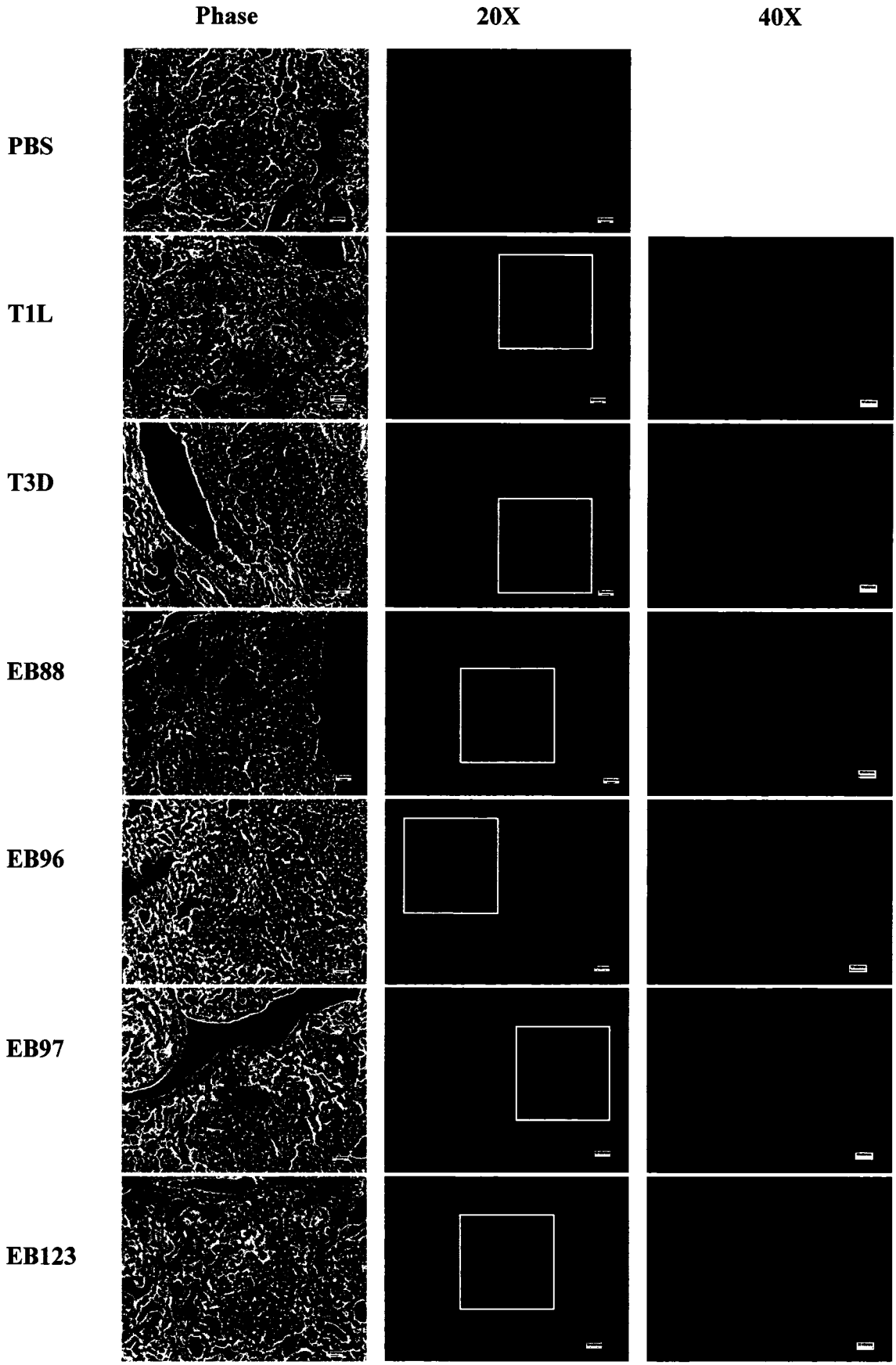

Figure 21: Fluorescent antibody staining for reovirus antigens in CT26 tumor bearing lungs 7 days post-treatment (20X and 40X magnification)
Balb/c mice bearing CT26 lung tumors were given a single dose of virus $1.0x10^7$ pfu intranasally and lungs were collected 7 days post-treatment. This composite is made up of photographs of Cy3 conjugated antibodies labeling reovirus antigens on frozen sections of mouse lung showing the location of viral infection. The 20X images contain both labeled viral antigen and Hoechst dye labeling the cell nucleus. The square in the 20X image represents the area magnified by the 40X image. The 40X images contain only Cy3 labeled viral antigen. The photographs were taken in areas containing CT26 tumors showing the most brightly fluorescing areas and may not be representative of the entire lung section. Scale bars are 10 microns

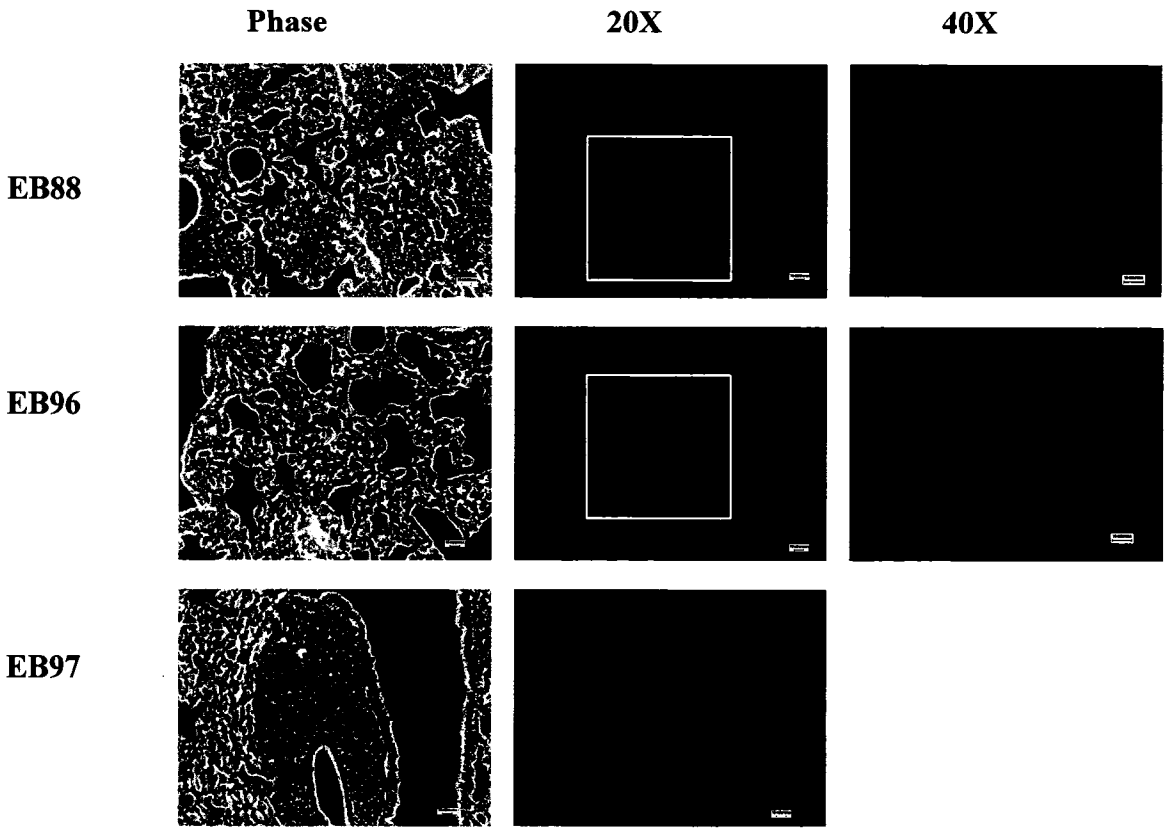

4.6.5 Detection of apoptosis markers in tumor bearing lungs

Balb/c mice bearing CT26 lung tumors were given a single treatment of virus 1.0 x 10^7 pfu *in* and lungs were collected at 1, 2, 3, and 7 days post-treatment. The lungs were stained for the presence of active caspase 3 and TUNEL positive cells (Figure 22, 23, 24, 25). Active caspase 3 and TUNEL positive cells are markers of apoptosis and the presence of these markers in lung tissue following viral treatment provide insight as to whether or not the tumor cells in the lungs have undergone cell death due to activation of the apoptotic pathway. At all of the time points post-treatment the presence of active caspase 3 could not be detected by immunohistochemistry. However, TUNEL positive cells were present in tumors in the lungs. At both 1 and 2 days post-treatment TUNEL positive cells could be detected in tumors present in lung tissue collected from mice treated with the reassortant viruses (Figure 22 & 23). The number of TUNEL positive cells was higher in tumors present in lungs treated with virus then PBS treated mice and normal lung tissue. Therefore, the presence of TUNEL positive cells is due to cell death caused by the virus. At 1 day post-treatment the highest amount of TUNEL positive cells were present in tumors from EB97 and EB123 treated lungs (qualitative analysis). At 2 days post-treatment the highest amount of TUNEL positive cells was present in tumors from EB123 treated lungs. TUNEL positive cells were also observed in tumors in lungs collected from mice treated with T1L and T3D. At 3 days post-treatment only a small number of TUNEL positive cells was observed in tumors present in lungs treated with EB96 (Figure 24). Interestingly by day 7 post treatment TUNEL positive cells were present in both tumors and lung tissue collected from mice treated with EB96 (Figure 25). TUNEL positive cells were detected following viral treatment and the amount of TUNEL positive cells was higher than in PBS treated lungs; therefore, cell death is occurring in tumors following viral treatment.

Figure 22: TUNEL positive cells in CT26 tumor bearing lungs at 1 day post-treatment (20X magnification)
Balb/c mice bearing CT26 lung tumors were given a single dose of virus $1.0x10^7$ pfu intranasally and lungs were collected 1 days post-treatment. **A.** PBS, T1L and T3D treated lungs. **B.** EB88, EB96, EB97 and EB123 treated lungs. This composite is made up of photographs of TUNEL labeled cells. The gray images are to demonstrate the location in the lung. The photographs were taken in areas containing CT26 tumors showing the most brightly fluorescing areas and may not be representative of the entire lung section. Scale bars are 10 microns.

A.

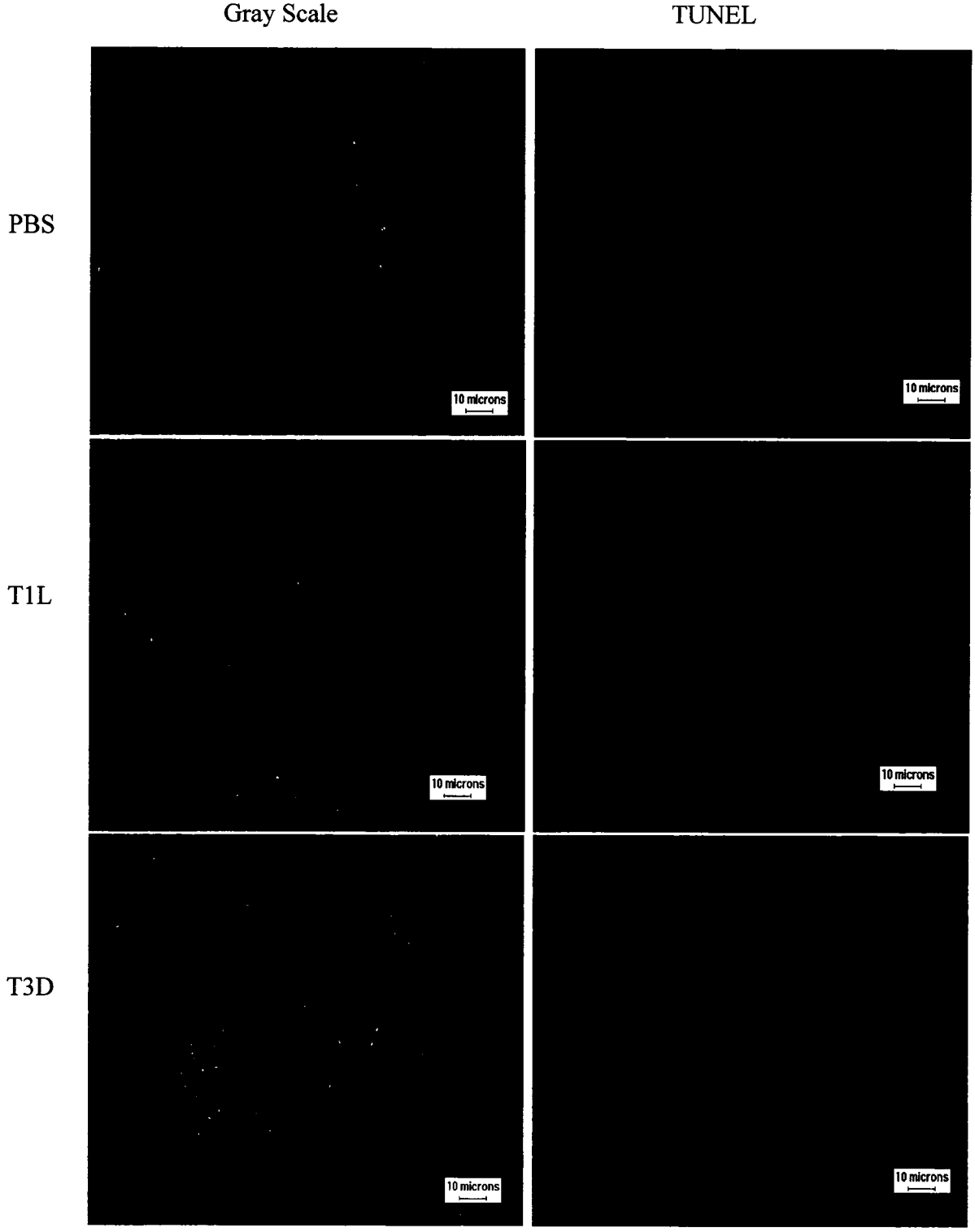

B.

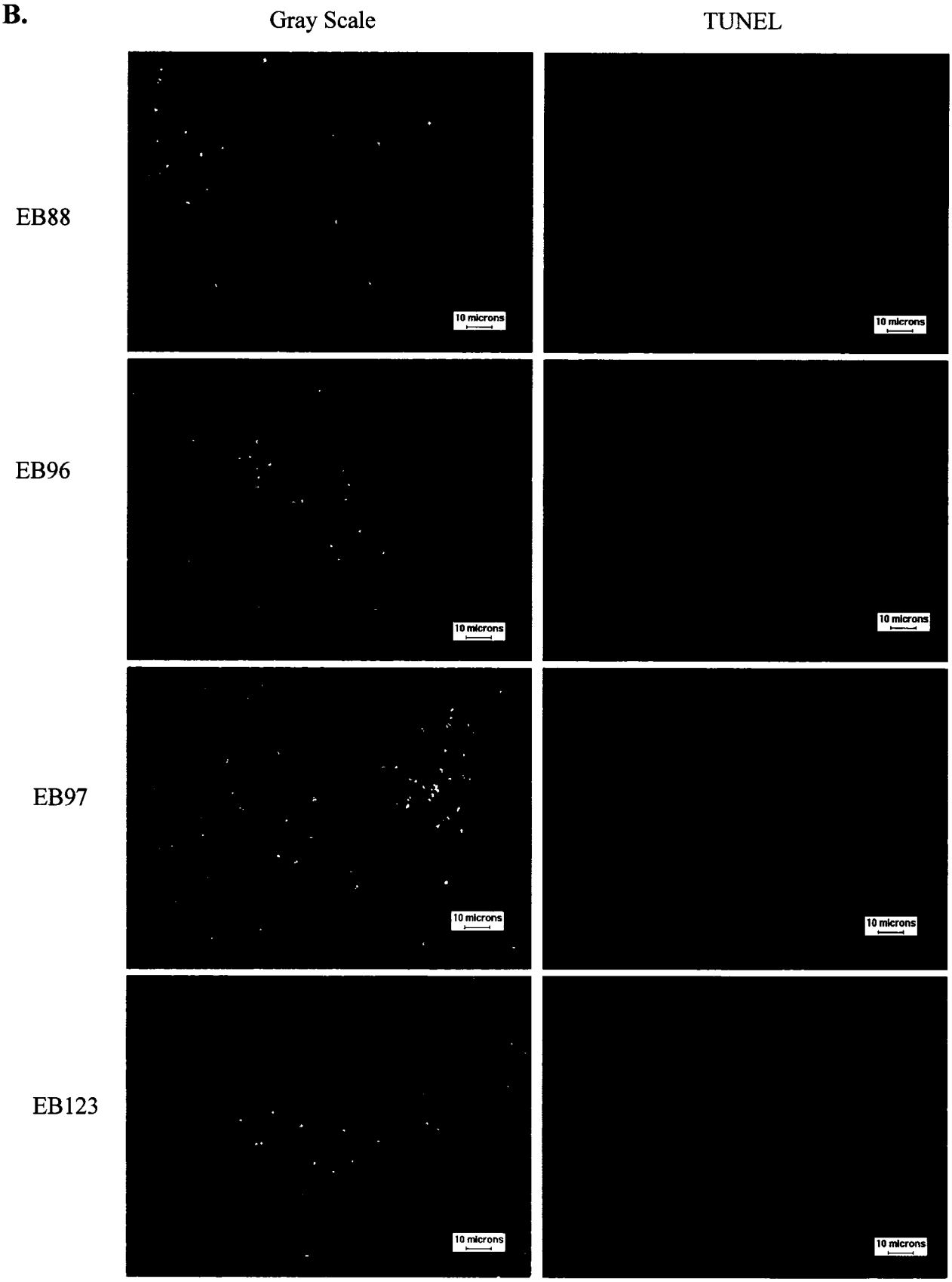

Figure 23: TUNEL positive cells in CT26 tumor bearing lungs at 2 day post-treatment (20X magnification)
Balb/c mice bearing CT26 lung tumors were given a single dose of virus $1.0x10^7$ pfu intranasally and lungs were collected 2 days post-treatment. **A.** PBS, T1L and T3D treated lungs. **B.** EB88, EB96, EB97 and EB123 treated lungs. This composite is made up of photographs of TUNEL labeled cells. The gray images are to demonstrate the location in the lung. The photographs were taken in areas containing CT26 tumors showing the most brightly fluorescing areas and may not be representative of the entire lung section. Scale bars are 10 microns.

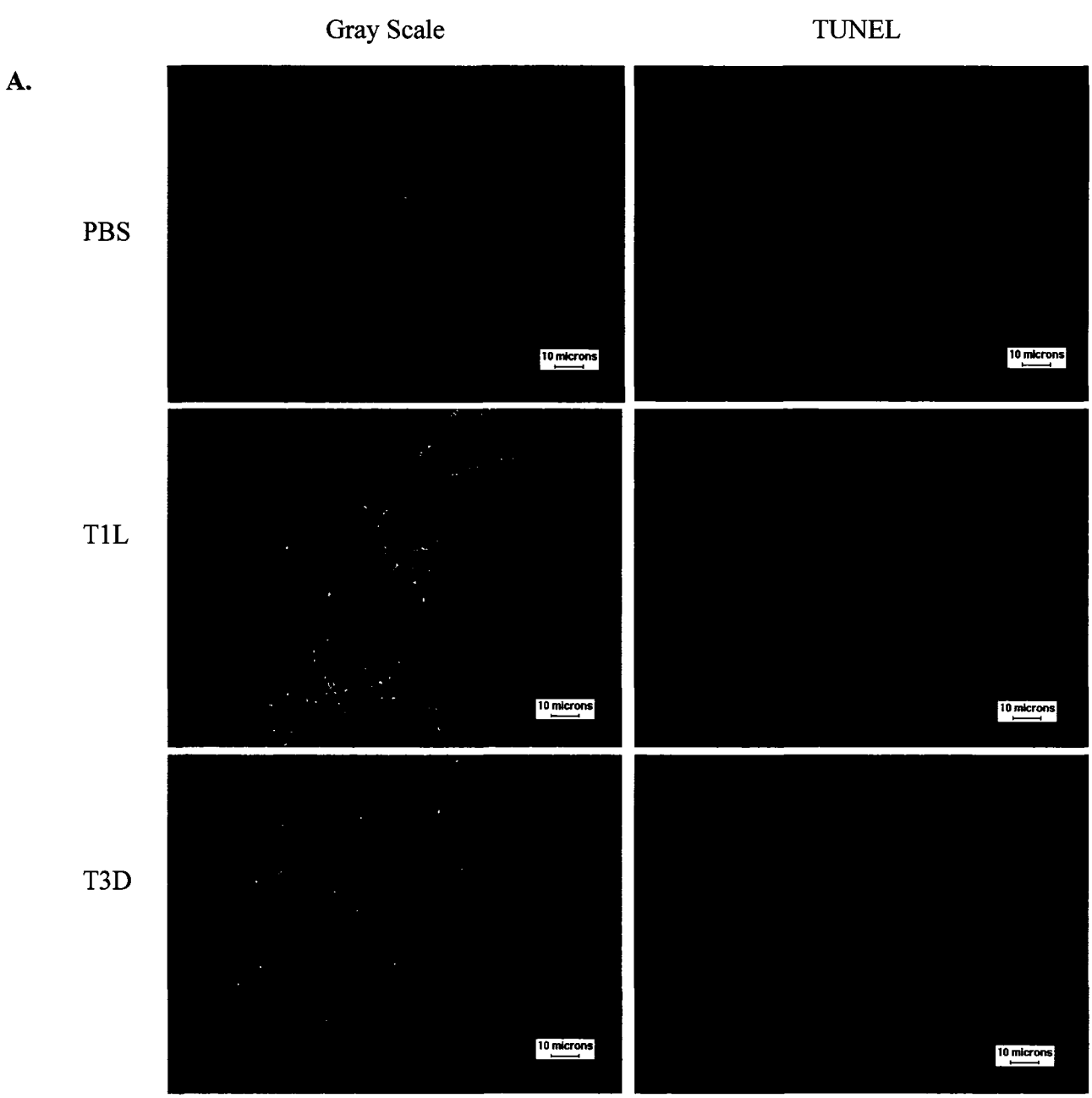

B.

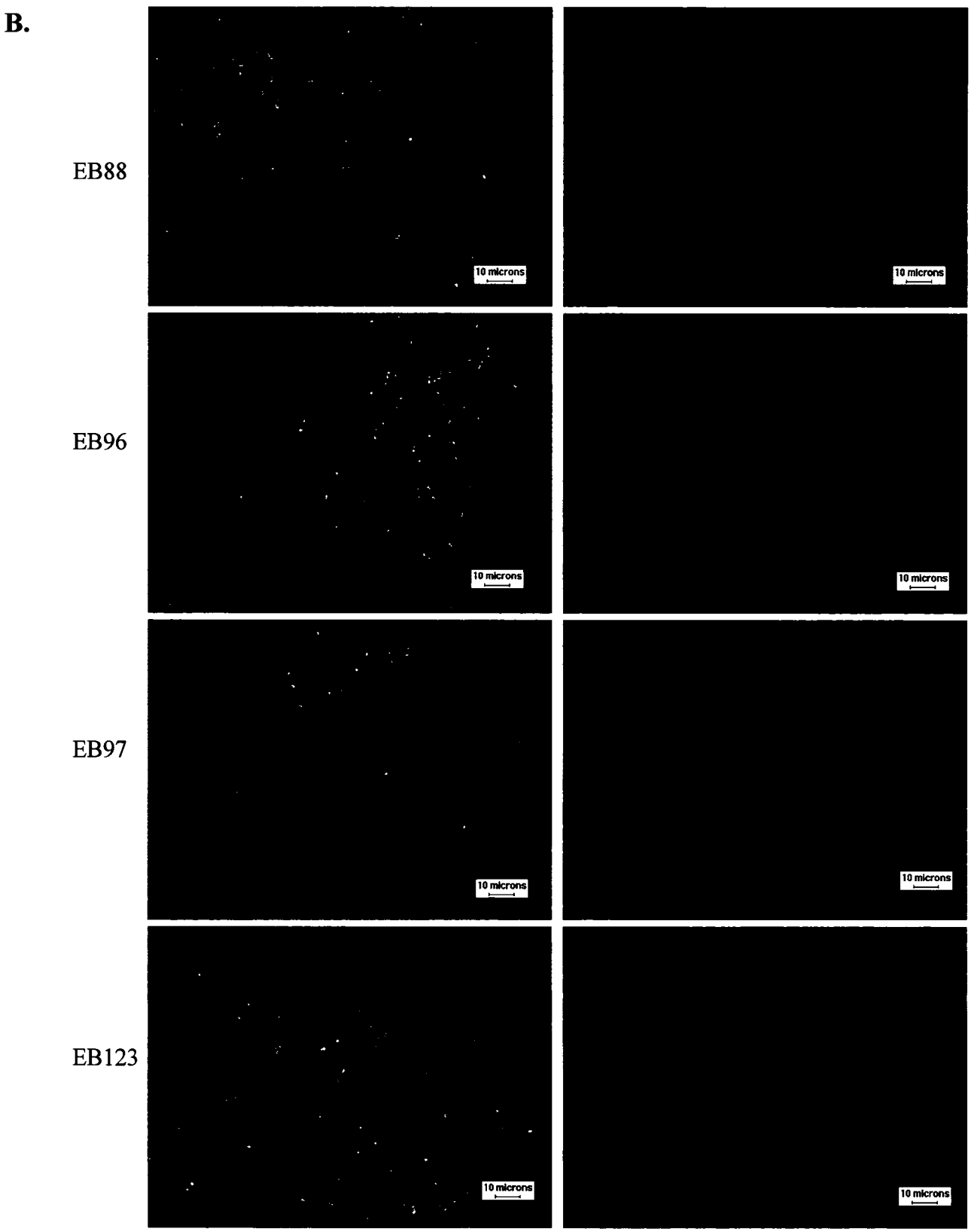

Figure 24: TUNEL positive cells in CT26 tumor bearing lungs at 3 day post-treatment (20X magnification)
Balb/c mice bearing CT26 lung tumors were given a single dose of virus $1.0x10^7$ pfu intranasally and lungs were collected 3 days post-treatment. **A.** PBS, T1L and T3D treated lungs. **B.** EB88, EB96, EB97 and EB123 treated lungs. This composite is made up of photographs of TUNEL labeled cells. The gray images are to demonstrate the location in the lung. The photographs were taken in areas containing CT26 tumors showing the most brightly fluorescing areas and may not be representative of the entire lung section. Scale bars are 10 microns.

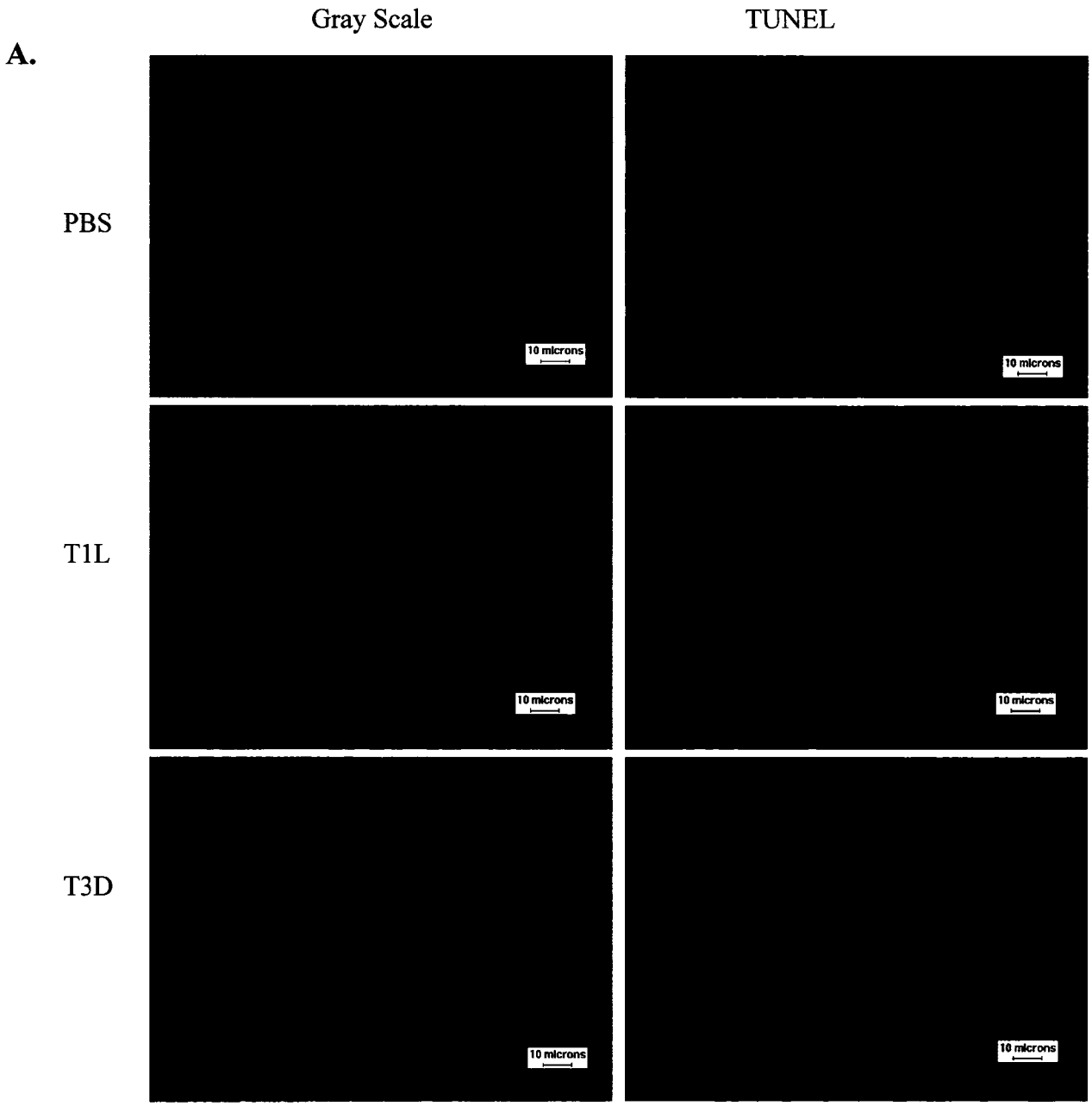

B.

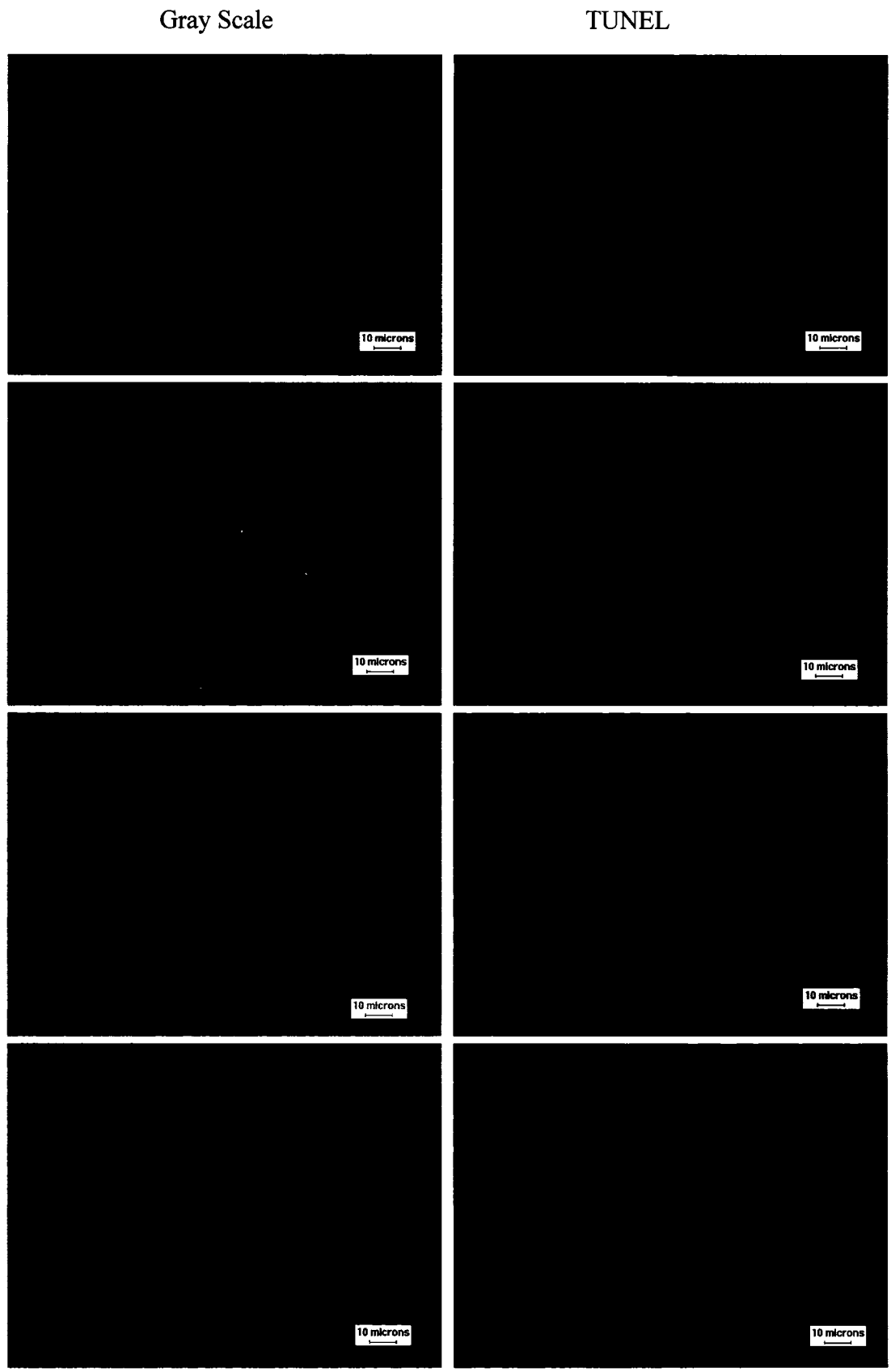

Figure 25: TUNEL positive cells in CT26 tumor bearing lungs at 7 day post-treatment (20X magnification)
Balb/c mice bearing CT26 lung tumors were given a single dose of virus $1.0x10^7$ pfu intranasally and lungs were collected 7 days post-treatment. EB88, EB96, EB97 treated lungs. This composite is made up of photographs of TUNEL labeled cells. The gray images are to demonstrate the location in the lung. The photographs were taken in areas containing CT26 tumors showing the most brightly fluorescing areas and may not be representative of the entire lung section. Scale bars are 10 microns.

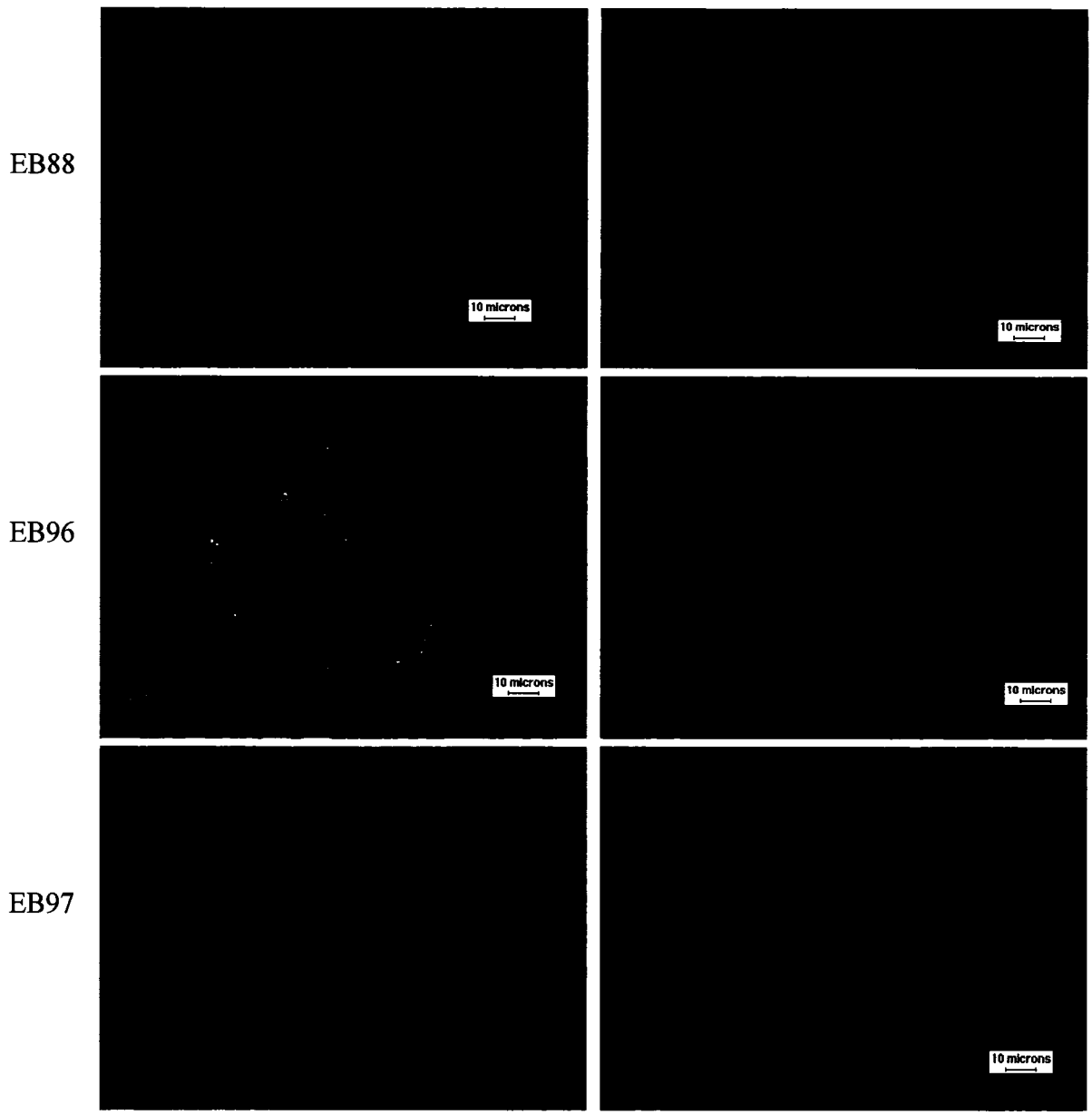

Chapter Five

5. Discussion

5.1 Reovirus in tumor bearing Balb/c mice

I have assessed the genetic basis for differences in the ability of reovirus reassortants to infect the CT26 colon carcinoma cell line that is resistant to lysis by the parental T1L and T3D reoviruses. The reassortants EB88, EB96, EB97, and EB123 have previously been shown to increase survival in Balb/c tumor bearing mice and therefore they were chosen to assess infection in tumor bearing lungs. The viral titers in the lungs of CT26 tumor bearing mice were compared. Two days post-treatment, reassortants EB123 and EB97 yielded higher titers than EB88 and EB96. These two reassortants were also shown to yield high titers in CT26 cells *in vitro*. EB123 and EB97 contain all of the T3D gene segments (S1, L1, L2, M2, and M3) that were determined to play a role in both infectious viral yield and protein production in CT26 cells *in vitro*. T1L yielded the highest titer of all 6 viruses and therefore this would suggest that the *in vitro* results do not completely correlate with the *in vivo* data with respect to viral yield or, at least oncolysis is not relative to viral yield.

The infected lungs were also stained to detect the presence of viral antigen in tumor bearing regions of the lungs. At 1, 2, and 3 days post-treatment EB123 had the highest amounts of viral antigen in tumor bearing regions of the lungs compared to the 3 other reassortants (qualitative analysis). By day 7 post-treatment surviving animals were only found in the groups of mice that were treated with EB88, EB96, and EB97. Interestingly, by day 7 post-treatment, viral antigens could still be detected in lungs of mice treated with EB88 and EB96. EB88 possesses all the gene segments that were required for high viral yield and protein production *in vitro* (S1, L2, and M3) except for the T3D M2 gene segment. EB96

has only one T3D gene segment, the L2 gene segment, which was shown to play a role in viral yield. This suggests that the gene segments involved in viral yield and protein production *in vitro* do not correlate with the extent of viral replication *in vivo*. Although the titers seen in tumor bearing lungs were low for both EB88 and EB96 at 2 days post-treatment their ability to persist in the lungs until day 7 may explain their enhanced tumor killing ability. The tumors that could be detected by H & E staining in lungs treated with EB88 and EB96 were greatly reduced in size by 7 days post-treatment. EB88 and EB96 display attractive oncolytic potential which exceeds that of the parental serotypes. Previous survival studies done by our lab have shown that these two reassortants are able to prolong survival in tumor bearing mice greater than 45 days post-infection. The results of these experiments also suggest that the gene segments important for replication *in vitro* are not necessarily the same as those required for *in vivo* oncolysis. EB88 is a single gene segment exchange reassortant with the T1L M2 gene segment on a T3D background suggesting that the T1L M2 gene segment plays an important role in viral oncolysis. However, the T1L M2 gene segment was not one of the gene segments important for *in vitro* oncolysis. Further study is required to determine which gene segments are beneficial for survival and tumor destruction *in vivo*.

The treated lungs were also assessed for the presence of apoptosis markers. TUNEL positive cells could be detected at both 1 and 2 days post-treatment in tumor bearing regions of the lungs for all 4 of the reovirus reassortants. This suggests that the reassortants are able to induce apoptosis in tumor cells in the lungs. On day 3 post-infection, TUNEL positive cells could not be detected in any of the treated lungs; however, on day 7 post-treatment TUNEL positive cells could once again be seen in lungs that had been treated with EB96. Immunohistochemistry was used to detect the presence of a second marker of apoptosis,

active caspase-3. At all time points post-treatment active caspase-3 could not be detected by immunohistochemistry. Reovirus has been shown to induce apoptosis in a wide variety of cultured cells *in vitro* and in tissue *in vivo* [25]. The presence of active caspase-3 detected in myocardial tissue after viral infection and apoptosis, has been demonstrated to be an important mechanism in the pathogenesis of myocardial injury [32]. It is possible that we were unable to detect caspase-3 in the infected lung because it was being broken down during reovirus infection of this tissue.

5.2 Reovirus viral growth and protein production in resistant CT26 cells line

The murine CT26 cell line is resistant to lysis by T1L and T3D and is therefore a challenging model in which to screen T1L x T3D reassortants for improved oncolytic ability. The use of T1L x T3D reassortants in this model allowed us to determine the key gene segments involved in oncolytic ability. These are gene segments involved in improved viral yield and protein production in the CT26 resistant tumor cell line. Using the non-parametric statistical analysis of Wilcoxin Rank-sum it was determined that the key gene segments involved in viral yield in CT26 cells are the L2 ($p = 0.0028$), M2 ($p = 0.0043$), M3 ($p = 0.0137$), and S1 ($p = 0.000036$) gene segments from T3D (Figure 7c), while the key gene segments involved in protein production are L1 ($p = 0.015$), M3 ($p = 0.0059$), and S1 ($p = 0.0000093$) gene segments from T3D (Table 6). For both viral yield and protein production the S1 gene segment was the most significant determinant. Previous data mapped the M1 gene segment to PKR dependent and independent replication in MEFs (unpublished results). Replication in mouse epithelium was controlled by the S1 gene segment indicating that PKR dependent growth differs between fibroblasts and epithelium. Since 99% of cancers are carcinomas of epithelial origin, replication in epithelial cells is presumably of greater relevance to oncolytic potential. Others in our lab identified that the L1, M1, and S1 gene

segments are antagonists of IFN induction in mouse fibroblasts and data by Sherry *et al.* indicates that the L2, M1, and S2 gene segments of T1L reduced the induction of IFN [83]. This means that the corresponding T3D genome segments are less effective IFN antagonists and therefore, are unable to block the induction of IFN synthesis. Since the working hypothesis of oncolytic viruses is that they exploit a defective IFN response, viruses like T3D, which is more IFN sensitive then T1L, will be highly dependent on the presence of a reduced IFN response for effective growth. Our initial assumption that viruses with the best replication ability in tumor cells will be more effective oncolytic agents was not supported by our findings here. The 2 best oncolytic viruses, EB88 and EB96, *in vivo* were the lowest yielding in CT26 cells for infectious virus and protein production in CT26, MEF and PKR -/- cells (Figure 26). The effectiveness of these viruses as oncolytic agents strongly suggests that tumor destruction involves infection induced cell death via apoptosis. This could be a consequence of direct virus infection or may be a bystander effect of cytokines or other factors induced by the infection of normal tissue.

According to their genotypes, the 4 oncolytic reassortants used in the *in vivo* model can be divided into 2 groups, EB88 and EB96 relative to EB97 and EB123. Considering the 2 groups as distinct and using the genotypes for characterizing features of the groups the only gene segment that discriminates them is the M2 gene segment, where EB88 and EB96 possess the T1L allele, and the less effective EB97 and EB123 possess the T3D allele. Differences in the T1L and T3D M2 gene segments relating to apoptosis have been identified. EB88 is also a single gene segment exchange reassortant possessing the T1L M2 gene segment on a T3D background and this demonstrates clearly that the exchange of this single gene segment has enhanced oncolysis where a single virus challenge can result in the

durable curing of fatal CT26 lung tumors. Observation of the 4 reassortants with improved oncolysis

Figure 26: Reovirus growth and protein production in CT26, MEF and PKR -/- cells
A. Viral growth in CT26 cells ranked from highest to lowest with the 4 reassortants that have improved oncolytic ability *in vivo* boxed in red. **B.** Protein production in CT26 cells ranked from highest to lowest with the 4 reassortants that have improved oncolytic ability *in vivo* boxed in red. **C.** Protein production in MEF cells ranked from highest to lowest with the 4 reassortants that have improved oncolytic ability *in vivo* boxed in red. **D.** Protein production in PKR -/- cells ranked from highest to lowest with the 4 reassortants that have improved oncolytic ability *in vivo* boxed in red.

A. Viral growth in CT26 cells

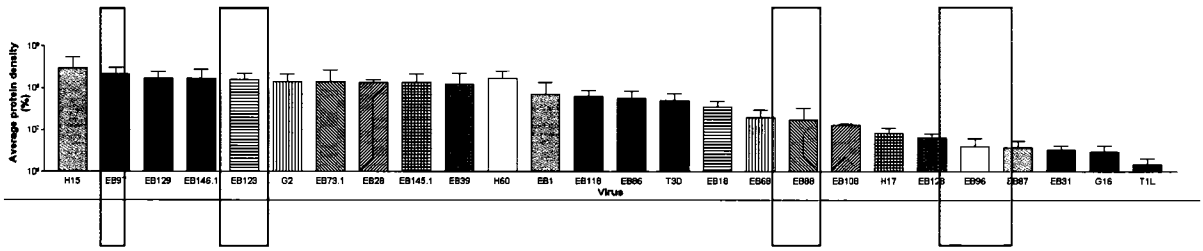

B. Protein production in CT26 cells

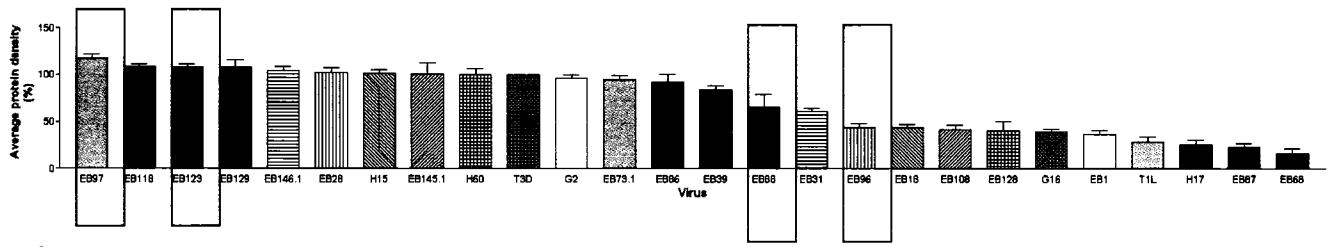

C. Protein production in MEF cells

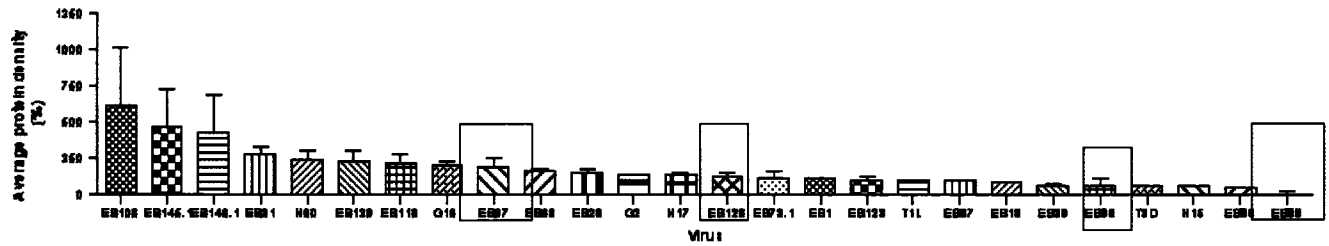

D. Protein production in PKR -/- cells

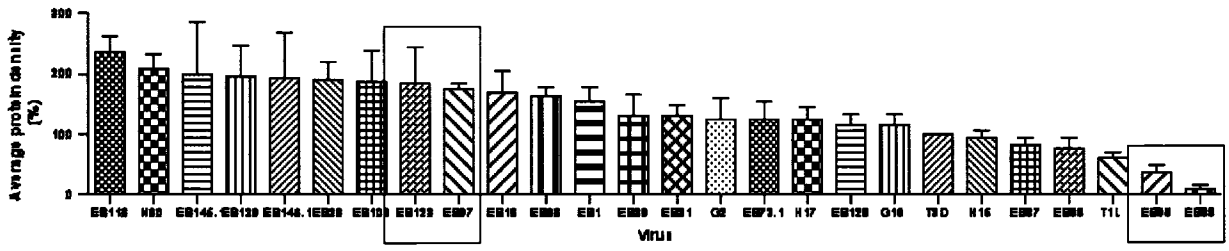

in vivo, they all possess the T3D L2 and M1 gene segments that lead to enhanced CT26 replication and IFN and PKR sensitivity, respectively. The overall pattern we observed suggests that improved oncolysis can be achieved by a combination of T3D L2 and M1 gene segments in addition to the T1L M2 gene segment.

5.3 Reovirus gene segments involved in oncolysis in CT26 cells

The S1 gene segment

The S1 gene segment is bicistronic and it codes for the receptor binding protein σ1, and for the nonstructural protein σ1s. The S1 gene segment has been shown to play a pivotal role in viral infection and tissue tropism. A possible explanation for the importance of the S1 gene segment in determining viral yield and protein production in CT26 cells is that the T3D σ1 protein is more specific for CT26 cell surface receptors than the σ1 protein of T1L and it is therefore more efficient during viral entry and spread. The S1 gene segment has previously been shown to be responsible for serotype differences seen in viral spread. T1L spreads to the CNS by a hematogenous route while T3D spreads to the CNS via microtubule-associated fast axonal transport [97]. It has also been demonstrated previously that the S1 gene segment was the critical determinant of serotype specific viral yield in the brains and intestines of SCID mice [40]. The capacity of reovirus to grow and survive in intestinal tissue has also been linked to the L2 and S1 gene segments of T1L [9]. T1L can be recovered from the intestines of neonatal mice up to 8 days post-peroral inoculation whereas T3D cannot be recovered past day 4 [9]. These results clearly demonstrate that the S1 gene segment plays a critical role in the serotype specific productivity of viral infection in different tissues and cell types; however, these studies did not differentiate between the receptor binding protein σ1 or the nonstructural protein σ1s.

Early studies demonstrated that the S1 gene segment is a critical determinant in the induction of apoptosis with T3D being able to induce apoptosis to a greater extent than T1L [76,98]. Early studies have shown that the binding of σ1 to cell surface sialic acid is involved in the induction of apoptosis. T3SA-, a non-sialic acid binding strain induces little or no apoptosis in HeLa and L cells, but the T3SA+, which does bind to sialic acid, does induce apoptosis [27]. The differences in the capacity of T3SA- and T3SA+ to induce apoptosis was not due to differences in protein synthesis or viral yield [27]. However, more recent studies have brought the importance of the S1 gene segment in reovirus-induced apoptosis into question. Danthi *et al.* demonstrated that in Chinese hamster ovary (CHO) cells expressing the Fc receptor but, not JAM-A or sialic acid, infection and reovirus-induced apoptosis could occur when the σ1 protein is prebound with monoclonal antibodies such that the Fc portion of the antibody mediates viral attachment [31]. The use of T1L x T3D reassortants in this study showed that the M2 gene segment is the only determinant for reovirus induced apoptosis [31]. This suggests that the S1 gene segment is not the critical determinant for apoptosis and that the signaling pathways activated by binding of σ1 to JAM-A and sialic acid are not needed for reovirus-induced apoptosis.

The σ1 protein is not the only S1 gene segment product that has been shown to be involved in apoptosis in infected cells, the nonstructural protein σ1s also plays a role. Two day old mice inoculated with either σ1s- or σ1s+ reovirus strains exhibited differences in the extent of apoptosis induced in both the heart and the CNS [45]. Viral replication was not affected by the presence or absence of σ1s but virus induced caspase-3 activation and histological tissue damage in both the heart and the brain was significantly reduced in σ1s- viruses [45]. This suggests that the nonstructural protein σ1s plays a role in pathogenesis and virulence.

Reovirus induced apoptosis occurs late in infection and this suggests that replication events are needed to amplify the apoptotic signals that accompany cell entry [19]. If σ1 binding is not a critical determinant for apoptosis it could be that the *de novo* expression of S1 gene products plays a role in inducing apoptosis. The ability of the S1 gene segment from T3D to induce apoptosis to a greater extent then the S1 gene segment from T1L is beneficial to viral spread since reovirus is released from the cell upon cell lysis. Therefore, the σ1 protein of T3D may be more efficient at viral entry and spread. When these features are combined with the increased viral yield and protein production observed in CT26 cells, it makes the S1 gene segment from T3D an attractive gene segment for an oncolytic virus. The requirement of the T3D S1 gene segment for infection of TIK-/- epithelial cells may be suggestive of its use in reassortants targeting cancerous epithelium. In support of this 3 of the 4 reassortants with improved oncolytic ability *in vivo* had the T3D S1 gene segment. However, EB96 possesses the T1L S1 gene segment indicating that the T3D S1 may not be absolute requirement in an oncolytic virus.

The M2 gene segment

The M2 gene segment from T3D plays a role in the serotype specific increase in viral yield observed in the CT26 cell line. The M2 gene segment encodes the major outer capsid protein μ1. There are 600 copies of the μ1 protein per virion and several studies suggest that one or more of the μ1 cleavage products interact with the cellular membranes to allow penetration of ISVPs into the cytoplasm [67,72]. The μ1 protein plays an important role in viral entry, and this could be the reason for the serotype specific viral yield seen in the resistant CT26 cells. If viruses with the T3D μ1 protein are more efficiently uncoated upon entry into the cell, this would result in more cells being infected and hence a greater viral yield. The recent evidence that implicates the M2 gene segment as the critical determinant for

apoptosis[31] may suggest that the increased ability to cause apoptosis leads to more efficient viral spread.

The M3 gene segment

The M3 gene segment of T3D plays a role in increased protein production in the CT26 cells. The M3 gene segment encodes the nonstructural protein μNS, responsible for the formation of viral inclusion bodies, which are the sites of reovirus replication [5,12,14]. The role that μNS plays in viral inclusion bodies may contribute to the serotype specific increase in viral yield observed in the CT26 cells.

The L1 gene segment

The L1 gene from T3D plays a role in the increased levels of protein production in the resistant CT26 cell line. This is not surprising since the L1 gene segment codes for the λ3 protein which is the viral RNA-dependent RNA polymerase. Therefore, if the λ3 protein of T3D is more efficient than that of T1L, more viral mRNA is available for translation and this results in a higher level of viral protein production.

The L2 gene segment

The L2 gene segment encodes the λ2 core spike protein which possesses guanyltransferase and methyltransferase activity. The L2 gene segment of T3D also seems to contribute to enhancing viral yields in the resistant CT26 cell line, although by an unknown mechanism.

5.4 Reovirus in the presence or absence of PKR *in vitro*

The panel of T1L x T3D reassortants was used to determine which genes were important for viral protein production in the presence or absence of PKR. The L3 gene segment codes for the λ1 protein which is a core capsid protein that has RNA binding ability as well as NTPase and helicase activities. The L3 gene segment has previously been shown

by our lab to be the main determinant for PKR independent growth in PKR-/- cells (unpublished data). In this study, the L3 gene segment from T1L was shown to be involved in the levels of protein production in the presence of PKR. The L1 gene from T1L and the M2 gene from T3D were important for viral protein production in the absence of PKR. It is interesting that in the CT26 cells, which are epithelial cells, the S1 gene is the primary determinant of both viral replication and protein production with the L2, M2 and M3 genes playing a secondary role in viral replication and the L1 and M3 genes playing a secondary role in protein production. The MEF cells are fibroblasts and therefore this suggests that different genes are important in different cell types. The difference observed could also be due to the fact that the CT26 cells are transformed and the MEF cells are normal cells. Therefore, the T1L L3 gene segment is important for protein production in the presence of PKR in normal fibroblast cells. The T1L L1 and the T3D M2 gene segments are important for protein production in the absence of PKR in normal fibroblast cells. Thus, these two gene segments may be good candidates for an oncolytic virus that is targeting fibroblast tumors with defective PKR due to activated Ras pathways.

Table 8: Summary of the T1L and T3D gene segments involved in infection and pathogenesis. Data in bold is from the work of this study.

	Gene Segments									
Role in infection	**L1**	**L2**	**L3**	**M1**	**M2**	**M3**	**S1**	**S2**	**S3**	**S4**
IFN-antagonist (L929)	D<			D<			D<			
IFN-antagonist (myocites)		D<		D<				D<		
PKR-antagonist (MEF)				D<						D/L
Bronchiial epithelium (BE)in TIK-/- mice							**D**			
Growth (MEF)			D<	D<						
Growth (L929)	D<		D<							
Growth (E/CT26)		**D>**			**D>**	**D>**	**D>>**			
Growth (myocites)	D<		D<	D<						
protein synth MEF			**L>**							
protein synth PKR -/-	**L>**				**D>**					
protein synth CT26	**D>**					**D>**	**D>>**			
Myocarditis (T1L)		L		L						
hepatits scid mice										
apoptosis L929 (L vs D)					D>		D>			
apoptosis MDCK (L vs D)					D>		D>			

5.5 Reovirus tropism in the absence of PKR

Earlier studies have shown that PKR plays a direct role in determining the resistance of untransformed cells to reovirus replication. The PKR gene is absent or inactive in many tumor types [6,84,93]. The downregulation of PKR in cancer cells provides a breach in the anti-viral defenses of the cell and this downregulation is beneficial in terms of oncolytic susceptibility to viruses such as reovirus [88], influenza virus mutants [8], and herpes simplex virus [35] as well as its mutants [47,61].

The genetic basis for reovirus PKR sensitivity, with respect to viral growth, was previously demonstrated in our lab (unpublished data). The replication of the T1L and T3D strains was compared in MEF and PKR -/- cells. It was observed that both T1L and T3D grew to higher titers in the PKR -/- cells, but that TIL grew better than T3D in both PKR-/- and MEF cells. A panel of T1L x T3D reassortants was then used to determine which genes were involved in generating high viral yields in the absence of PKR. As a result of this study, it was demonstrated that the M1 gene segment from T3D controls PKR sensitivity and the T1L L3 gene segment controlled the increased viral yield in the absence of PKR. To better understand which genes are involved in the absence of PKR *in vivo* we infected PKR-/- mice with T1L and T3D reovirus. PKR-/- mice are much more susceptible to killing by oncolytic viruses such as vesicular stomatitis virus [87] and herpes simplex virus [53]. Infection of the PKR-/- mice with the parental strains revealed a serotype specific tropism that occurred when PKR was knocked out. T3D but not T1L could infect the bronchial epithelial cells that are protected from infection in wild-type Balb/c mice with active PKR. To determine what genes were involved PKR-/- mice were infected with a panel of T1L x T3D reassortant viruses and the tropism in the absence of PKR mapped to the S1 gene segment of T3D. To confirm that the S1 gene segment of T3D was the sole determinant for bronchial

epithelial tropism in the lungs of PKR-/- mono-reassortant viruses 1HA3 and 3HA1 were used. The 1HA3 virus contained all the gene segments of T1L with only the S1 gene segment being derived from T3D. The 3HA1 contained all of the T3D gene segments except for the S1 gene segment derived from T1L. Infection of PKR-/- mice with the mono-reassortant viruses confirmed that the S1 gene segment from T3D is the sole determinant for the serotype specific viral tropism seen in the PKR-/- mice. This suggests that in wild-type mice the bronchial epithelial cells are protected from reovirus infection and that in the absence of PKR the bronchial epithelial cells become susceptible to infection by T3D or viruses with the T3D S1 gene segment. Mono-reassortant 1HA3 and 3HA1 viruses were also used to confirm the role of the S1 gene segment in the CNS cell tropism of reovirus T1L and T3D. In the CNS, T1L infects ependymal cells whereas T3D infects neuronal cells; this is due to differences in their S1 gene segments [100]. The serotype specific cell tropism that occurs in the absence of PKR may be a result of interactions with specific cell surface receptors leading to a block in viral entry for T1L but not for T3D, but could also be due to the nonstructural protein σ1s once the virus has entered the cell. This cell type specificity may also involve a step in viral replication preceding protein synthesis that occurs after the virus has entered the cell. However, it is important to understand the gene segments involved in viral cell tropism so that the novel reassortant viruses may contain the optimal combination of gene segments that will make them more specific for the tumor cell types for which they are targeted.

5.6 Conclusions

1) Different reovirus genes are involved in the productivity and permissiveness of infection in different cell types. In fibroblasts the T1L L3 gene was important for protein production in the presence of PKR in MEF and the T1L L1 and T3D M2 genes segments were involved in protein production in the absence of PKR. However, in epithelial cells the primary gene segment involved in viral yield and protein production in CT26 cells was the T3D S1 gene segment. This gene segment was also the primary determinant of PKR replication in bronchial epithelial cells in the TIK -/- mouse lung. This suggests that the genetic basis for permissive replication differs between fibroblasts and epithelium. These data also suggest that the mechanisms for PKR action are dependent on the cell type and presumably the tumor type.

2) From the T1L x T3D reassortant experiments it was shown that in normal MEF the T1L L3 gene segment is important for protein production in the presence of PKR. In the PKR -/- cells the T1L L1 and T3D M2 gene segments are important for protein production in the absence of PKR.

3) The reassortant EB88 has improved oncolytic ability *in vivo* and has a single gene segment exchange possessing the T1L M2 gene segment on a T3D background. This clearly demonstrates that the T1L M2 gene plays an important role in improved oncolytic ability *in vivo.* The 4 reassortants (EB88, EB96, EB97 and EB123) with improved oncolytic ability *in vivo* all possess the T3D L2 and M1 gene segments. This suggests that improved oncolysis can be achieved by a combination of T3D L2 and M1 gene segments in addition to the T1L L3 gene segment.

4) High levels of viral replication do not necessarily translate into better oncolysis and tumor killing. EB88 and EB96 yielded the lowest levels of infectious virus and protein in

CT26 cells *in vitro*. However, as seen in the survival study and the H & E images, these reassortants were able to prolong survival in CT26 tumor bearing mice and visually reduce tumor size and burden in the lungs 7 days post-infection following a singe dose of virus. The effectiveness of these viruses as oncolytic agents strongly suggests that tumor destruction involves infection induced cell death via apoptosis. This could be a consequence of direct virus infection or by a bystander effect of cytokines or other factors induced by the infection of normal tissue.

5) The data in this thesis provide a proof of principle that the oncolytic ability of reovirus can be improved to include resistant tumor types through the creation of reovirus reassortants possessing specific gene combinations that are optimal for oncolysis of different tumor types.

Reference List

1. Alain, T., K. Hirasawa, K. J. Pon, S. G. Nishikawa, S. J. Urbanski, Y. Auer, J. Luider, A. Martin, R. N. Johnston, A. Janowska-Wieczorek, P. W. Lee, and A. E. Kossakowska. 2002. Reovirus therapy of lymphoid malignancies. Blood 100:4146-4153.

2. Antczak, J. B. and W. K. Joklik. 1992. Reovirus genome segment assortment into progeny genomes studied by the use of monoclonal antibodies directed against reovirus proteins. Virology 187:760-776.

3. Barton, E. S., J. C. Forrest, J. L. Connolly, J. D. Chappell, Y. Liu, F. J. Schnell, A. Nusrat, C. A. Parkos, and T. S. Dermody. 2001. Junction adhesion molecule is a receptor for reovirus. Cell 104:441-451.

4. Bass, D. M., D. Bodkin, R. Dambrauskas, J. S. Trier, B. N. Fields, and J. L. Wolf. 1990. Intraluminal proteolytic activation plays an important role in replication of type 1 reovirus in the intestines of neonatal mice. J. Virol. 64:1830-1833.

5. Becker, M. M., M. I. Goral, P. R. Hazelton, G. S. Baer, S. E. Rodgers, E. G. Brown, K. M. Coombs, and T. S. Dermody. 2001. Reovirus sigmaNS protein is required for nucleation of viral assembly complexes and formation of viral inclusions. J. Virol. 75:1459-1475.

6. Bell, J. C., K. A. Garson, B. D. Lichty, and Stojdl.D.F. 2002. Oncolytic viruses: programmable tumor hunters. Curr. Gene Ther.243-254.

7. Bell, J. C., B. Lichty, and D. Stojdl. 2003. Getting oncolytic virus therapies off the ground. Cancer Cell 4:7-11.

8. Bergmann, M., I. Romirer, M. Sachet, R. Fleischhacker, A. Garcia-Sastre, P. Palese, K. Wolff, H. Pehamberger, R. Jakesz, and T. Muster. 2001. A genetically engineered influenza A virus with ras-dependent oncolytic properties. Cancer Res. 61:8188-8193.

9. Bodkin, D. K. and B. N. Fields. 1989. Growth and survival of reovirus in intestinal tissue: role of the L2 and S1 genes. J. Virol. 63:1188-1193.

10. Brentano, L., D. L. Noah, E. G. Brown, and B. Sherry. 1998. The reovirus protein mu2, encoded by the M1 gene, is an RNA-binding protein. J. Virol. 72:8354-8357.

11. Breun, L. A., T. J. Broering, A. M. McCutcheon, S. J. Harrison, C. L. Luongo, and M. L. Nibert. 2001. Mammalian reovirus L2 gene and lambda2 core spike protein sequences and whole-genome comparisons of reoviruses type 1 Lang, type 2 Jones, and type 3 Dearing. Virology 287:333-348.

12. Broering, T. J., M. M. Arnold, C. L. Miller, J. A. Hurt, P. L. Joyce, and M. L. Nibert. 2005. Carboxyl-proximal regions of reovirus nonstructural protein muNS necessary and sufficient for forming factory-like inclusions. J. Virol. 79:6194-6206.

13. Broering, T. J., J. Kim, C. L. Miller, C. D. Piggott, J. B. Dinoso, M. L. Nibert, and J. S. Parker. 2004. Reovirus nonstructural protein mu NS recruits viral core surface proteins and entering core particles to factory-like inclusions. J. Virol. 78:1882-1892.

14. Broering, T. J., J. S. Parker, P. L. Joyce, J. Kim, and M. L. Nibert. 2002. Mammalian reovirus nonstructural protein microNS forms large inclusions and colocalizes with reovirus microtubule-associated protein micro2 in transfected cells. J. Virol. 76:8285-8297.

15. Brown, E. G., M. L. Nibert, and B. N. Fields. 1983. The L2 gene of reovirus serotype 3 controls the capacity to interfere, accumulate deletions and establish persistent infections. Double-Streanded RNA Viruses, p. 275-287. *In* R. W. Compans and D. H. L. Bishop (eds.), Elviser Science Publishing Co., Inc..

16. Canning, W. M. and B. N. Fields. 1983. Ammonium chloride prevents lytic growth of reovirus and helps to establish persistent infection in mouse L cells. Science 219:987-988.

17. Chandran, K. and M. L. Nibert. 1998. Protease cleavage of reovirus capsid protein mu1/mu1C is blocked by alkyl sulfate detergents, yielding a new type of infectious subvirion particle. J. Virol. 72:467-475.

18. Chappell, J. D., V. L. Gunn, J. D. Wetzel, G. S. Baer, and T. S. Dermody. 1997. Mutations in type 3 reovirus that determine binding to sialic acid are contained in the fibrous tail domain of viral attachment protein sigma1. J. Virol. 71:1834-1841.

19. Clarke, P., R. L. Debiasi, R. Goody, C. C. Hoyt, S. Richardson-Burns, and K. L. Tyler. 2005. Mechanisms of reovirus-induced cell death and tissue injury: role of apoptosis and virus-induced perturbation of host-cell signaling and transcription factor activation. Viral Immunol. 18:89-115.

20. Clarke, P., R. L. Debiasi, S. M. Meintzer, B. A. Robinson, and K. L. Tyler. 2005. Inhibition of NF-kappa B activity and cFLIP expression contribute to viral-induced apoptosis. Apoptosis. 10:513-524.

21. Clarke, P., S. M. Meintzer, S. Gibson, C. Widmann, T. P. Garrington, G. L. Johnson, and K. L. Tyler. 2000. Reovirus-induced apoptosis is mediated by TRAIL. J. Virol. 74:8135-8139.

22. Clarke, P., S. M. Meintzer, A. C. Spalding, G. L. Johnson, and K. L. Tyler. 2001. Caspase 8-dependent sensitization of cancer cells to TRAIL-induced apoptosis following reovirus-infection. Oncogene 20:6910-6919.

23. Clarke, P., S. M. Meintzer, Y. Wang, L. A. Moffitt, S. M. Richardson-Burns, G. L. Johnson, and K. L. Tyler. 2004. JNK regulates the release of proapoptotic mitochondrial factors in reovirus-infected cells. J. Virol. 78:13132-13138.

24. Clarke, P., S. M. Richardson-Burns, R. L. Debiasi, and K. L. Tyler. 2005. Mechanisms of apoptosis during reovirus infection. Curr. Top. Microbiol. Immunol. 289:1-24.

25. Clarke, P. and K. L. Tyler. 2003. Reovirus-induced apoptosis: A minireview. Apoptosis. 8:141-150.

26. Coffey, M. C., J. E. Strong, P. A. Forsyth, and P. W. Lee. 1998. Reovirus therapy of tumors with activated Ras pathway. Science 282:1332-1334.

27. Connolly, J. L., E. S. Barton, and T. S. Dermody. 2001. Reovirus binding to cell surface sialic acid potentiates virus-induced apoptosis. J. Virol. 75:4029-4039.

28. Connolly, J. L., S. E. Rodgers, P. Clarke, D. W. Ballard, L. D. Kerr, K. L. Tyler, and T. S. Dermody. 2000. Reovirus-induced apoptosis requires activation of transcription factor NF-kappaB. J. Virol. 74:2981-2989.

29. Coombs, K. M. 2006. Reovirus structure and morphogenesis. Curr. Top. Microbiol. Immunol. 309:117-167.

30. Coombs, K. M. 2006. Reovirus structure and morphogenesis. Curr. Top. Microbiol. Immunol. 309:117-167.

31. Danthi, P., M. W. Hansberger, J. A. Campbell, J. C. Forrest, and T. S. Dermody. 2006. JAM-A-independent, antibody-mediated uptake of reovirus into cells leads to apoptosis. J. Virol. 80:1261-1270.

32. Debiasi, R. L., B. A. Robinson, B. Sherry, R. Bouchard, R. D. Brown, M. Rizeq, C. Long, and K. L. Tyler. 2004. Caspase inhibition protects against reovirus-induced myocardial injury in vitro and in vivo. J. Virol. 78:11040-11050.

33. Dryden, K. A., G. Wang, M. Yeager, M. L. Nibert, K. M. Coombs, D. B. Furlong, B. N. Fields, and T. S. Baker. 1993. Early steps in reovirus infection are associated with dramatic changes in supramolecular structure and protein conformation: analysis of virions and subviral particles by cryoelectron microscopy and image reconstruction. J. Cell Biol. 122:1023-1041.

34. Duncan, M. R., S. M. Stanish, and D. C. Cox. 1978. Differential sensitivity of normal and transformed human cells to reovirus infection. J. Virol. 28:444-449.

35. Farassati, F., A. D. Yang, and P. W. Lee. 2001. Oncogenes in Ras signalling pathway dictate host-cell permissiveness to herpes simplex virus 1. Nat. Cell Biol 3:745-750.

36. Gillian, A. L., S. C. Schmechel, J. Livny, L. A. Schiff, and M. L. Nibert. 2000. Reovirus protein sigmaNS binds in multiple copies to single-stranded RNA and shares properties with single-stranded DNA binding proteins. J. Virol. 74:5939-5948.

37. Gomatos, P. J., O. Prakash, and N. M. Stamatos. 1981. Small reovirus particle composed solely of sigma NS with specificity for binding different nucleic acids. J. Virol. 39:115-124.

38. Gomatos, P. J., N. M. Stamatos, and N. H. Sarkar. 1980. Small reovirus-specific particle with polycytidylate-dependent RNA polymerase activity. J. Virol. 36:556-565.

39. Guglielmi, K. M., E. M. Johnson, T. Stehle, and T. S. Dermody. 2006. Attachment and cell entry of mammalian orthoreovirus. Curr. Top. Microbiol. Immunol. 309:1-38.

40. Haller, B. L., M. L. Barkon, G. P. Vogler, and H. W. Virgin. 1995. Genetic mapping of reovirus virulence and organ tropism in severe combined immunodeficient mice: organ-specific virulence genes. J. Virol. 69:357-364.

41. Hashiro, G., P. C. Loh, and J. T. Yau. 1977. The preferential cytotoxicity of reovirus for certain transformed cell lines. Arch. Virol. 54:307-315.

42. Hazelton, P. R. and K. M. Coombs. 1995. The reovirus mutant tsA279 has temperature-sensitive lesions in the M2 and L2 genes: the M2 gene is associated with decreased viral protein production and blockade in transmembrane transport. Virology 207:46-58.

43. Helander, A., K. J. Silvey, N. J. Mantis, A. B. Hutchings, K. Chandran, W. T. Lucas, M. L. Nibert, and M. R. Neutra. 2003. The viral sigma1 protein and glycoconjugates containing alpha2-3-linked sialic acid are involved in type 1 reovirus adherence to M cell apical surfaces. J. Virol. 77:7964-7977.

44. Hirasawa, K., S. G. Nishikawa, K. L. Norman, T. Alain, A. Kossakowska, and P. W. Lee. 2002. Oncolytic reovirus against ovarian and colon cancer. Cancer Res. 62:1696-1701.

45. Hoyt, C. C., S. M. Richardson-Burns, R. J. Goody, B. A. Robinson, R. L. Debiasi, and K. L. Tyler. 2005. Nonstructural protein sigma1s is a determinant of reovirus virulence and influences the kinetics and severity of apoptosis induction in the heart and central nervous system. J. Virol. 79:2743-2753.

46. Huismans, H. and W. K. Joklik. 1976. Reovirus-coded polypeptides in infected cells: isolation of two native monomeric polypeptides with affinity for single-stranded and double-stranded RNA, respectively. Virology 70:411-424.

47. Hunter, W. D., R. L. Martuza, F. Feigenbaum, T. Todo, T. Mineta, T. Yazaki, M. Toda, J. T. Newsome, R. C. Platenberg, H. J. Manz, and S. D. Rabkin. 1999. Attenuated, replication-competent herpes simplex virus type 1 mutant G207: safety evaluation of intracerebral injection in nonhuman primates. J. Virol. 73:6319-6326.

48. Ikeda, Y., G. Nishimura, S. Yanoma, A. Kubota, M. Furukawa, and M. Tsukuda. 2004. Reovirus oncolysis in human head and neck squamous carcinoma cells. Auris Nasus Larynx 31:407-412.

49. Jagus, R., B. Joshi, and and Barber GN. 1999. PKR, apoptosis and cancer. Int. J. Biochem. Cell Biol 31:123-138.

50. Joklik, W. K. and M. R. Roner. 1995. What reassorts when reovirus genome segments reassort? J. Biol. Chem. 270:4181-4184.

51. Kominsky, D. J., R. J. Bickel, and K. L. Tyler. 2002. Reovirus-induced apoptosis requires both death receptor- and mitochondrial-mediated caspase-dependent pathways of cell death. Cell Death. Differ. 9:926-933.

52. Lee, P. W. and R. Gilmore. 1998. Reovirus cell attachment protein sigma 1: structure-function relationships and biogenesis. Curr. Top. Microbiol. Immunol. 233:137-153.

53. Leib, D. A., M. A. Machalek, B. R. Williams, R. H. Silverman, and H. W. Virgin. 2000. Specific phenotypic restoration of an attenuated virus by knockout of a host resistance gene. Proc. Natl. Acad. Sci. U. S. A 97:6097-6101.

54. Lucia-Jandris, P., J. W. Hooper, and B. N. Fields. 1993. Reovirus M2 gene is associated with chromium release from mouse L cells. J. Virol. 67:5339-5345.

55. Luongo, C. L., K. M. Reinisch, S. C. Harrison, and M. L. Nibert. 2000. Identification of the guanylyltransferase region and active site in reovirus mRNA capping protein lambda2. J. Biol Chem. 275:2804-2810.

56. Luongo, C. L., X. Zhang, S. B. Walker, Y. Chen, T. J. Broering, D. L. Farsetta, V. D. Bowman, T. S. Baker, and M. L. Nibert. 2002. Loss of activities for mRNA synthesis accompanies loss of lambda2 spikes from reovirus cores: an effect of lambda2 on lambda1 shell structure. Virology 296:24-38.

57. Mao, Z. X. and W. K. Joklik. 1991. Isolation and enzymatic characterization of protein lambda 2, the reovirus guanylyltransferase. Virology 185:377-386.

58. Matoba, Y., W. S. Colucci, B. N. Fields, and T. W. Smith. 1993. The reovirus M1 gene determines the relative capacity of growth of reovirus in cultured bovine aortic endothelial cells. J. Clin. Invest 92:2883-2888.

59. Matoba, Y., B. Sherry, B. N. Fields, and T. W. Smith. 1991. Identification of the viral genes responsible for growth of strains of reovirus in cultured mouse heart cells. J. Clin. Invest 87:1628-1633.

60. Miller, C. L., T. J. Broering, J. S. Parker, M. M. Arnold, and M. L. Nibert. 2003. Reovirus sigma NS protein localizes to inclusions through an association requiring the mu NS amino terminus. J. Virol. 77:4566-4576.

61. Mineta, T., S. D. Rabkin, T. Yazaki, W. D. Hunter, and R. L. Martuza. 1995. Attenuated multi-mutated herpes simplex virus-1 for the treatment of malignant gliomas. Nat. Med 1:938-943.

62. Morin, M. J., A. Warner, and B. N. Fields. 1996. Reovirus infection in rat lungs as a model to study the pathogenesis of viral pneumonia. J. Virol. 70:541-548.

63. Nibert, M. L. and B. N. Fields. 1992. A carboxy terminal fragment of protein μ1/μ1c is present in infectious subvirion particles of mammalian Reoviruses and is proposed to have a role in penetration. J. Virol. 66:6408-6418.

64. Nibert, M. L., R. L. Margraf, and K. M. Coombs. 1996. Nonrandom segregation of parental alleles in reovirus reassortants. J. Virol. 70:7295-7300.

65. Nibert, M. L., A. L. Odegard, M. A. Agosto, K. Chandran, and L. A. Schiff. 2005. Putative autocleavage of reovirus mu1 protein in concert with outer-capsid disassembly and activation for membrane permeabilization. J. Mol. Biol 345:461-474.

66. Nibert, M. L. and L. A. Schiff. 2001. Reoviruses and thier replication; Fields virology, p. 1679-1719. Lippincott Williams & Wilkins, Philidelphia.

67. Nibert, M. L., L. A. Schiff, and B. N. Fields. 1991. Mammalian reoviruses contain a myristoylated structural protein. J. Virol. 65:1960-1967.

68. Nonoyama, M. and A. F. Graham. 1970. Appearance of defective virions in clones of reovirus. J. Virol. 6:693-694.

69. Nonoyama, M., Y. Watanabe, and A. F. Graham. 1970. Defective virions of reovirus. J. Virol. 6:226-236.

70. Norman, K. L., M. C. Coffey, K. Hirasawa, D. J. Demetrick, S. G. Nishikawa, L. M. DiFrancesco, J. E. Strong, and P. W. Lee. 2002. Reovirus oncolysis of human breast cancer. Hum. Gene Ther. 13:641-652.

71. Norman, K. L., K. Hirasawa, A. D. Yang, M. A. Shields, and P. W. Lee. 2004. Reovirus oncolysis: the Ras/RalGEF/p38 pathway dictates host cell permissiveness to reovirus infection. Proc. Natl. Acad. Sci. U. S. A 101:11099-11104.

72. Odegard, A. L., K. Chandran, X. Zhang, J. S. Parker, T. S. Baker, and M. L. Nibert. 2004. Putative autocleavage of outer capsid protein micro1, allowing release of myristoylated peptide micro1N during particle uncoating, is critical for cell entry by reovirus. J. Virol. 78:8732-8745.

73. Parato, K. A., D. Senger, P. Forsyth, and J. C. Bell. 2005. Recent progress in the battler between oncolytic viruses and tumors. Nature Rev. Cancer 5:965-976.

74. Parker, J. S., T. J. Broering, J. Kim, D. E. Higgins, and M. L. Nibert. 2002. Reovirus core protein mu2 determines the filamentous morphology of viral inclusion bodies by interacting with and stabilizing microtubules. J. Virol. 76:4483-4496.

75. Richardson-Burns, S. M. and K. L. Tyler. 2004. Regional differences in viral growth and central nervous system injury correlate with apoptosis. J. Virol. 78:5466-5475.

76. Rodgers, S. E., E. S. Barton, S. M. Oberhaus, B. Pike, C. A. Gibson, K. L. Tyler, and T. S. Dermody. 1997. Reovirus-induced apoptosis of MDCK cells is not linked to viral yield and is blocked by Bcl-2. J. Virol. 71:2540-2546.

77. Roner, M. R., K. Bassett, and J. Roehr. 2004. Identification of the 5' sequences required for incorporation of an engineered ssRNA into the Reovirus genome. Virology 329:348-360.

78. Schiff, L. A. 1998. Reovirus capsid proteins sigma 3 and mu 1: interactions that influence viral entry, assembly, and translational control. Curr. Top. Microbiol. Immunol. 233:167-183.

79. Selb, B. and B. Weber. 1994. A study of human reovirus IgG and IgA antibodies by ELISA and western blot. J. Virol. Methods 47:15-25.

80. Sharpe, A. H., L. B. Chen, and B. N. Fields. 1982. The interaction of mammalian reoviruses with the cytoskeleton of monkey kidney CV-1 cells. Virology 120:399-411.

81. Sherry, B., C. J. Baty, and M. A. Blum. 1996. Reovirus-induced acute myocarditis in mice correlates with viral RNA synthesis rather than generation of infectious virus in cardiac myocytes. J. Virol. 70:6709-6715.

82. Sherry, B. and M. A. Blum. 1994. Multiple viral core proteins are determinants of reovirus-induced acute myocarditis. J. Virol. 68:8461-8465.

83. Sherry, B., J. Torres, and M. A. Blum. 1998. Reovirus induction of and sensitivity to beta interferon in cardiac myocyte cultures correlate with induction of myocarditis and are determined by viral core proteins. J. Virol. 72:1314-1323.

84. Shimada, A., G. Shiota, H. Miyata, T. Kamahora, H. Kawasaki, K. Shiraki, S. Hino, and T. Terada. 1998. Aberrant expression of double-stranded RNA-dependent protein kinase in hepatocytes of chronic hepatitis and differentiated hepatocellular carcinoma. Cancer Res. 58:4434-4438.

85. Shmulevitz, M., P. Marcato, and P. W. Lee. 2005. Unshackling the links between reovirus oncolysis, Ras signaling, translational control and cancer. Oncogene 24:7720-7728.

86. Stamatos, N. M. and P. J. Gomatos. 1982. Binding to selected regions of reovirus mRNAs by a nonstructural reovirus protein. Proc. Natl. Acad. Sci. U. S. A 79:3457-3461.

87. Stojdl.D.F, N. Abraham, S. Knowles, R. Marius, A. Brasey, B. Lichty, E. G. Brown, N. Sonenberg, and J. C. Bell. 2000. The murine double-stranded RNA-dependent protein kinase PKR is required for resistance to vesicular stomatitis virus. J. Virol. 75:9580-9585.

88. Strong, J. E., M. C. Coffey, D. Tang, P. Sabinin, and P. W. Lee. 1998. The molecular basis of viral oncolysis: usurpation of the Ras signaling pathway by reovirus. EMBO J. 17:3351-3362.

89. Strong, J. E. and P. W. Lee. 1996. The v-erbB oncogene confers enhanced cellular susceptibility to reovirus infection. J. Virol. 70:612-616.

90. Strong, J. E., D. Tang, and P. W. Lee. 1993. Evidence that the epidermal growth factor receptor on host cells confers reovirus infection efficiency. Virology 197:405-411.

91. Takai Y, Sasaki T, and Matozaki T. 2001. Small GTP-binding proteins. Phys. Rev 81:153-208.

92. Tang, D., J. E. Strong, and P. W. Lee. 1993. Recognition of the epidermal growth factor receptor by reovirus. Virology 197:412-414.

93. Terada, T., K. E. K. Maeta, and T. Ohta. 2000. Protein expression of double-stranded RNA-activated protein kinase in thyroid carcinomas: correlation with histologic types, pathologic parameters, and Ki-67 labeling. Hum. Pathol. 31:817-821.

94. Thirukkumaran, C. M., J. M. Luider, D. A. Stewart, T. Alain, J. A. Russell, I. A. Auer, P. Forsyth, and D. G. Morris. 2005. Biological purging of breast cancer

cell lines using a replication-competent oncolytic virus in human stem cell autografts. Bone Marrow Transplant. 35:1055-1064.

95. Tosteson, M. T., M. L. Nibert, and B. N. Fields. 1993. Ion channels induced in lipid bilayers by subvirion particles of the nonenveloped mammalian reoviruses. Proc. Natl. Acad. Sci. U. S. A 90:10549-10552.

96. Tyler, K. L., P. Clarke, R. L. Debiasi, D. Kominsky, and G. J. Poggioli. 2001. Reoviruses and the host cell. Trends Microbiol. 9:560-564.

97. Tyler, K. L., D. A. McPhee, and B. N. Fields. 1986. Distinct pathways of viral spread in the host determined by reovirus S1 gene segment. Science 233:770-774.

98. Tyler, K. L., M. K. Squier, A. L. Brown, B. Pike, D. Willis, S. M. Oberhaus, T. S. Dermody, and J. J. Cohen. 1996. Linkage between reovirus-induced apoptosis and inhibition of cellular DNA synthesis: role of the S1 and M2 genes. J. Virol. 70:7984-7991.

99. Watanabe, Y., H. Kudo, and A. F. Graham. 1967. Selective inhibition of reovirus ribonucleic acid synthesis by cycloheximide. J. Virol. 1:36-44.

100. Weiner, H. L., M. L. Powers, and B. N. Fields. 1980. Absolute linkage of virulence and central nervous system cell tropism of reoviruses to viral hemagglutinin. J. Infect. Dis. 141:609-616.

101. Wenske, E. A., S. J. Chanock, L. Krata, and B. N. Fields. 1985. Genetic reassortment of mammalian reoviruses in mice. J. Virol. 56:613-616.

102. Wiener, J. R. and W. K. Joklik. 1989. The sequences of the reovirus serotype 1, 2, and 3 L1 genome segments and analysis of the mode of divergence of the reovirus serotypes. Virology 169:194-203.

103. Wilcox, M. E., W. Yang, D. Senger, N. B. Rewcastle, D. G. Morris, P. M. Brasher, Z. Q. Shi, R. N. Johnston, S. Nishikawa, P. W. Lee, and P. A. Forsyth. 2001. Reovirus as an oncolytic agent against experimental human malignant gliomas. J. Natl. Cancer Inst. 93:903-912.

104. Yang, W. Q., D. Senger, H. Muzik, Z. Q. Shi, D. Johnson, P. M. Brasher, N. B. Rewcastle, M. Hamilton, J. Rutka, J. Wolff, C. Wetmore, T. Curran, P. W. Lee, and P. A. Forsyth. 2003. Reovirus prolongs survival and reduces the frequency of spinal and leptomeningeal metastases from medulloblastoma. Cancer Res. 63:3162-3172.

105. Zou, S. and E. G. Brown. 1992. Identification of sequence elements containing signals for replication and encapsidation of the reovirus M1 genome segment. Virology 186:377-388.

APPENDIX I

Figure 27: Survival graph of Balb/c mice bearing CT26 lung tumors following a single intranasal dose of virus ($1.0x10^7$ pfu)
Balb/c mice bearing CT26 lung tumors were treated with a single dose of one of the following viruses EB88, EB96, EB97, or EB123 in order to assess survival post-treatment.

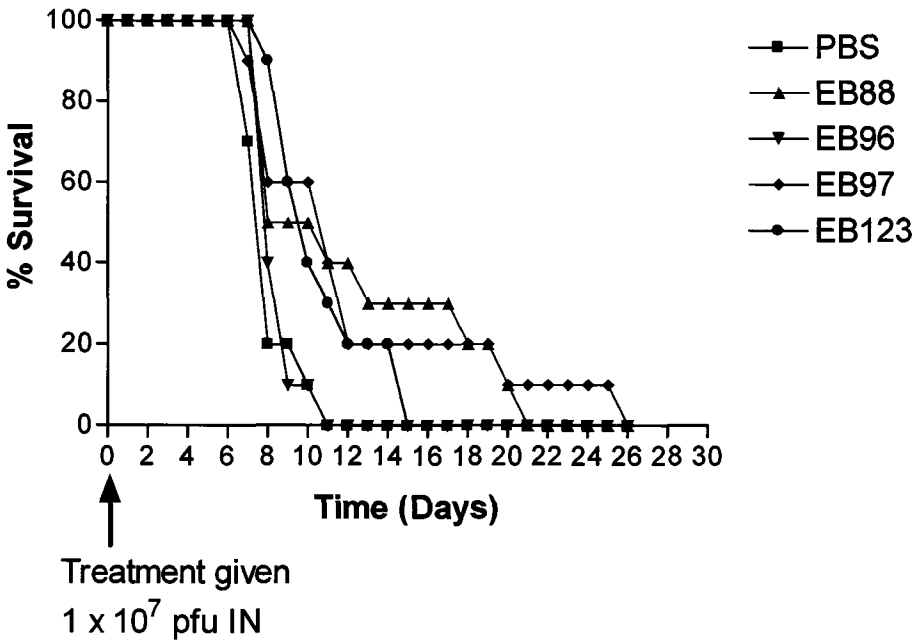

Figure 28: Survival graph of Balb/c mice bearing CT26 lung tumors following three intranasal doses of virus ($1.0x10^7$ pfu)
Balb/c mice bearing CT26 lung tumors were treated three times with $1.0x10^7$ pfu of virus intranasssally on days 0, day 2 and day 4, with one of the following viruses T1L, T3D EB88, EB96, EB97, or EB123 in order to assess survival post-treatment.

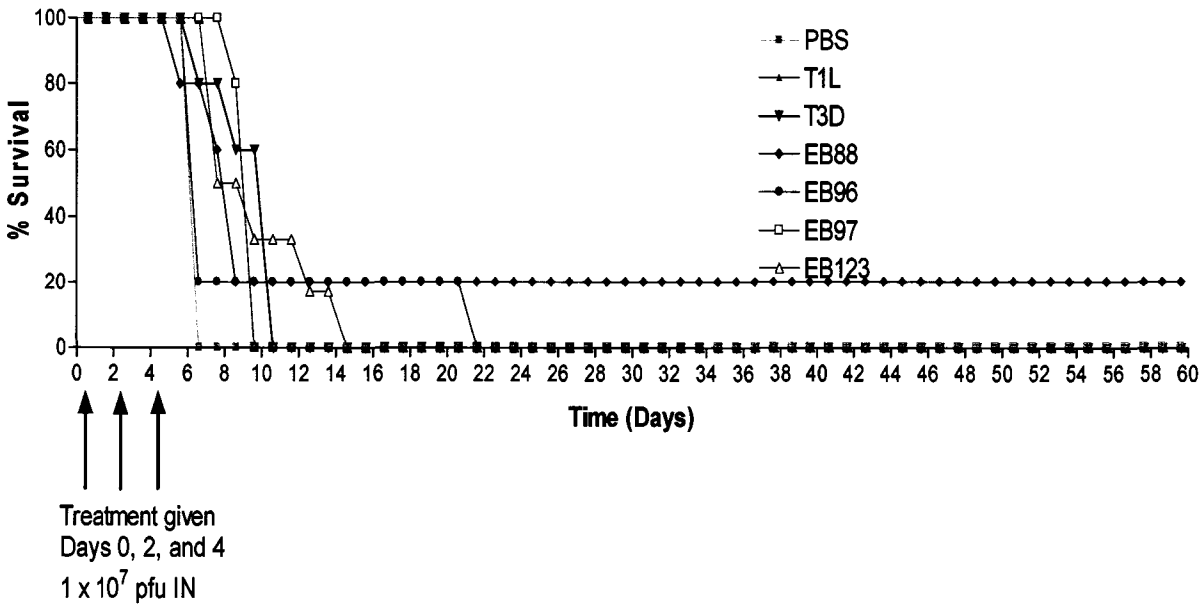

Figure 29: Survival graph of Balb/c mice bearing CT26 lung tumors following three intravenous doses of virus ($1.0x10^8$ pfu)
Balb/c mice bearing CT26 lung tumors were treated three times with $1.0x10^8$ pfu of virus intranasssally on days 0, day 2 and day 4, with one of the following viruses T1L, T3D, or EB88 in order to assess survival post-treatment.

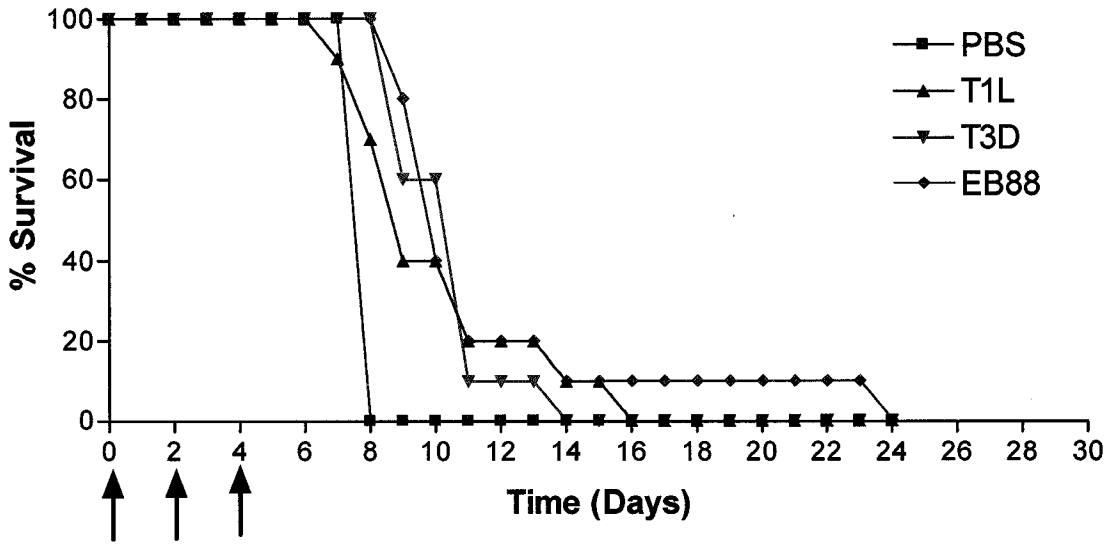

Treatments given
Day 0, 2, and 4
1×10^8 pfu IV
EB88 only recieved 1×10^7 pfu IV